Deutsches Geodätisches Forschungsinstitut

ANNUAL REPORT 2014

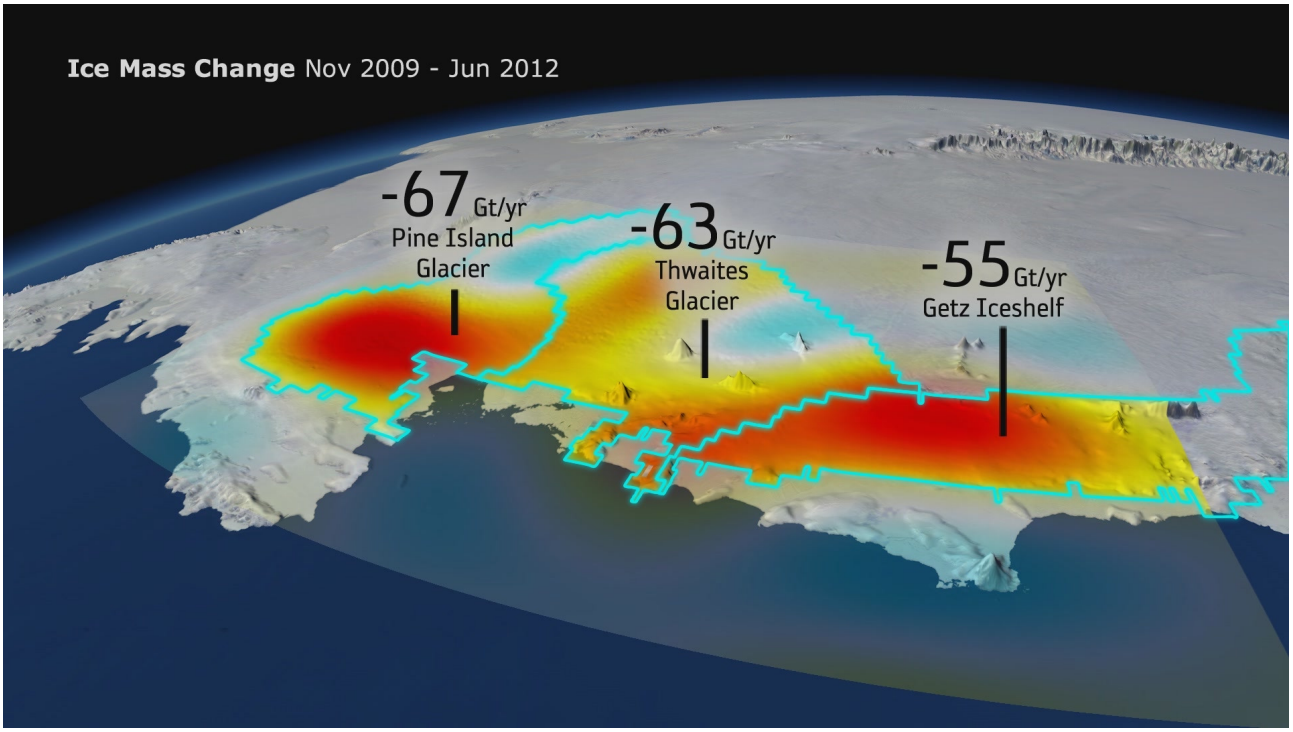

Ice mass change for basins in the Amundsen Sea sector, Antarctica, determined from a combination of GRACE and GOCE, for details see Bouman et al. (GRL, 2014) and Section 2.2; image courtesy of ESA

Deutsches Geodätisches Forschungsinstitut (DGFI)
Alfons-Goppel-Str. 11, 80539 München
Tel.: 089 / 23031-1107 Fax: 089 / 23031-1240
E-mail: mailer.dgfi@tum.de Internet: http://www.dgfi.tum.de

Contents

The Institute

2014: A year of transition for the DGFI

The year 2014 was a year of transition for the Deutsches Geodätisches Forschungsinstitut (DGFI). Established in 1952 at the Bavarian Academy of Sciences and Humanities (BAdW) as an autonomous research institute, the DGFI was affiliated with BAdW's German Geodetic Commission (DGK) for more than 62 years. During this time the institute was the largest purely geodetic research institution in Germany, and it has continuously been involved in various national and international research activities.

During the past decades the institute has performed notable geodetic basic research, and today *DGFI* is a well-known acronym in the geoscientific community all over the world. During the first decades after the foundation of the DGFI, outstanding results were achieved particularly in the fields of geodetic-astronomical observations and electro-optical distance measurements for the determination of the German and European triangulation as well as in gravimetric surveys for gravity networks. The DGFI was involved in the first worldwide network of satellite triangulation and played an important role in the development of dynamical methods of satellite geodesy for precise orbit determination, point positioning and gravity field modelling. A key aspect of DGFI's research has always been the realisation of global and regional horizontal and vertical terrestrial reference systems and of the celestial reference system.

Based on a decision of the Bavarian State Ministry of Education, Science and the Arts (StMBKWK) following a structural evaluation in the year 2012 (StrukBY2013), the DGFI was transferred to the Technische Universität München (TUM). In August 2014, a respective agreement between StMBKWK and TUM was signed, according to which the DGFI has been integrated into the TUM effective from January 1st, 2015. As part of TUM's Faculty of Civil, Geo and Environmental Engineering (BGU), the institute will presume its internationally recognised geodetic basic research under its new official name Deutsches Geodätisches Forschungsinstitut der Technischen Universität München (DGFI-TUM) from 2015 onward.

National and international collaboration

The DGFI is strongly cross-linked with other institutions around the world. Intensive collaborations exist in particular within the framework of the international scientific organisations IUGG (International Union of Geodesy and Geophysics), IAU (International Astronomical Union) and IAG (International Association of Geodesy). The DGFI recognises the outstanding role of the IAG services for science and practice and cooperates in these services as data, analysis and combination centre. Scientists of the DGFI have taken leading positions and supporting functions in IAG's Commissions, Services, Projects, Working and Study Groups, and in its Global Geodetic Observing System (GGOS). Furthermore, the DGFI staff is prominently involved in the management of international scientific organisations, such as the European Geosciences Union (EGU) and the IAU. The DGFI also participates in research programmes and bodies of the European Union (EU) and the European Space Agency (ESA). It cooperates in several United Nations' (UN) and intergovernmental institutions and activities.

On the national level, the DGFI has been a member of the Forschungsgruppe Satellitengeodäsie (FGS) since 1984. The FGS is a follow-on cooperation of the former DFG-Sonderforschungsbereich SFB 78, closely affiliated with the Geodetic Observatory Wettzell in the Bavarian Forest. In the framework of the FGS, the DGFI is cooperating with other units of the TUM (Institut für Astronomische und Physikalische Geodäsie [IAPG], Forschungseinrichtung Satellitengeodäsie [FESG]), the Bundesamt für Kartographie und Geodäsie in Frankfurt/Main (BKG) and the Institut für Geodäsie und Geoinformation of the University of Bonn (IGG).

Within the framework of the Centre of Geodetic Earth System Research (CGE), the DGFI is connected with IAPG, FESG, and the section "Geodesy" of BAdW's Commission for Geodesy and Glaciology (KEG) since 2010. The institutions forming the CGE work together according to a joint research and development programme, guided by the vision that geodesy can provide a high-precision, consistent and long-term valid metric for Earth system sciences. The research and development programme is realised by scientific collaborations across the institutions and within joint third-party funded projects.

DGFI - Geodetic basic research for Earth system science

Geodesy has developed towards an important discipline for Earth system research during the last decades through new technological achievements in Earth observation systems, in particular in satellite technology and in the field of scientific computing. In the context of global change, geosciences are facing new challenges. Large-scale changes in the Earth system come along with implications on environment and living conditions, and catastrophic consequences of natural disasters become more frequent. Research of processes and interactions in the system Earth is of increasing importance. This fundamentally requires reliable observations of changes on various spatial scales over long time spans. Geodesy contributes to Earth system research in particular by providing highly precise geometrical and physical parameters from terrestrial, airborne and satellite-based observation systems. Time series of a variety of geodetic parameters have been determined for many decades. As geodynamic processes and environmental change map into the temporal variations of these parameters, their analysis provides valuable information of long-term changes in the Earth system. As fundamental backbone for referencing the observations and, thus, for enabling a reliable interpretation over long time spans, a consistent global and long-term stable reference system is indispensable.

The DGFI possesses unique competence on several geodetic research fields, in particular in the fields of reference frame determination and satellite altimetry. The institute takes a leading position in the realisation of global and regional horizontal and vertical terrestrial reference systems and of the celestial reference system from a combined analysis of various geometrical space geodetic observing systems. The DGFI regularly computes solutions for the highly precise International Terrestrial Reference Frame (ITRF) as an ITRS Combination Centre. The ITRF is a prerequisite for the use of global navigation and positioning systems and surveying. For its realisation, the IAG requires an accuracy of 1 mm for the positions of globally distributed observing stations and of 0.1 mm per year for their linear velocities. This accuracy is necessary in order to detect very small changes in the Earth system (e.g., the global mean sea level rise of about 3 mm per year) reliably.

In the field of satellite altimetry, the DGFI computes global and regional variations of the sea level on different time scales from all altimetry missions since 1992 and investigates variations of ocean currents. Strong research activities in 2014 were also related to the rather new and challenging topic of inland applications of satellite altimetry. Via its Open Altimeter Database (OpenADB) the DGFI distributes various altimetry products free of charge. Further prominent research topics of the DGFI include theoretical and applied aspects of gravity field determination and atmosphere research. For the latter, the research in 2014 was predominantly focused on investigations of the Earth's ionosphere from the combination of data from various space geodetic observing systems.

DGFI research programme

The scientific activities of the DGFI are oriented towards geodetic basic research. They are embedded in the overall topic "Geodetic Earth System Research" of CGE. The CGE programme is divided into the research areas (1) Geometric Techniques, (2) Gravity Field, (3) Geodetic Earth System Modelling, (4) Methodological Foundations and (5) New Technologies. Research activities within CGE are coordinated by scientists of the contributing partners.

According to the current research programme, the DGFI research areas are consistent with the research areas (1) to (4) of the CGE programme:

1. Geometric Techniques
2. Gravity Field
3. Geodetic Earth System Modelling
4. Methodological Foundations

The DGFI research programme was set up for the period from 2011 to 2014. In November 2010, it was evaluated and approved by an international scientific council (Wissenschaftlicher Beirat).

Dynamic processes and interactions within and between individual components of the Earth system (e.g., atmosphere, hydrosphere, solid Earth) map into temporal variations of geodetic parameters that describe the rotation, the gravity field and the surface geometry of the Earth. Thus, the investigation of time series resulting from the analysis and combination of geodetic observations delivers important information and contributes to Earth system research. On the one hand, geodetic research at the DGFI aims at a further improvement of accuracy and consistency of geodetic parameters related to the Earth's geometry (research area 1) and its gravity field (research area 2). This work is related to and benefits strongly from DGFI's activities in international services. On the other hand, the DGFI aims at the interpretation of geodetic parameters and their application for Earth system research in interdisciplinary cooperations. Accordingly, research area 3 is dedicated to geodetic contributions to Earth system science. One of the main tasks in research area 3 is the application of geodetic data in order to enhance the understanding of dynamical processes in the Earth system and to develop and improve respective empirical and physical models. In particular, the data analysed and provided by the DGFI (which are to a very large extent based on global satellite observations) contribute information about those components of the Earth system in which processes act on large spatial scales. The geodetic observations allow for conclusions with respect to large-scale mass redistributions and exchange processes of angular momentum that involve temporal changes of gravity field, surface geometry, and rotation of the Earth. Furthermore, by suitable combination of observation techniques with different sensitivity for different processes and numerical models the DGFI aims at the separation of integral parameters into contributions of individual system components and underlying dynamical processes. Finally, the cross-cutting research area 4 provides methodological foundations and support for the other research areas by the development and provision of tools, common standards and the necessary infrastructure.

1 Geometric Techniques

This research field is primarily concerned with the analysis and combination of the space geodetic observations contributing to determine geometric parameters describing the shape and orientation of the Earth. In addition, also the low degree spherical harmonic coefficients of the Earth's gravity field are studied as they are directly correlated with the datum parameters to realize the terrestrial reference system. The work relies on the space geodetic observation techniques Very Long Baseline Interferometry (VLBI), Satellite and Lunar Laser Ranging (SLR/LLR), Global Navigation Satellite Systems (GNSS), Doppler Orbitography and Radiopositioning Integrated by Satellite (DORIS) as well as satellite altimetry. The tasks cover the full processing chain from the original observations to the generation of geodetic results and products. They are divided into four major themes:

1.1 Observation systems, data acquisition and provision

1.2 Model development and analysis of the space geodetic observations

1.3 Analysis and refinement of combination methods

1.4 Computation of global and regional reference frames

The work in this research field benefits from the DGFI engagement in the international scientific services of the International Association of Geodesy (IAG). The institute operates - mostly by virtue of long-term commitments - data centres, analysis centres, and combination centres (Müller and Bloßfeld (2014); Sánchez et al. (2014); Schmid et al. (2014); Seitz et al. (2014a)). Table 1.1 summarizes the IAG activities that are closely related to the research field "Geometric Techniques". These responsibilities require an operational analysis of SLR, VLBI and GNSS data and a timely generation of geodetic products. The specific software packages (DOGS-OC for SLR and OCCAM/DOGS-RI for VLBI) and the DGFI combination software DOGS-CS need to be updated regularly according to the latest version of conventions, models and processing standards. Besides the activities listed below, scientists of DGFI took over various responsibilities and functions in IAG (see Sect. 5.4).

The engagement in the IAG services and commissions is a backbone of this research field. It ensures the direct access to the original data of the space geodetic techniques and to the products generated by the scientific services. This is, on the one hand, of great benefit for the research activities at DGFI like, e.g., the combination of space geodetic observations (see Sect. 1.3) and the computation of geodetic reference frames (see Sect. 1.4). On the other hand, the basic research performed at the institute ensures a high-quality generation of geodetic products.

Table 1.1: *Long-term commitments of DGFI in the IAG Services.*

IAG Service	Responsibility of DGFI
International Earth Rotation and Reference Systems Service (IERS)	ITRS Combination Centre
International GNSS Service (IGS)	Regional Network Associate Analysis Centre for SIRGAS (RNAAC-SIR) Tide Gauge Monitoring Working Group (TIGA)
International Laser Ranging Service (ILRS)	Global Data and Operation Centre (EDC) Analysis Centre
International VLBI Service for Geodesy and Astrometry (IVS)	Analysis Centre Combination Centre (jointly with BKG)

1.1 Observation systems, data acquisition and provision

Operation of permanent GNSS stations

DGFI currently is in charge of five continuously operating GNSS stations along the Bavarian Alps and eight stations in South America (3 in Bolivia, 3 in Chile and 2 in Peru). The operation of these stations is supported by local partner institutions, which take care of the appropriate functioning of the equipment and the timely data delivery to DGFI, where the data are archived and distributed to the processing centres. DGFI regularly processes these data in the frame of the following projects: modelling of regional deformations, computation of the regional reference frame SIRGAS, GNSS monitoring of tide gauges, and vertical datum unification in South America. These stations additionally contribute to the IGS Tide Gauge Benchmark Working Group (TIGA), the IGS Multi-GNSS Experiment (MGEX), and the regional densification of the ITRF in Latin America.

ILRS Global Data and Operation Center

Since the foundation of the International Laser Ranging Service (ILRS) in 1998, the EUROLAS Data Center (EDC) acts as one of two global ILRS data centres, the EDC at DGFI-TUM and the Crustal Dynamics Data Information System (CDDIS) at NASA.

The EDC, as ILRS Operation Center (OC) and ILRS Data Center (DC) has to ensure the quality of submitted data sets by checking their format. Furthermore, a daily and hourly data exchange with the NASA OC and CDDIS is performed. All data sets and products are publicly available for the ILRS community via FTP (ftp://edc.dgfi.tum.de) and website (http://edc.dgfi.tum.de).

EDC is running several mail exploders for the exchange of information, data and results. The Consolidated Prediction Format (CPF) files (43164 in 2014) of 78 satellites are exploded automatically on a daily and sub-daily basis and stored at the FTP server. Mailing lists such as SLR-Mail (77 in 2014), SLR-Report (1117 in 2014), Urgent and Rapid-Service-Mail (22 in 2014) are maintained by EDC.

In 2014, 42 SLR stations observed 78 satellites. There were six new satellite missions tracked by SLR stations, namely Glonass-132, Glonass-133, Glonass-134, Galileo-201, IRNSS-1A, and IRNSS-1B. Furthermore, the ILRS station network was extended by the new stations Brasilia (Brazil), Irkutsk (Russia) and Wettzell-SOSW (Germany). Figure 1.1 shows the ILRS station network in 2014.

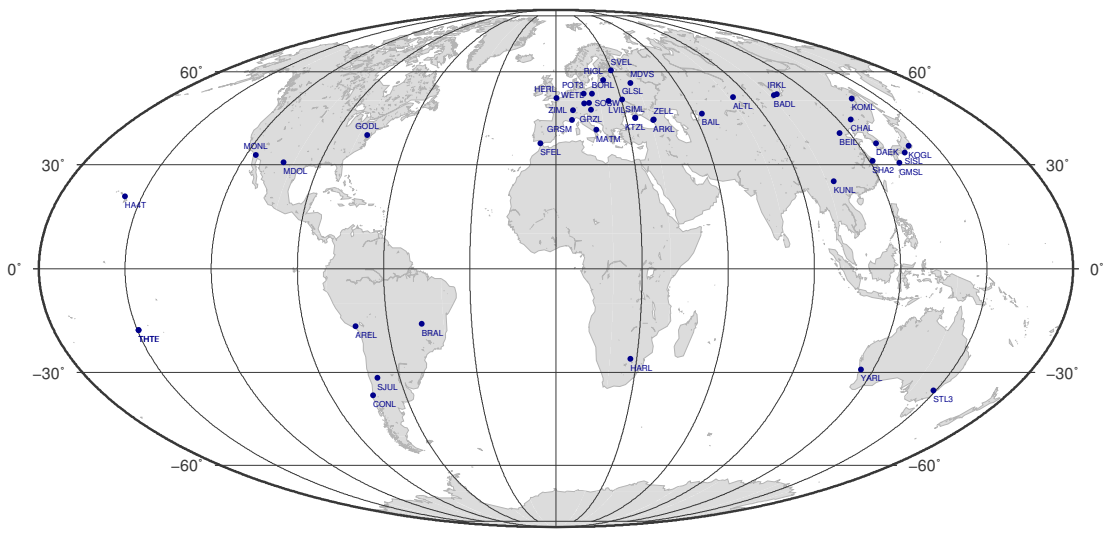

Fig. 1.1: The ILRS station network in 2014

1.2 Model development and analysis of space geodetic observations

SLR contribution to ITRF2014

In 2014, the ILRS Analysis Centre at DGFI reprocessed the SLR observations for the time period from January 1983 to December 2014 according to the latest processing standards of the ILRS as input for the new terrestrial reference frame realization, the ITRF2014. Starting from January 1993, weekly arcs of Lageos 1 and 2 (15-day arcs of Lageos 1 for earlier data) were computed. At the end of 2014, DGFI delivered an updated version 61 (v61) for the whole period, using a new DOGS-OC version (see Sect. 4.1). The loosely constrained solutions including station coordinates and EOP were submitted to the ILRS combination centres. First comparisons of the DGFI solution with the preliminary combined ILRS solution over the period 1983 to 2013 show a good agreement after similarity transformation using the core stations (see Fig. 1.2).

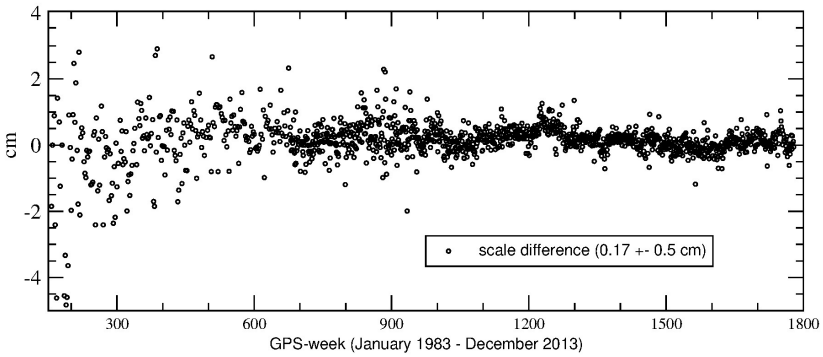

Fig. 1.2: *Scale difference between ILRS v60 and DGFI v61 using core stations.*

SLR multi-satellite solution

SLR plays a key role for the common estimation of orbit parameters, station coordinates, EOP and Stokes coefficients of the Earth's gravitational field. Since SLR is sensitive to all these parameters, this space technique can be used to study interactions and correlations between them. During 2014, DGFI investigated the potential of SLR for a common adjustment of all parameters using a multi-satellite SLR solution. This solution contains observations to multiple (up to ten) different spherical satellites which are combined using a variance component estimation (VCE). The investigations are published in Bloßfeld et al. (2014a,b).

In Bloßfeld et al. (2014a), the mathematical parameterization of the temporal behavior of station positions (linear model) in the most recent ITRF realization is discussed and an alternative epoch-wise estimation of station coordinates is presented. Thereby, the special role of SLR for the TRF datum is emphasized. SLR is used for the realization of the TRF origin and, together with VLBI, for the realization of the TRF scale. Due to the non-homogeneous global distribution of observing stations, common translations due to neglected non-linear station variations alias into common rotations of all stations (network orientation). As a consequence, the terrestrial pole coordinates as complementary parameters to the network orientation (non-equatorial rotations) are biased.

In Bloßfeld et al. (2014b), the systematics in the excess length-of-day (ΔLOD) estimates of satellite observation techniques are investigated. ΔLOD describes the difference between LOD and 86400 s and is related to ΔUT1 through d/dt(ΔUT1)=-(ΔLOD)/(86400 s). This rotation is complementary to rotations of the orbital plane caused by the Stokes coefficient C_{20} (Earth's flattening). Figure 1.3 shows systematics in ΔLOD caused by different C_{20} a priori models. If ΔLOD and C_{20} are estimated in a joint adjustment,

at least two different satellite inclinations are necessary to decorrelate the parameters (see Fig. 1.4). Furthermore, Bloßfeld et al. (2014b) investigate the effect of relativistic accelerations due to the Lense-Thirring and deSitter effect on ΔLOD. In total, both accelerations cause a constant offset of 0.0087 ms in ΔLOD if they are neglected.

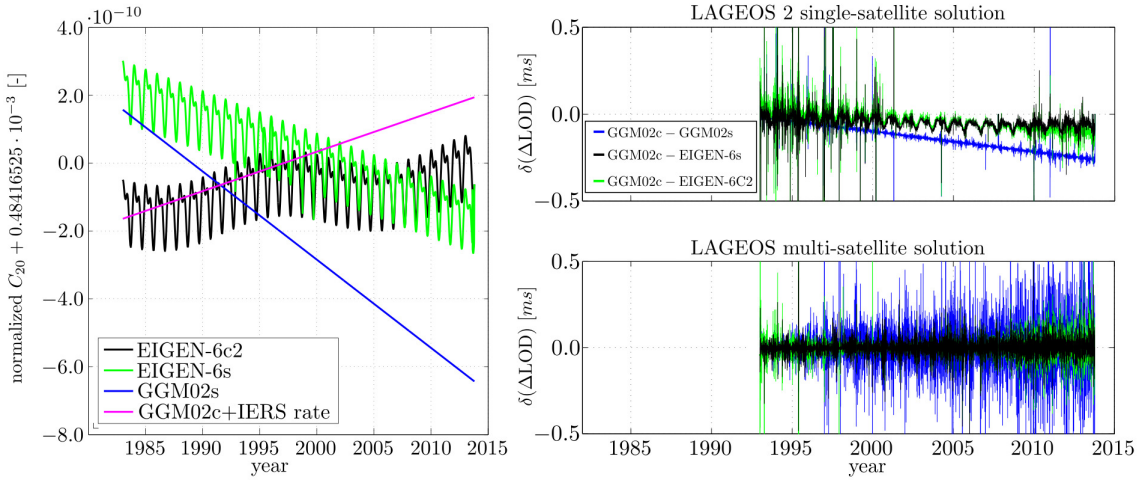

Fig. 1.3: Different C_{20} a priori models (left panel); systematics of ΔLOD caused by the different C_{20} a priori models for the LAGEOS 2 single-satellite solution (upper right panel) and the LAGEOS 1/2 multi-satellite solution (lower right panel).

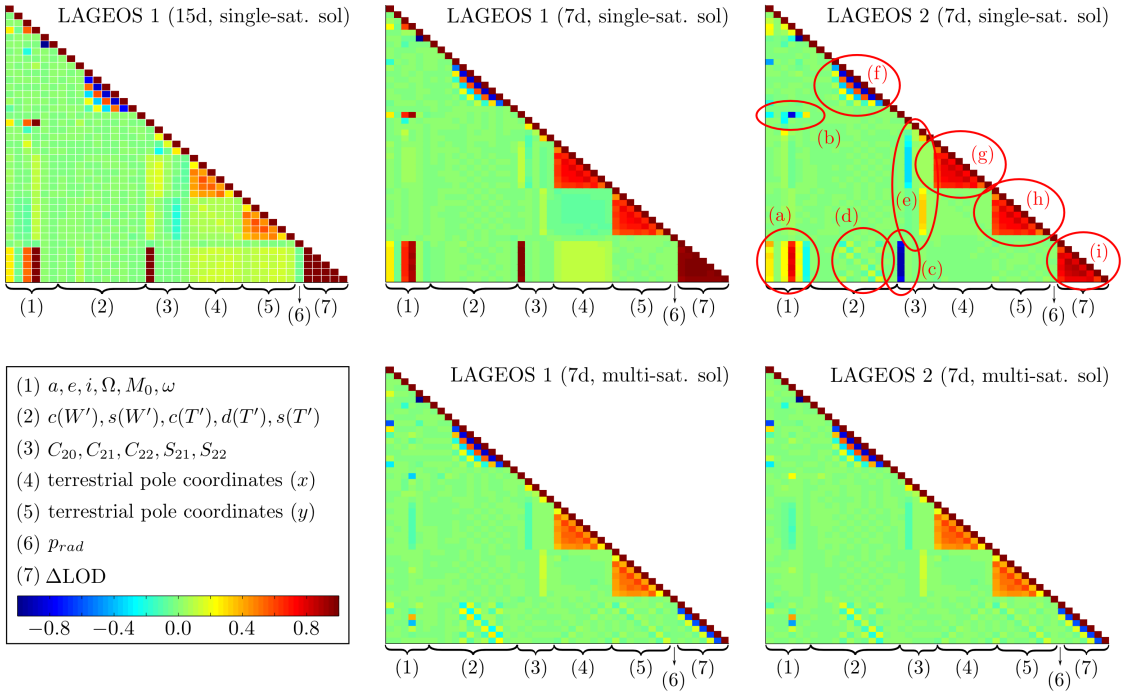

Fig. 1.4: Mean correlation matrices of LAGEOS 1 and 2 single-satellite solutions and satellite-separated multi-satellite solutions. Due to the varying number of stations per week, the station-related (coordinates and biases) rows and columns are not shown. The correlations (a) to (i) are explained in Bloßfeld et al. (2014b).

Multi-mission cross calibration of SARAL/AltiKa

In the framework of the regular calibration of all satellite altimeter missions, DGFI performed a comprehensive analysis of SARAL sea surface heights (SSH, Bosch et al., 2014).
SARAL is a French/Indian satellite mission developed as a collaboration between ISRO and CNES. SARAL was launched on February 25, 2013 and is equipped with two independent main payloads: ARGOS-3 and AltiKa. The latter is an innovative single-frequency altimeter system measuring in Ka-band (35.75 GHz). SARAL follows the same orbit with a 35-day repeat cycle as the multi-disciplinary phases of ERS-1, ERS-2, and ENVISAT extending their long-term time series. In order to connect the SARAL time series with ENVISAT a careful validation and calibration of the new mission is necessary. Moreover, it is important to ensure consistency with other current altimeter missions such as Jason-2, Cryosat-2, and HY-2A allowing multi-mission altimetry applications. This will improve the spatial and temporal resolution for manifold applications regarding ocean dynamics and variability.
The 1 Hz data of the first 1.5 years of the SARAL mission are used to perform a comprehensive quality assessment by means of a global multi-mission crossover analysis. This approach compares SARAL SSH with data from other current missions, mainly Jason-2 and Cryosat-2, in order to reveal its accuracy and consistency with other altimeter systems. Alongside with global mean range biases and instrumental drifts, investigations on geographically correlated errors as well as on the realization of the systems' origin are performed. The study proved the high quality and reliability of SARAL. The mission shows only a small range bias of about -5 cm with respect to Jason-2 and neither a significant time-tag bias nor instrumental drifts. With about 1.3 cm the scatter of radial errors is in the same order of magnitude as for Cryosat-2 and Jason-1 GM and will probably further improve using an enhanced sea state bias (SSB) model. However, the wet tropospheric corrections derived from the SARAL radiometer still show some systematic effects (see Fig. 1.5) influencing the range bias as well as geographically correlated error patterns and the z-component of the origin. Improved in-flight calibration will be necessary to overcome these effects. More details can be found in Dettmering et al. (2014).

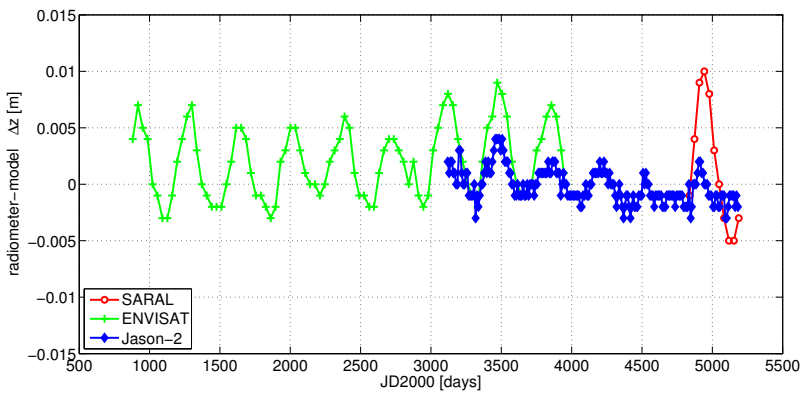

Fig. 1.5: Wet tropospheric correction for different altimeter missions. The z-component of the differences between radiometer-derived corrections and model corrections is shown for a time period of about 12 years.

Cryosat-2 SAR multi-looked waveform retracking

The Cryosat-2 satellite was launched in April 2010 to measure floating sea ice and land ice sheets. It is the first satellite which has a synthetic aperture interferometric radar altimeter (SIRAL) onboard which measures in three modes depending on the geographic location:

- Low resolution mode (LRM) like a conventional radar altimeter,
- Synthetic aperture radar (SAR) mode and
- SAR interferometry (SIN) mode.

Table 1.2: *Standard deviation σ of the differences between the geoid heights and the retracked sea surface heights along with the improvement percentage (IMP) with respect to the Cryosat-2 SAR L2 data.*

retracker	L2	OCOG	TR 75 %	ITR 75 %	Beta5	SAMOSA2
σ [m]	0.14	0.23	0.14	0.14	0.12	0.09
IMP [%]		−52.71	4.75	5.82	16.20	36.96

At DGFI, we started to use Cryosat-2 SAR measurements to determine water level heights. Compared to the conventional radar altimeter, the SAR altimeter is not pulse-limited so that the full Doppler bandwidth can be exploited to increase the spatial resolution in along-track direction. Each ground location is sensed multiple times due to the fact that the satellite moves forward. By averaging the echoes for each location multi-looked waveforms (L1b data) are obtained. These waveforms show different characteristics than the classical radar altimetry waveforms, e.g., they are much "peakier".
We tested 4 standard altimeter retrackers: Offset Center Of Gravity (OCOG); Threshold Retracker (TR); Improved Threshold Retracker (ITR); and Beta5. It was studied how well these retrackers perform for SAR multi-looked waveforms over the open ocean and over inland water. For comparisons we determined the sea surface heights also with the SAR Versatile Altimetric Toolkit for Ocean Research & Exploitation (SARvatore) which uses the SAMOSA2 retracker developed within the ESA project "Development of SAR Altimetry Studies and Applications over Ocean, Coastal zones and Inland waters (SAMOSA)".
For the **open ocean**, the sea surface heights are compared with the Cryosat-2 SAR L2 data (retracked by ESA) and the geoid heights derived from the Earth Gravitational Model 2008 (EGM08). The standard deviations of the differences between the geoid heights and the retracked sea surface heights are computed along with the improvement percentage with respect to the Cryosat-2 SAR L2 data (see Table 1.2). The TR (75 %) and ITR (75 %) retrackers provide only slightly improved results with respect to the Cryosat-2 SAR L2 data whereas the Beta5 retracker provides significantly improved results. Thus, the standard altimeter retracker can be also used to retrack SAR multi-looked waveforms. However, much better results can be achieved with the SAMOSA2 retracker developed for SAR ocean waveforms.
For **inland water**, the sea surface heights are reduced by the geoid heights in order to compare the orthometric heights with measurements of gauging stations. Figure 1.6 shows the Cryosat-2 tracks which cross the lake Tonle Sap in Cambodia together with the different retracking results for the orthometric heights. Furthermore, the standard deviations with respect to the gauging station Prek kdam are listed in Figure 1.6 along with the improvement percentage with respect to the Cryosat-2 SAR L2 data. Here, the ITR (75 %) and Beta5 retrackers provide only slightly improved results. The SAMOSA2 retracker cannot be used for inland water because it is based on a physical model for SAR ocean waveforms.
The experiences gathered with Cryosat-2 SAR will enable us to deal with data from Sentinel-3, which will be launched in 2015 and provide global SAR data coverage.

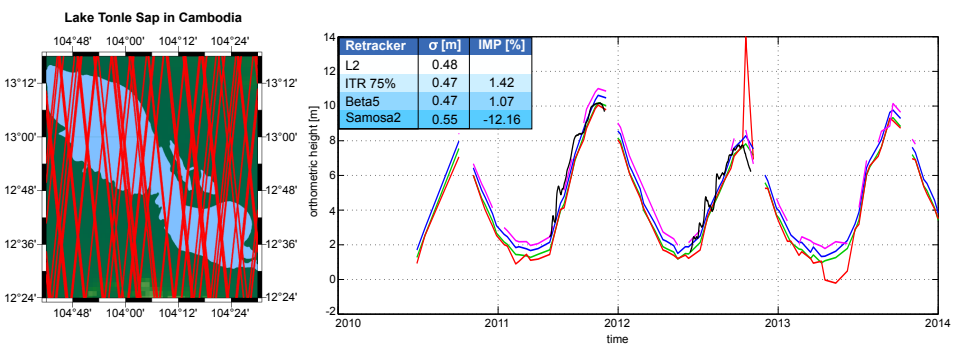

Fig. 1.6: *Orthometric heights for the lake Tonle Sap in Cambodia derived from Cryosat-2 SAR L1b data by using the retracker: ITR 75% (green), Beta5 (blue) and SAMOSA2 (magenta). For comparison, the orthometric heights from the Cryosat-2 SAR L2 data (red) and the gauging station Prek kdam (black) are shown. The table includes the standard deviations σ with respect to the gauging station Prek kdam along with the improvement percentage (IMP) with respect to the Cryosat-2 SAR L2 data.*

1.3 Analysis and refinement of combination methods

The combination of space geodetic observations is a major research topic at DGFI. The combinations are performed on the level of datum-free normal equations with the DGFI software DOGS-CS. This software is continuously updated to enable the implementation of refined methodologies. The work within this theme provides the basis for the computation of global and regional reference frames (see Sect. 1.4) and for the contribution to various IAG services (e.g., ITRS Combination Centre, IVS Combination Centre jointly with BKG) and working groups (e.g., IERS WG "Combination at the Observation Level", Joint WG 1.4 of IAG Commission 1 and the IERS "Strategies for epoch reference frames").

In 2014, a major part of the work was accomplished in the framework of the Research Unit (FOR 1503) "Space-time reference systems for monitoring global change and for precise navigation in space" funded by the German Research Foundation (DFG). DGFI is involved in two out of six projects: Project PN5 is devoted to "Consistent celestial and terrestrial reference frames by improved modeling and combination", and project PN6 aims at "Consistent dynamic satellite reference frames and terrestrial geodetic datum parameters".

Project PN5

The main goals of this joint project of BKG and DGFI are to develop and apply improved combination methods for reference frame computations, to use advanced strategies for handling non-linear station motions, and to generate consistent celestial and terrestrial reference frames including EOP.

The results are generated by combining constraint-free normal equations derived from VLBI, SLR and GNSS observations. The latter are processed homogeneously considering a unified set of processing standards. As radio source positions were fixed to their a priori values in the routine VLBI solutions submitted to the IVS until the end of 2012, a VLBI reprocessing was started to have source positions included. Together with the operational solutions from 2014, a consistent VLBI time series covering six and a half years was available at the end of 2014. As regards SLR, weekly 10-satellite solutions are available for combination back to the year 2000. The advantage of multi-satellite solutions is a better decorrelation of the estimated parameters compared to the standard LAGEOS1/2 solutions. So far, five years of global GNSS data from 2006 to 2011 were used for the reference frame computations.

A major focus in 2014 was on an improved handling of non-linear station motions by an extended parameterization (e.g., for seasonal signals). In order to allow for the estimation of periodic station signals besides the linear station velocities, the amplitudes of sine and cosine waves were implemented as additional parameters into DOGS-CS, DGFI's combination software. This extended parameterization was applied to a global GNSS solution computed over a time span of 5 years. The results were compared with the standard approach (linear station motion model) and with the BKG results obtained from improved geophysical fluid models. As an example, Figure 1.7 shows the height time series for the GNSS station Zwenigorod (Russia) in comparison with the geophysical model results and the estimated annual signal.

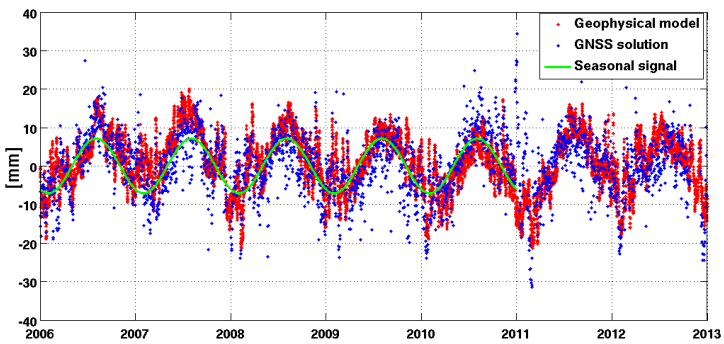

Fig. 1.7: GNSS height time series for the GNSS station Zwenigorod (blue) with deformation from geophysical models (red) and estimated seasonal signal (green).

Project PN6

The focus of the work in 2014 was on a further improvement of low gravity field coefficients from an SLR multi-satellite solution, the investigation of the sensitivity of GNSS orbits to the subdaily pole model and the implementation of Jason-2 satellite models into the DGFI orbit determination software DOGS-OC.

Estimation of Stokes coefficients using SLR observations to multiple spherical satellites

The combination of SLR observations to multiple spherical satellites with different orbit characteristics allows the decorrelation of orbit parameters such as the right ascension of the ascending node Ω and the even-degree Stokes coefficients of the Earth's gravitational field (esp. C_{20}). This leads to an increased accuracy for all estimated parameters. The joint estimation of orbit parameters and second-degree Stokes coefficients mostly benefits from a combination of LAGEOS-1/2, Ajisai, Stella, Starlette and LARES whereas the inclusion of Etalon-1/2, Larets and BLITS does not have a significant impact. The increase of the sensitivity of the orbit constellation to the Earth's gravitational field is essential for a consistent and highly accurate realization of a dynamic satellite reference frame and terrestrial geodetic datum parameters.

Analysis of SLR observations to Jason-2

The altimeter satellite Jason-2, launched in 2008, is also equipped with an SLR reflector, a GNSS and a DORIS antenna. Due to its low orbit height of 1300 km and the availability of three different observing techniques over a time span of currently 6.5 years, the satellite is valuable for combination studies and for research on the computation of low-degree gravity field coefficients. DOGS-OC was upgraded with the modeling of non-gravitational perturbations (solar radiation pressure, Earth infrared (IR) radiation, Earth albedo, atmospheric drag) for non-spherical satellites, such as Jason-2 (see Sect. 4.1).

Sensitivity of GNSS orbits to the subdaily pole model

The IERS2000 subdaily Earth rotation parameter (ERP) model commonly used for the analysis of space geodetic observations is known to show uncertainties of about 20%. In order to investigate the impact of these uncertainties on the datum of the dynamic reference frame, a GNSS solution was set up in which the parameterized subdaily ERP are transformed into tidal signals. Estimating orbits by fixing the amplitudes of these signals to artificially falsified a priori values (IERS2000 model with an offset for one tidal term) allowed to study the interactions of Keplerian elements and parameters related to non-gravitational disturbances. The errors of the subdaily ERP model (characterized by pro- and retrograde terms of a daily differential wave and a linear drift in x- and y-pole) lead to a shift (translation) of single satellite orbits, an orientation change of the whole satellite constellation in the intertial space and an offset in the daily ERP (see Fig. 1.8).

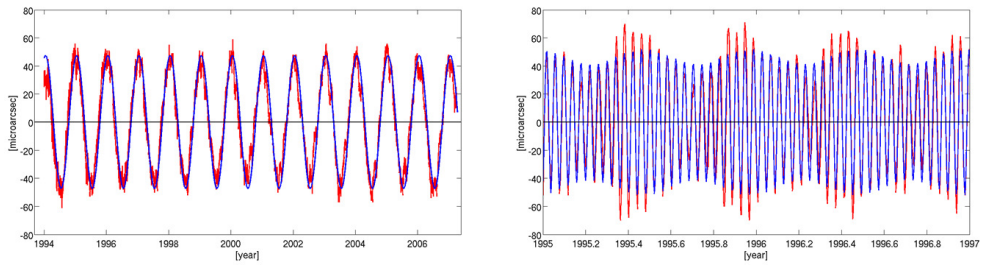

Fig. 1.8: *x-rotations between orbits estimated with different ERP subdaily models (IERS2000 and IERS2000 plus 100 µas; red) and theoretical values derived from the differential model waves (blue). Left: S1 term (24 h), right: O1 term (25.2 h).*

1.4 Computation of global and regional reference frames

DTRF2014, the new ITRS realization: first steps

In 2014, the work of the ITRS Combination Centre at DGFI concentrated on the new ITRS realization, ITRF2014. In December the ITRS Centre decided – after consulting the technique centres - to extend the input data series by one year and to switch from the initially planned ITRF2013 to an ITRF2014 solution. The reason was a time delay for some of the input data series. However, the DORIS data provided by the IDS were available almost in time, and SLR and VLBI input data were provided in late 2014. These data were analyzed and multi-year solutions per technique were generated. The ITRF2014 will, for the first time, consider non-tidal atmospheric loading signals. The implementation of the necessary procedures was one task in 2014 (see also Sect. 4.1).

For DORIS, 1093 weekly SINEX files (1993.0–2014.0) were provided and analyzed. They contain station positions and terrestrial pole coordinates. As the applied constraints are not given in the SINEX files, they cannot be removed. Therefore, seven parameters of a similarity transformation have to be introduced to reconstruct the weekly normal equations. These normal equations are solved and station position time series are generated. Due to a better phase center modelling applied by the IDS, some ITRF2008 discontinuities caused by equipment changes could now be removed. Thus, the number of discontinuities decreased from 48 (ITRF2008) to 33 (ITRF2014, data until 2013.0), even though the number of stations increased from 136 to 149 and the time series were extended by five more years of data. Nevertheless, 25% of the station time series are shorter than 2.5 years. For ITRF2008, stations with less than 2.5 years of data were reduced because otherwise the annual station signals affected the estimated station velocity and the position at the reference epoch. As the application of non-tidal atmospheric loading corrections will reduce annual signals, detailed analyses will be necessary to define the minimal length of the time series. The analysis of the time series of the initial DORIS datum parameters reflects the accuracy of the DORIS solutions. The analysis provided reduced RMS values compared to ITRF2008. Besides, the large long-term scale drift is reduced, and only a short-term drift in 2011 – possibly related to the satellites HY-2A and Saral launched in this time period – was detected (Figure 1.9). The correlation of the z-translation with the solar cycle is also reduced but still significant. The comparison of the DORIS EOP series with IERS 08 C04 shows clear periodic signals in the x-pole for harmonics of Jason-2 and GPS draconitic periods.

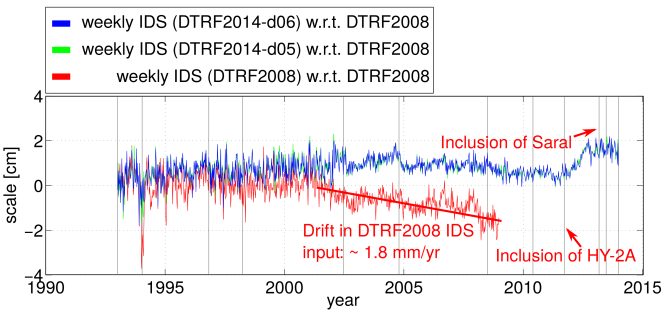

Fig. 1.9: Time series of the initial scale of DORIS input data for DTRF2014 (blue/green) and DTRF2008 (red). The main difference between the two DTRF2014 input data sets is the relative weighting of the Analysis Centre contributions.

In case of SLR, 1338 weekly SINEX files (1983.0–2014.0) derived from LAGEOS-1/2 and Etalon-1/2 observations (Etalon by some ACs only) were provided, including station positions, pole coordinates and LOD. The applied loose constraints can remain on the normal equations. The analysis of the station position time series shows that the number of discontinuities (34) is slightly larger compared to ITRF2008 (31). However, 33% of the stations observed for less than 2.5 years. For a first SLR multi-year solution, 57 stations with either less than 2 years of data or less than 10 weeks are reduced. A final decision on the minimum length of the time series will be made after the analysis of all techniques by applying non-tidal atmospheric loading corrections. The analysis of the datum parameter time series provided an RMS comparable to ITRF2008. The scale time series shows a smaller annual signal for DTRF2014 (Figure 1.10), possibly due to a new CoM model.

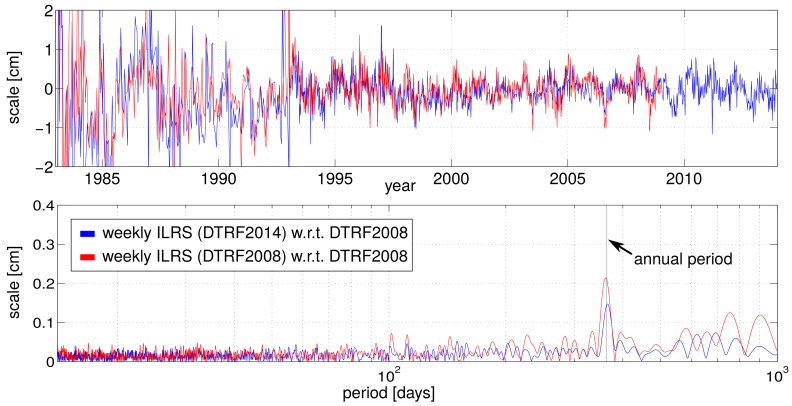

Fig. 1.10: *Scale time series for DTRF2014 (blue) and DTRF2008 (red) SLR input data as well as the corresponding amplitude spectra.*

A first SLR multi-year solution agrees with DTRF2008 within 0.7 mm for the translation and 0.2 mm for the scale. The agreement for the corresponding rates is 0.5 mm/yr and 0.2 mm/yr, respectively. The RMS of the transformation is 3 mm for station positions and 0.7 mm/yr for the velocities. The good results are an indication for the high accuracy of up-to-date ITRF solutions. However, the differential rates should be further reduced. The analysis of the SLR-EOP series shows the well-known effect of outliers during Christmas holidays. Furthermore tidal frequencies are visible in LOD differences with respect to IERS 08 C04 (also for DTRF2008). Therefore, the question arises, whether all analysis centres used exactly the same subdaily ERP model. The annual signal that was visible in the LOD difference series for DTRF2008 fully disappeared.

The IVS provided 5359 session-wise SINEX files (1980.2-–2014.0) including constraint-free normal equations. The explicitly estimated parameters are station positions, pole coordinates and rates, UT1, LOD and nutation offsets. 259 files include one-baseline sessions that cannot be used for reference frame computation. Furthermore, 26 stations which are observed in one or two sessions only had to be reduced. The analysis of the station position time series provides RMS values comparable to DTRF2008 and only a few outliers resulting from weak sessions of regional networks with three stations only. The scale time series is homogeneous and does not show any drift or systematic effect except for the very beginning, which is also characterized by large noise (Figure 1.11). The scale of a first multi-year solution agrees with DTRF2008 within 0.0 mm and 0.4 mm/yr. However, the list of station discontinuities is not yet finalized and a further improvement of the scale rate agreement can be expected.

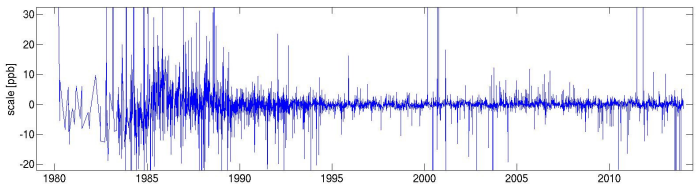

Fig. 1.11: *Scale time series for DTRF2014 VLBI input data.*

In early 2015, the technique centres will provide SINEX series until the end of 2014 and the final ITRF solution is expected to be finished before mid of the year.

Consistent computation of TRF and CRF

In 2014, a new consistent realization of ITRS and ICRS was performed. This solution was computed from long-term VLBI, GNSS and SLR observations until the end of 2010. In case of VLBI, most of the X/S sessions (4341) observed in this time span and all 24 VCS sessions are included now so that the CRF solution is more complete and comparable to ICRF-2. The parameters determined explicitly include station coordinates, source coordinates, pole coordinates, UT1 and nutation parameters. Altogether, 57032 parameters were estimated. A first precise solution was computed by combining VLBI and GNSS, as the early SLR EOP exhibited some problems. In particular, the combination has an impact on the EOP

and, thus, indirectly also on the CRF. The combined EOP series are continuous during the satellite era and benefit as regards their standard deviations and scatter. Due to the decrease of EOP standard deviations, also the standard deviations of the sources decrease. Position changes are mainly visible for VCS sources as well as for sources observed in RDV sessions. Detailed investigations on the CRF results are under progress.

Modelling seismic deformations within the SIRGAS reference frame

The Maule 2010 earthquake in Chile generated the largest displacements of geodetic observation stations ever observed in terrestrial reference frames. Coordinates changed by up to 4 m, and deformations were measurable in distances of up to more than 1000 km from the epicentre. The station velocities in the regions adjacent to the epicentre changed dramatically after the seism. While they were oriented eastward with approximately 2 cm/yr before the event, they are now directed westward with about 1 cm/yr. The 2010 Baja California earthquake in Mexico caused displacements on the dm level also followed by anomalous velocity changes. The main problem for geodetic applications is the fact that there is no reliable reference frame available in the region. To overcome this inconvenience, DGFI, acting as the IGS-RNAAC-SIR (IGS Regional Network Associate Analysis Centre for SIRGAS), computed a new multi-year solution for the SIRGAS reference frame (Figure 1.12) considering only the four years after the seismic event (from mid-2010 until mid-2014). The obtained station positions and velocities refer to the IGb08 reference frame (the IGS realization of the ITRF2008), epoch 2013.0. The averaged rms precision is ±1.4 mm horizontally and ±2.5 mm vertically for the station positions at the reference epoch, and ±0.8 mm/yr horizontally and ±1.2 mm/yr vertically for the constant velocities. Based on this solution, a new continuous deformation model for SIRGAS was computed (Figure 1.13). It is clear that the tectonic structure in South America has to be redefined. The area south of 35° to 40° was considered as a stable part of the South American plate. Now we see that there are large and extended crustal deformations.

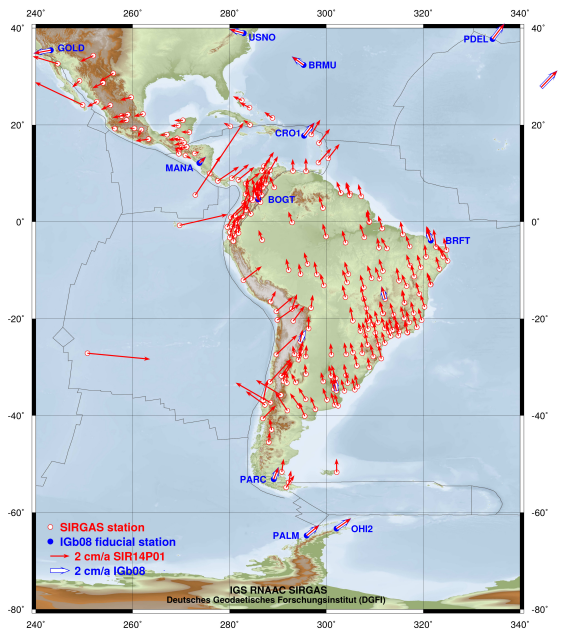

Fig. 1.12: Horizontal velocities of the multi-year solution SIR14P01 (ITRF2008, 2013.0).

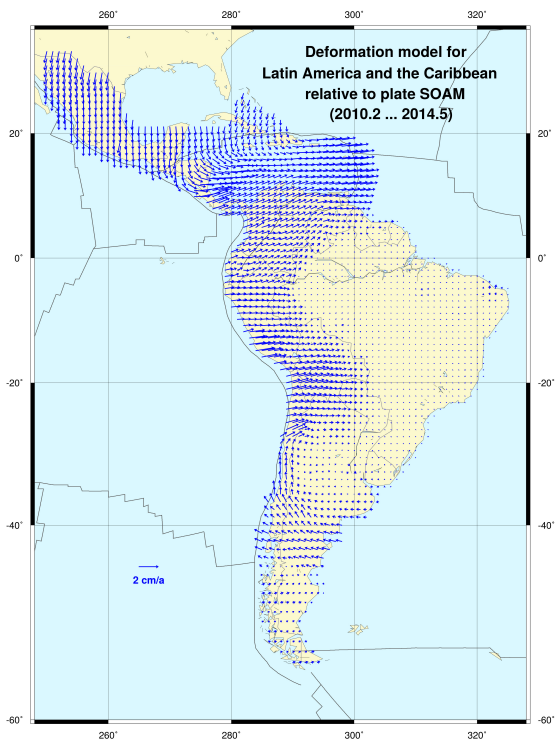

Fig. 1.13: Post-seismic deformation model after the 2010 earthquakes in Latin America.

Acknowledgements

The activities performed by DGFI as IGS-RNAAC-SIR are strongly supported by more than 30 Latin American and Caribbean institutions which not only make the measurements of the GNSS stations available, but also operate SIRGAS Analysis Centres processing the observational data on a routine basis. The weekly solutions computed by the SIRGAS Analysis Centres are provided to DGFI for further analysis of the reference frame. This support is highly appreciated.

Related publications

Bloßfeld M., Seitz M., Angermann D.: *Non-linear station motions in epoch and multi-year reference frames*. Journal of Geodesy 88(1): 45-63, Springer, 10.1007/s00190-013-0668-6, 2014a

Bloßfeld M., Gerstl M., Hugentobler U., Angermann D., Müller H.: *Systematic effects in LOD from SLR observations*. Advances in Space Research 54(6): 1049-1063, 10.1016/j.asr.2014.06.009, 2014b

Bosch W., Dettmering D., Schwatke C.: *Multi-mission cross-calibration of satellite altimeters: constructing a long-term data record for global and regional sea level change studies*. Remote Sensing 6(3): 2255-2281, 10.3390/rs6032255, 2014

Dettmering D., Schwatke C., Bosch W.: *Global calibration of SARAL/AltiKa using multi-mission sea surface height crossovers*. Marine Geodesy, 10.1080/01490419.2014.988832, 2014

Jacobs C.S., Arias F., Boboltz D., Boehm J., Bolotin S., Bourda G., Charlot P., de Witt A., Fey A., Gaume R., Gordon D., Heinkelmann R., Lambert S., Ma C., Malkin Z., Nothnagel A., Seitz M., Skurikhina E., Souchay J., Titov O.: *ICRF-3: roadmap to the next generation ICRF*. In: Capitaine N. (Ed.) Proceedings of the Journées 2013, Scientific developments from highly accurate space-time reference systems, 51-56, Observatoire de Paris, ISBN 978-2-901057-69-7, 2014

Müller H., Bloßfeld M.: *Quality and possible improvements of the official ILRS products*. Proceedings of the 18th International Workshop on Laser Ranging, 13-0202, 2014

Panafidina N., Hugentobler U., Seitz M.: *Interaction between subdaily Earth rotation parameters and GPS orbits*. IAG Symposia, Springer, accepted

Sánchez L., Drewes H., Brunini C., Mackern M.V., Martínez-Díaz W.: *SIRGAS core network stability*. IAG Symposia 143, in press

Sánchez L.: *IGS Regional Network Associate Analysis Centre for SIRGAS (IGS RNAAC SIR)*. In: Dach R., Jean Y. (Eds.) International GNSS Service Technical Report 2013, 103-114, 2014

Schmid R., Gerstl M., Seitz M., Angermann D.: *DGFI Analysis Center Annual Report 2013*. In: Baver K.D., Behrend D., Armstrong K.L. (Eds.) International VLBI Service for Geodesy and Astrometry 2013 Annual Report, 263-264, NASA/TP-2014-217522, 2014

Schmid R.: *IGS Antenna Working Group*. In: Dach R., Jean Y. (Eds.) International GNSS Service Technical Report 2013, 133-136, IGS Central Bureau, 2014

Seitz M., Angermann D., Blossfeld M., Gerstl M., Müller H.: *ITRS Combination Centre at DGFI*. IERS Annual Report 2013, BKG, Frankfurt a.M., 2014a

Seitz M., Steigenberger P., Artz T.: *Consistent adjustment of combined terrestrial and celestial reference frames*. In: Rizos C., Willis P. (Eds.) Earth on the Edge: Science for a Sustainable Planet, IAG Symposia 139: 215-221, Springer, 10.1007/978-3-642-37222-3_28, 2014b

Seitz M., Angermann D., Gerstl M., Bloßfeld M., Sánchez L., Seitz F.: *Geometrical Reference Systems*. Handbook of Geomathematics (Second Edition), in press

2 Gravity Field

The Earth's gravitational field serves on the one hand as a reference surface for many dynamic processes in the Earth system, while on the other hand the observation of the gravitational field itself together with its variations in time characterize mass distribution and mass transport, which in turn describe geophysical processes. Typical examples of research areas for which the gravitational field is of importance are geodesy, geophysics, oceanography, and navigation. A central theme is therefore the observation, modelling and determination of the Earth's mean and time-variable gravitational field at all temporal and spatial scales.

In 2014, we focussed on three main topics related to the gravitational field. The first topic dealt with refinements in our regional gravity field analysis, exploiting satellite altimeter data, airborne gravity data as well as Gravity field and steady-state Ocean Circulation Explorer (GOCE) gravity gradient data (Sect. 2.1). The time-variable gravity field (Sect. 2.2) was studied at different spatial scales using a combination of satellite laser ranging (SLR) and Gravity Recovery And Climate Experiment (GRACE) data, as well as combining GRACE and gravity gradients from GOCE. A final topic was devoted to height systems and their application (Sect. 2.3). Highlights of these three topics are discussed below.

2.1 Regional gravity fields

Generation of a software application for producing highly precise regional gravity models as a height reference surface (RegGRAV)

The project RegGRAV, funded by the Bundeswehr Geoinformation Centre (BGIC) located in Euskirchen, expired in January 2015. It comprised two funding periods: the first two-year phase was scheduled from July 2009 to June 2011, the final phase started after a break of more than two years in December 2013. The project tends to the development of a software package for the generation of regional gravity fields out of heterogeneous data.

The basic feature of the project is the spectral combination of measurements from various observation techniques such as terrestrial and satellite gravimetry by means of a multi-resolution representation (MRR). A MRR means a decomposition of a target signal $F \approx F_{J+1}$, e.g. the gravitational potential, into a number of detail signals according to Eq. (1) of Fig. 2.1. Following Eq. (2) of the same figure, each detail signal G_j with $j = j', \ldots, J$ is expanded in a series in terms of level$-j$ wavelet functions $\psi_{j,k}$ covering a specified spectral band. Since the summation limits N_j and N_{j-1} in Eq. (2) are subject to the inequality condition $N_j > N_{j-1}$, the whole set of series coefficients $d_{j,k}$ for $j = j', \ldots, J$ form an upside-down pyramid as symbolized in Fig. 2.1 by the gray-coloured triangle. In other words, the detail signal G_J of the highest level J describes the finest structures of the target function and needs the largest number of coefficients $d_{J,k}$. Figure 2.1 shows schematically the setup of the developed procedure: the detail signals G_j depending on the resolution level j are estimated from appropriate observation techniques sensitive to the frequency band defined by the wavelet functions $\psi_{j,k}$. The sum of the estimated detail signals and a low-pass filtered version $F_{j'}$ of the target function establishes the MRR; for more details see, e.g., Lieb et al. (2014).

Figure 2.2 shows exemplarily the selection of different observation techniques for the estimation of the detail signals. Different criteria have been chosen, namely (1) the sensitivity of the measurement system, (2) the level of correlation between the observation techniques, and (3) the spatial distribution of the observation sites. If the latter are spatially not dense enough, prior information might be added if it allows for the necessary spectral resolution. Since we use the Shannon kernel for the estimation of the series coefficients $d_{j,k}$ in Eq. (2), the detail signals G_j and G_{j-1} are uncorrelated as far as different input

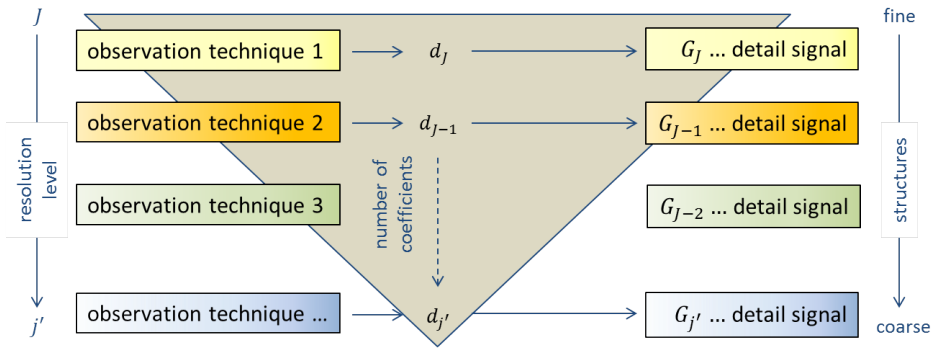

$$F_{J+1} = F_{j'} + \sum_{j=j'}^{J} G_j \qquad (1) \qquad\qquad G_j = \sum_{k=1}^{N_j} d_{j,k}\, \psi_{j,k} \qquad (2)$$

Fig. 2.1: *Scheme of the developed procedure: the detail signals G_j with $j = j', \ldots, J$ are estimated from measurements of appropriate observation techniques which are assumed to be uncorrelated; the Shannon function is used for setting up the wavelet functions $\psi_{j,k}$. The sum of the detail signals and a low-pass filtered version $F_{j'}$ represents the final estimation of the target function F.*

Observation	j = 8 (L = 255)	j = 9 (L = 511)	j = 10 (L = 1023)	j = 11 (L = 2047)
GOCE V_{xx}	1			
GOCE V_{xy}	10^{-4}			
GOCE V_{xz}	10^{-1}			
GOCE V_{yy}	1			
GOCE V_{yz}	10^{-4}			
GOCE V_{zz}	1			
ERS-1e		1	10^{-2}	10^{-3}
ERS-1f		1	10^{-2}	10^{-3}
Jason-1 GM		1	10^{-1}	10^{-3}
Envisat EM		1	10^{-1}	10^{-3}
Cryosat RADS		1	10^{-2}	10^{-3}
Airb. North Sea			1	1
Airb. Baltic Sea			10^{-1}	10^{-2}
Terrestrial Data			1	1
Sea ground				10^{-1}
a priori Information GOCO03s d/o 127	10^{-3}	10^{-4}	10^{-4}	10^{-5}

criteria
- high sensitivity
- level of correlation
- spatial distribution (prior information not dense enough)

Computation of the detail signals from different data sets by means of parameter estimation

Fig. 2.2: *Choice of appropriate observation techniques: since, for instance, the gravity gradients measured by GOCE are sensitive up to degree 250, they are used to estimate the coefficients $d_{8,k}$ of the detail signal G_8. Since the quality of the 6 GOCE gradients differs, the applied variance component estimation provides different weighting factors for the gradients. As can be seen the gradients V_{xy} and V_{yz} are down-weighted by a factor of 10^{-4}. Similar explanations hold for the other data sets shown in the table.*

data are chosen. An overview about the sensitivity and the corresponding spatial resolution of different observation techniques was provided in Fig. 2.3 of DGFI's Annual Report 2013. The GOCE gravity gradients, for instance, cover a spectral band up to degree 250 at most, i.e. this data can be used to estimate the detail signal G_8. In a similar way the input data sets for the higher levels $9, 10$ and 11 have been chosen. The procedure as well as the results of this MRR combination have been presented at the AGU 2014 Fall Meeting in San Francisco. All computation steps of the software application can be executed via a graphical user interface.

Deflections of the vertical for regional gravity field modelling

In the context of the project UHR-GravDat, regional gravity field modelling by means of local base functions has been realized for several types of observations like gravity anomalies, altimeter data, and gravity gradients. Deflections of the Vertical (DoV) were not yet considered. If, however, terrestrial gravity data is sparse it may be helpful to introduce DoV as a priori information. For example, synthetic Earth models taking into account the Earth topography and models of the Earth's crust may be used. In order to account for uncertainties in density and crustal thickness the synthetic Earth models should not be used in an absolute sense but relative only by the DoV as they represent the derivatives of the gravitational potential. This justifies to consider DoV as an additional observation type.

Let a residual disturbing potential δT

$$\delta T(\mathbf{p}) = \sum_{k=1}^{K} c_k B(\mathbf{p}, \mathbf{q}_k) \tag{2.1}$$

be represented by local base functions $B(\mathbf{p}, \mathbf{q}_k)$ with

$$B(\mathbf{p}, \mathbf{q}_k) = \sum_{n=0}^{N} \frac{2n+1}{4\pi} \left(\frac{R}{r}\right)^{n+1} B_n P_n(\cos\psi) \tag{2.2}$$

where ψ is the spherical distance between the computation point $\mathbf{p}$ and a support point $\mathbf{q_k}$. The residual DoV are defined by

$$\left\{ \begin{array}{c} \delta\xi \\ \delta\eta \end{array} \right\} = \frac{1}{\gamma R} \left\{ \begin{array}{c} \dfrac{\partial}{\partial\theta} \\ -\dfrac{1}{\sin\theta}\dfrac{\partial}{\partial\lambda} \end{array} \right\} \delta T \tag{2.3}$$

with co-latitude θ and longitude λ. By applying the chain rule and re-ordering the terms the following expression is obtained

$$\left\{ \begin{array}{c} \delta\xi \\ \delta\eta \end{array} \right\} = \frac{1}{\gamma R} \sum_k c_k \left\{ \begin{array}{c} \dfrac{\partial\cos\psi}{\partial\theta} \\ -\dfrac{1}{\sin\theta}\dfrac{\partial\cos\psi}{\partial\lambda} \end{array} \right\} \sum_n \frac{2n+1}{4\pi} \left(\frac{R}{r}\right)^{n+1} B_n \frac{\partial P_n(\cos\psi)}{\partial\cos\psi} \,. \tag{2.4}$$

Based on these relationships a software module has been developed to treat residual DoV as observations and to accumulate the corresponding normal equations such that they can be combined with normals set up for other types of observations. In order to validate the module the high-resolution gravity field EGM2008 was used up to degree 2190 to simulate DoV observations within a small study area around Crete in the Eastern Mediterranean. This area is known to have rather large variations in the gravity potential. Using the smooth satellite-only gravity model GOCO03S up to degree 180 as reference field, the EGM2008 potential was recovered by means of the simulated DoV. Figure 2.3 illustrates the result of these computations. The estimated potential (top right) shows a similar pattern as the residual potential (bottom right), but is smoother due to the coarse spacing of the local base functions.

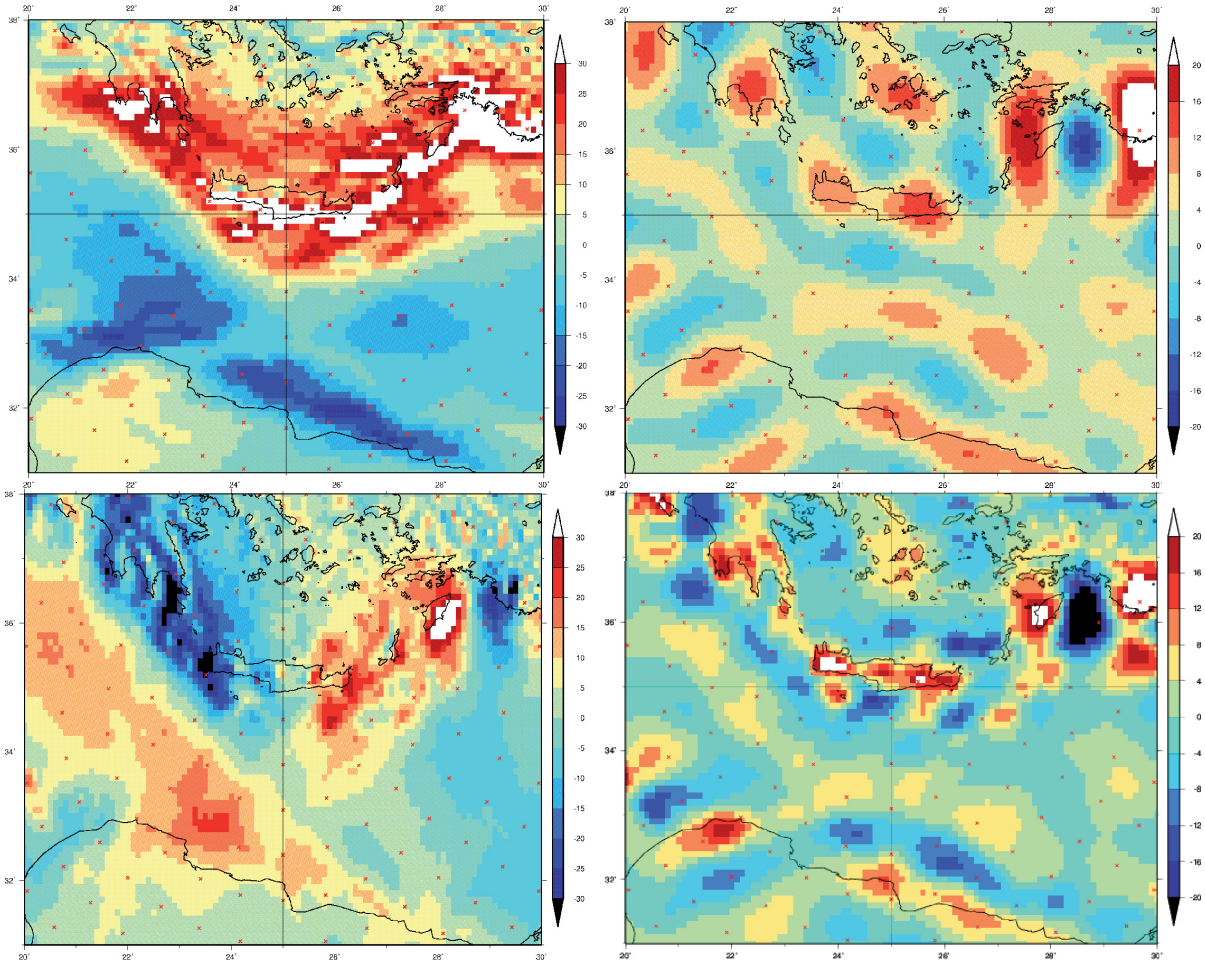

Fig. 2.3: Local gravity modeling with deflections of the vertical (DoV). Left: simulated DoV from EGM2008 with ξ ["] on top and η ["] on the bottom. Top right: residual potential δT $[m^2/s^2]$ estimated with local base functions at the positions of the red dots. Bottom right: The potential difference EGM2008 minus GOCO03S.

GOCE gravity gradients for application in geosciences

ESA's satellite gravity mission GOCE delivered scientific data from November 2009 until November 2013. Four gravity gradients have high accuracy especially at medium to shorter wavelengths. In the context of the GOCE+ GeoExplore project, we enhanced the GOCE gravity gradients combining them for long wavelengths with the GRACE-based global gravity field model GOCO03s. Enhanced gravity gradients were then used for regional gravity field determination. Tesseroid densities were estimated in overlapping regions of $15^\circ \times 15^\circ$ where GOCE data are available. The tesseroid solution was then used to generate gravity gradient grids at GOCE satellite altitude with the idea that these grids are more straightforward to use in geoscientific applications. Figure 2.4 shows the vertical gravity gradient signal at 225 km that was computed from the GOCE data in lower orbit phase towards the end of the mission using the tesseroid approach. Also shown are the differences with respect to GOCO03s, which are related to topography and bathymetry. As no global regularization is applied for our regional grids, the tesseroids are able to extract more gradient signal at satellite altitude. More information is available at http://goce4interior.dgfi.tum.de.

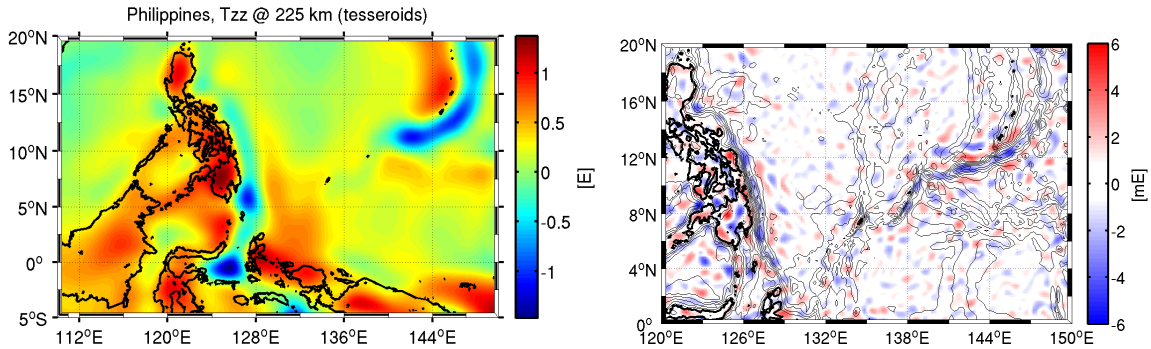

Fig. 2.4: Vertical gravity gradient signal at 225 km above the Earth (left) and differences with respect to GOCO03s (right).

2.2 Time-variable gravity field

Antarctic ice mass loss uncertainty induced by C_{20}

An accurate determination of the time-varying gravitational field of the Earth is a fundamental prerequisite for reliable geophysical interpretations. Within the Stokes coefficients, especially C_{20} plays an important role since it is about three orders of magnitude larger than other Stokes coefficients and describes the Earth's flattening. One example which emphasizes the importance of an accurate determination is the estimation of long-period ice mass loss in the Antarctic region. This region is highly influenced by the value of C_{20} due to its geographical location at the polar cap. For current estimates of the Antarctic ice mass loss, monthly gravitational fields based on GRACE data are used. Therein, the C_{20} coefficients of GRACE are replaced by SLR-derived coefficients since SLR is able to determine a more accurate estimate than GRACE. In Bloßfeld et al. (2015), two ice mass loss estimates are compared using a monthly time series of C_{20} coefficients of the Center for Space Research (CSR) and of DGFI. The top panel of Figure 2.5 shows the total Antarctic ice mass change between 2003.0 and 2013.0 using GRACE and the two C_{20} time series. Additionally, the two different C_{20}-induced ice mass changes are shown. In the bottom panel of Figure 2.5, on the left and in the middle, the trend estimates for various time intervals and a minimum/maximum time span of four/ten years are shown. For the trend estimates starting from 2003.0, the CSR solutions show larger trends than the DGFI solutions. The other trend estimates (time intervals longer than six years or starting after 2006.0) agree very well. On the right of the bottom panel, the difference of the trend estimates derived from GRACE fields between the CSR and the DGFI C_{20} time series is illustrated. It can be clearly seen that the long-term trend estimate between 2003.0 and 2013.0 differs by about 13% (12.3 Gt/yr). This difference is solely caused by different C_{20} values applied for the computation. This result emphasizes clearly that the uncertainty of C_{20} must be included when quantifying and interpreting the Antarctic ice mass loss.

Antarctic ice mass balance from a combination of GRACE and GOCE

The dramatic ice mass loss in West Antarctica, in particular in the Amundsen Sea sector, is visible in the GRACE monthly gravity field solutions. Although GOCE was not meant and not expected to sense related changes, it turns out that it does (Bouman et al., 2014). We combined existing GRACE monthly solutions with GOCE gravity gradients for the period 2009–2012. For this time period, we estimated equivalent water height (EWH) trends using 4-monthly gravity field solutions. Figure 2.6 displays these trends after applying a Gaussian filter of 250 km (typical for GRACE, left panel) and 90 km (right panel), where the maximum spherical harmonic degree is L = 90 and L = 110, respectively. The most negative EWH trends are roughly related to the Pine Island glacier (eastern minimum) and the Smith/Haynes/Kohler glaciers (western minimum). The solution may contain systematic errors, but it seems to be possible to separate different basins studying the GOCE data.

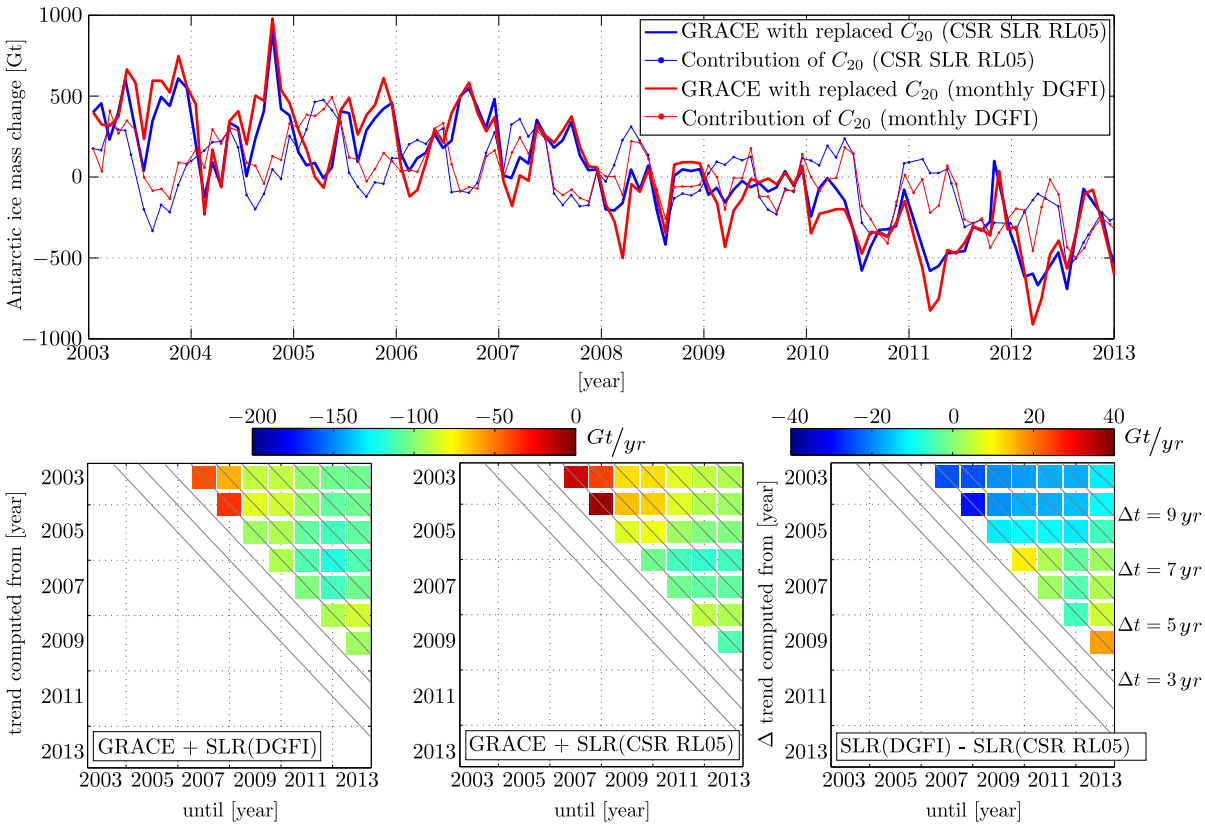

Fig. 2.5: *The top panel shows the Antarctic ice mass changes computed from the CSR SLR RL05 and the monthly DGFI C_{20} estimates between 2003.0 and 2013.0. The left and middle bottom panels show the linear trends derived from the CSR SLR RL05 and the DGFI solution computed for various time intervals between 2003.0 and 2013.0. In addition, on the right of the bottom panel, the trend differences between both solutions are shown for different time intervals.*

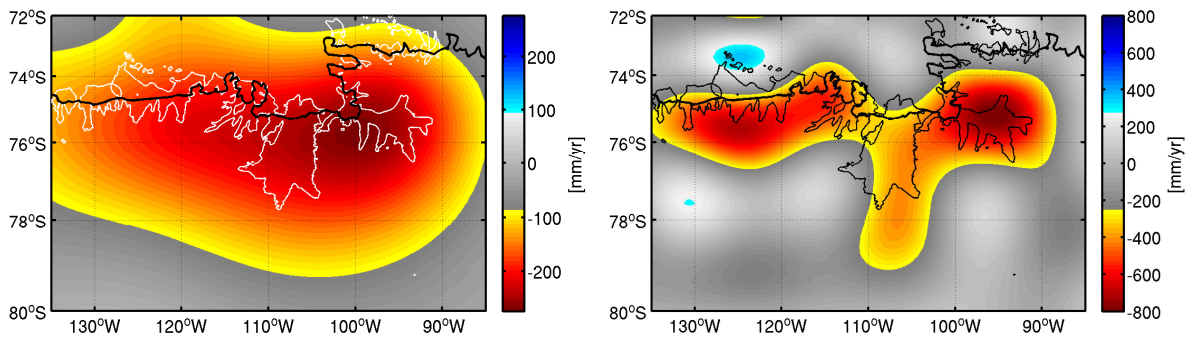

Fig. 2.6: *Equivalent water height trend in the Amundsen Sea sector for 2009–2012 from a combination of GRACE and GOCE. The left panel shows the EWH trend for a Gaussian filter of 250 km and L = 90, the right panel for 90 km and L = 110.*

We extended the study area to cover the whole of Antarctica. Here, the gap in the GOCE data around the poles has to be considered, which is caused by the orbit inclination of 83°. To avoid edge effects, we filled up the gap in the grid of combined GRACE-GOCE T_{zz} values with T_{zz} values calculated from existing monthly GRACE gravity fields. Then, four monthly solutions were merged to one 4-month solution covering the same time period as the corresponding GRACE-GOCE 4-month solution. Based on the T_{zz} values we estimated Stokes coefficients and transformed the resulting coefficients to EWH, replacing C_{20} with SLR values (see above). Before calculating ice mass balances, the EWH values have to be corrected for glacial isostatic adjustment effects and for degree L = 1. The EWH values are transformed to ice mass, and the trend is then calculated from all 4-month solutions. For smoothing, a Gaussian filter with a radius of 90 km and 250 km was applied. The GRACE models to fill the polar gap are CSR's

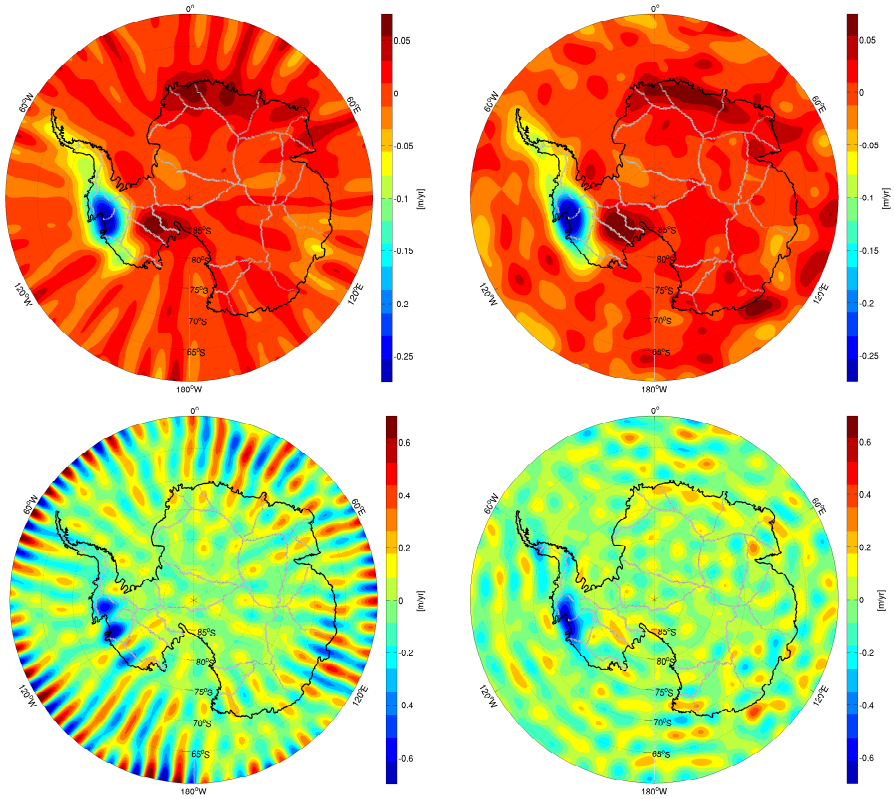

Fig. 2.7: Ice mass trend in Gt between November 2010 and September 2013. Left column: GRACE-only, right column: GRACE + GOCE. The coast line is shown in black, basin borders in grey. The top panels are filtered with a Gaussian filter with a radius of 250 km, the bottom ones with a 90 km filter.

monthly solutions. The enormous ice mass loss in West Antarctica is clearly visible in both data sets, but the combined one shows less stripes (see Fig. 2.7). The 250 km filter reduces the noise compared to the 90 km filter, but also the signal.

For each basin, we calculated total ice mass balances by summation over the basin area. The basins show different behaviour depending on the region in Antarctica: ice mass loss occurs mainly in the west and at the peninsula, whereas ice mass gain can be detected for East Antarctica. For some basins, seasonal effects are visible. Finally, we compared the GRACE-GOCE results with monthly GRACE-only results from GFZ and CSR and with a solution from CryoSat-2 data of the same time period (McMillan et al., 2014[1]). This is done for each basin, but also for three larger regions, the East Antarctic ice shield, the West Antarctic ice shield and the Antarctic Peninsula. For all three regions, the gravimetry missions show a good agreement, but the GRACE-GOCE combined solution and the CSR GRACE solution agree better. This is due to the fact that CSR was used for the GRACE-GOCE combination and the polar gap. For West Antarctica an the Peninsula CryoSat-2 shows the same negative but smaller ice mass trends, for East Antarctica, CryoSat-2 sees a small ice mass loss, but the gravimetry missions a large ice mass gain (see Fig. 2.8).

Post-seismic analysis following the 2011 Tohoku-Oki earthquake

The 2011 Tohoku-Oki 9.0 Mw earthquake had a devastating impact on the eastern coastal area of Japan. After the main shock in March 2011, several aftershocks took place leading to a vast deformation of the continental plate. With the dense GPS network of Japan it is possible to monitor such deformation processes over periods of seconds to years. We analyzed the post-seismic change for a period of two

[1] McMillan, M., A. Shepherd, A. Sundal, K. Briggs, A. Muir, A. Ridout, A. Hogg, and D. Wingham (2014): Increased ice losses from Antarctica detected by CryoSat-2, Geophysical Research Letters, 41(11): 3899-3905, doi:10.1002/2014GL060111.

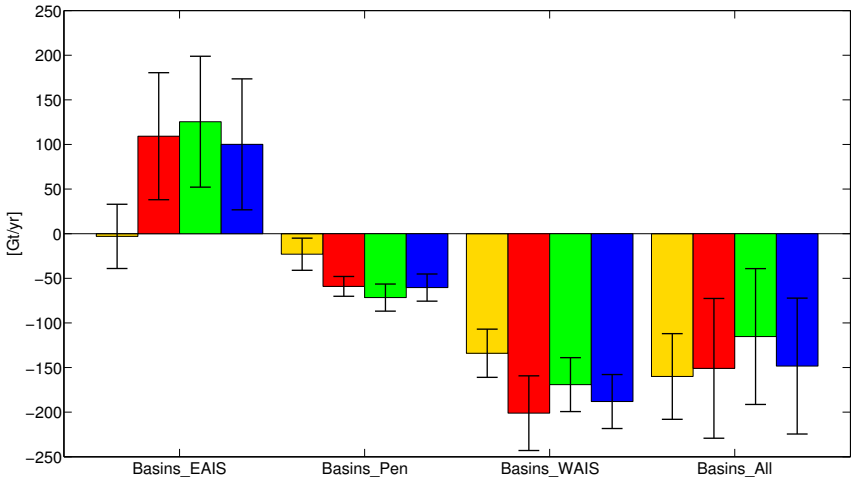

Fig. 2.8: Comparison of four different trend estimates: CryoSat-2 (yellow), GRACE-GOCE combined solution (red), GFZ GRACE-only solution (green), CSR GRACE-only solution (blue). Black bars show error estimates. Basins are concatenated to East Antarctic Ice Shield (EAIS), Antarctic Peninsula (Pen), West Antarctic Ice Shield (WAIS) and complete Antarctica.

years to evaluate the net contribution of afterslip and post-seismic relaxation. The first effect takes place instantaneously with a strong net contribution that decays within approximately half a year after earthquake occurrence. The second effect becomes measurable as soon as the afterslip decay is in the order of the net contribution caused by the viscoelastic mantle relaxation. Poroelastic effects are negligible since they should take place in the first period having a minor net contribution.

We analyzed a combination of GPS and GRACE data to reveal the afterslip caused by the 2011 Tohoku-Oki earthquake as precise as possible evaluating the short-term post-seismic trend for an interval of three months (Fuchs et al., 2014). Figure 2.9 shows the distributed slip solution. It can be stated that afterslip takes place mainly in areas not affected by the main shock of the 2011 Tohoku-Oki earthquake. Moreover, GRACE mostly is sensitive to deep dip-slip and offers an additional independent constraint for a solution merely computed from GPS data. However, the resolution of the GRACE information is limited and introduces an additional smoothing of the slip solution. The derived distributed slip solution is in agreement with Yamagiwa et al. (2015[2]) who used GPS data and sea-floor GNSS measurements to improve the resolution of the GPS GeoNet solution evaluating afterslip also for a period of two years.

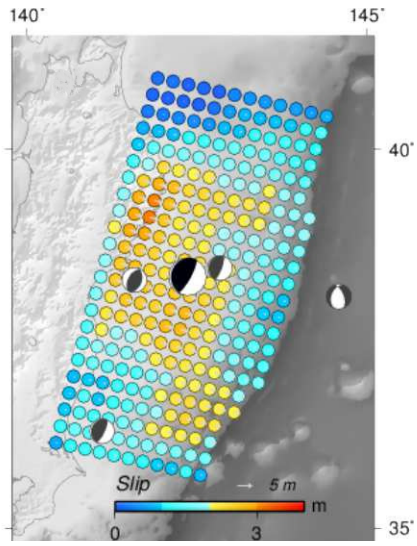

Fig. 2.9: Post-seismic change evaluated for an interval of three months (April to June 2011) using GPS and GRACE data (Fuchs et al., 2014).

Moreover, we used a post-seismic period of two years to evaluate the net contribution of viscoelastic mantle relaxation. For that purpose, we expanded the monthly GRACE gravity solutions with measurements of the GOCE mission to be most sensitive at small spatial scales. This expansion may improve the sectorial information of the long-term trend and, moreover, could improve the resolution of the GRACE-CSR series which are truncated typically at degree and order 96. Evaluating a two years period of the combined data it can be stated that the yearly trend can be estimated at GOCE mean orbit height with a formal accuracy of 0.28 mE/year (up to degree and order ≈180). Up to now no post-seismic trend could be indicated evaluating the fine-scale gravity changes. This might be due to the fact that viscoelastic mantle relaxation may map at larger scale due to the rebound properties of the elastic mantle medium. Applying a proper filter technique improves the detection capabilities optimizing the signal to noise ratio. The geophysical evaluation of the derived large-scale signals are the object of current investigations.

[2]Yamagiwa, S., S. Miyazaki, K. Hirahara, and Y. Fukahata (2015), Afterslip and viscoelastic relaxation following the 2011 Tohoku-oki earthquake (Mw9.0) inferred from inland GPS and seafloor GPS/Acoustic data, Geophys. Res. Lett., 42, 66–73, doi:10.1002/2014GL061735.

2.3 Height systems

Most of the existing vertical reference systems do not fulfil the accuracy requirements of modern geodesy. They refer to local sea surface levels, are stationary (do not consider variations in time), realize different physical height types (orthometric, normal, normal-orthometric, etc.), and their combination in a global frame presents uncertainties at the m level. To provide a precise geodetic infrastructure for monitoring the Earth system, the *Global Geodetic Observing System* (GGOS) of the *International Association of Geodesy* (IAG) promotes the standardization of the various height systems. The main purpose is to establish a global vertical reference system related to the gravity field that

- supports a highly precise (at the cm level) combination of physical and geometric heights,
- allows the unification of all existing local height datums, and
- guarantees vertical coordinates with global consistency (the same accuracy everywhere) and long-term stability (the same accuracy at any time).

DGFI supports this initiative through

- participation in the GGOS Theme 1 *Unified Height Datum*, whose main objective is to outline the basic strategy for the definition and realization of an *International Height Reference System* (IHRS),
- chairing the GGOS Working Group *Vertical Datum Standardization*, which concentrates on the establishment of a global vertical datum based on a new best estimate of the reference value W_0,
- developing strategies for the precise integration of the existing height systems into the global one proposed by GGOS.

The DGFI proposal is based on an IHRS comprising two components: a geometric component consisting of ellipsoidal heights as coordinates and a level ellipsoid as the reference surface, and a physical component consisting of geopotential numbers as coordinates and an equipotential surface defined by a conventional W_0 value as the reference surface. The definition of the physical component is based on potential parameters in order to provide reference to any type of physical heights (normal, orthometric, etc.). The conversion of geopotential numbers into metric heights and the modelling of the reference surface (geoid or quasigeoid determination) are considered as steps of the realization.

The DGFI vertical datum unification strategy is based on

- the physical connection of height datums to determine their discrepancies,
- the joint analysis of satellite altimetry data and tide gauge records to determine time variations of sea level at reference tide gauges,
- the analysis of GNSS time series at reference tide gauges to separate crustal movements from sea level changes, and
- the combination of geometrical and physical heights (referring to a common epoch) in a well-distributed and highly precise reference frame to estimate the relationship between the individual vertical levels and the global one.

The final vertical transformation parameters are provided by the common adjustment of the observation equations derived with three approaches: in the ocean areas around the reference tide gauges (ocean approach), at the reference tide gauges (coastal approach), and at the reference stations of the geocentric reference system (continental approach).

To evaluate the reliability of this proposal, the described procedure was applied to the height systems existing in South America. The input data (see Fig. 2.10) include 15 reference tide gauges, first-order levelling lines covering about 100 000 km, 90 SIRGAS reference stations, and 600 reference stations belonging to the national densifications of SIRGAS. The accuracy of the vertical datum transformation parameters (see Fig. 2.11) could be assessed to be about ± 5 cm for those countries with a good coverage of measurements (Argentina, Brazil-Imbituba, Colombia, Ecuador, Uruguay, and Venezuela). For the

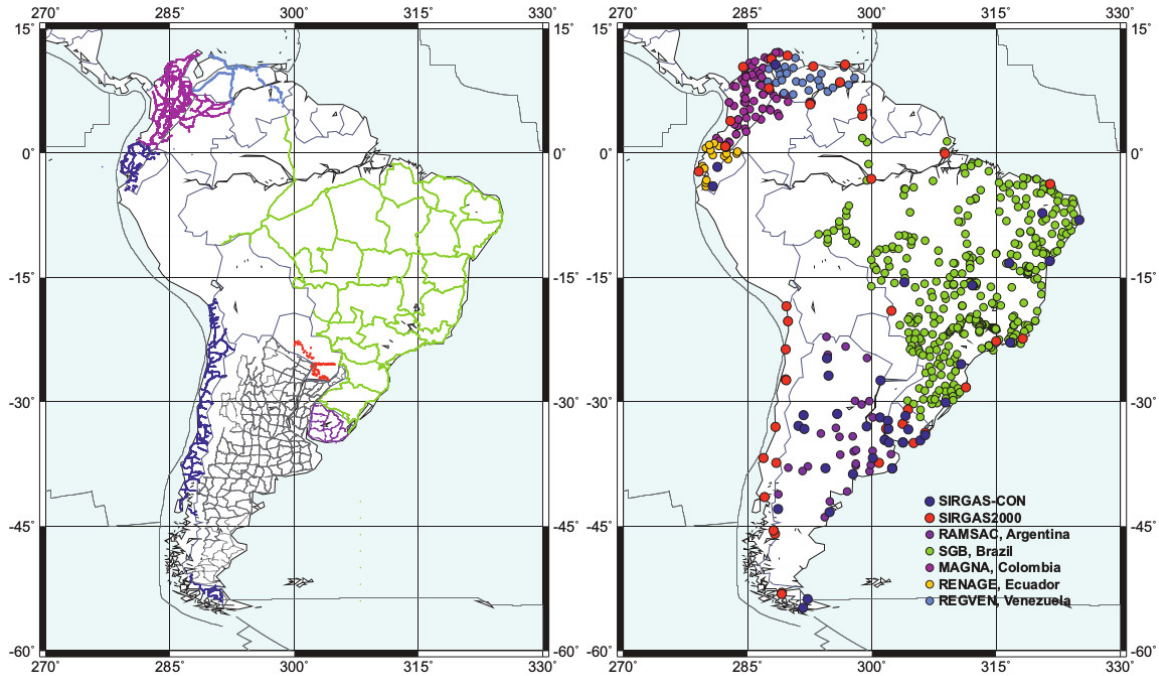

Fig. 2.10: *First-order levelling lines and SIRGAS reference stations available for the vertical datum unification in South America.*

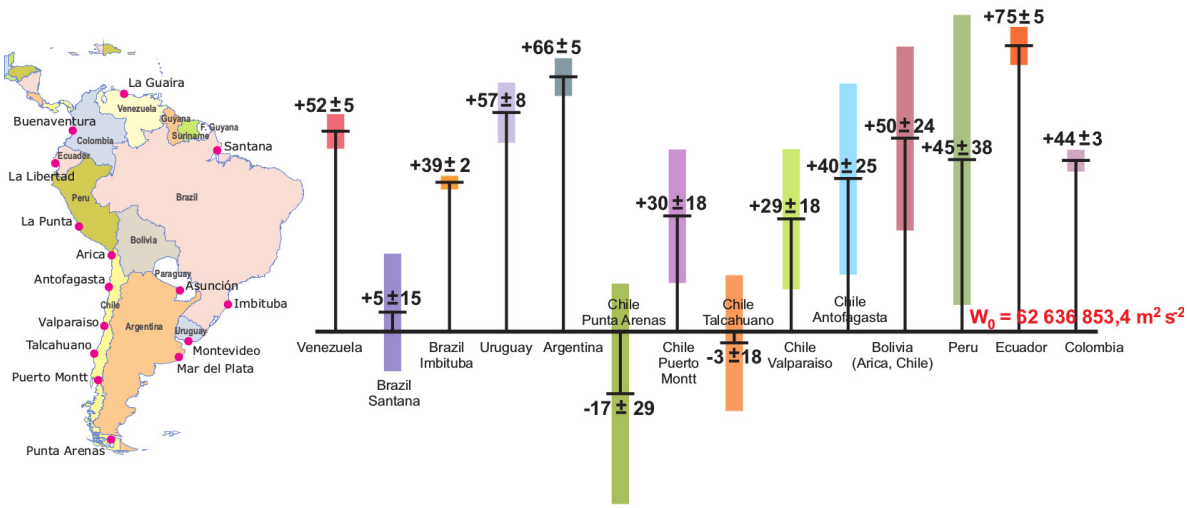

Fig. 2.11: *Vertical transformation parameters in [m] for the existing South American height systems with respect to a global vertical reference level defined by W_0 = 62 636 853.4 $m^2 s^{-2}$.*

regions with poor data coverage or high uncertainties in the data quality (Brazil-Santana, Bolivia, Peru, and Chile), the accuracy is about ±2 ... ±3 dm. The level differences are generally positive, i.e., local vertical datums are above the global reference level W_0. This and the north-south increase along the Atlantic coast as well as the south-north increase along the Pacific coast reflect the behaviour of the sea surface topography in these regions.

Related publications

Alothman A., Bouman J., Gruber T., Lieb V., Alsubaei M., Alomar A., Fuchs M., Schmidt M.: Validation of regional geoid models for Saudi Arabia using GPS/levelling data and GOCE models. In: Marti U. (Ed.) Gravity, Geoid and Height Systems (GGHS2012), IAG Symposia 141: 193-199, 10.1007/978-3-319-10837-7_25, 2014

Bloßfeld M., Müller H., Gerstl M., Štefka V., Bouman J., Göttl F.: Second degree Stokes coefficients from multi-satellite SLR. Journal of Geodesy (in review), 2015

Bouman J., Fuchs M., Ivins E., van der Wal W., Schrama E., Visser P., Horwath M.: Antarctic outlet glacier mass change resolved at basin scale from satellite gravity gradiometry. Geophysical Research Letters 41(16): 5919-5926, 10.1002/2014GL060637, 2014

Bouman J., Fuchs M., Lieb V., Bosch W., Dettmering D., Schmidt M.: GOCE gravity gradients: combination with GRACE and satellite altimetry. In: Flechtner F., Sneeuw N., Schuh W.-D. (Eds.) Observation of the System Earth from Space - CHAMP, GRACE, GOCE and future missions, Advanced Technologies in Earth Sciences, 89-94, Springer, 10.1007/978-3-642-32135-1_11, 2014

Bouman J., Fuchs M., Broerse T., Vermeersen B., Visser P., Schrama E., Schmidt M.: Modelling and observing the Mw 8.8 Chile 2010 and Mw 9.0 Japan 2011 earthquakes using GOCE. In: Rizos C., Willis P. (Eds.) Earth on the Edge: Science for a Sustainable Planet, IAG Symposia 139: 303-310, Springer, 10.1007/978-3-642-37222-3_40, 2014

Bouman J., Ebbing J., Meekes S., Fattah R.A., Fuchs M., Gradmann S., Haagmans R., Lieb V., Schmidt M., Dettmering D., Bosch W.: GOCE gravity gradient data for lithospheric modeling. Int. J. of Applied Earth Observation and Geoinformation, 35: 16-30, 10.1016/j.jag.2013.11.001, 2015

Ebbing J., Bouman J., Fuchs M., Gradmann S., Haagmans R.: Sensitivity of GOCE gravity gradients to crustal thickness and density variations: case study for the Northeast Atlantic region. In: Marti U. (Ed.) Gravity, Geoid and Height Systems (GGHS2012), IAG Symposia 141: 291-298, 10.1007/978-3-319-10837-7_37, 2014

Fuchs M., Broerse T., Hooper A., Pietrzak J., Bouman J.: GRACE gravity data to enhance the modeling of coseismic slip distribution for the Tohoku-Oki 2011 earthquake. IAG Symposia, 2015

Lieb V., Bouman J., Dettmering D., Fuchs M., Schmidt M.: Combination of GOCE gravity gradients in regional gravity field modelling using radial basis functions. IAG Symposia (accepted), 2015

Visser P.N.A.M., van der Wal W., Schrama E.J.O., van den IJssel J., Bouman J.: Assessment of observing time-variable gravity from GOCE GPS and accelerometer observations. Journal of Geodesy 88(11): 1029-1046, 10.1007/s00190-014-0741-9, 2014

3 Geodetic Earth System Modelling

The main components of the Earth system are the atmosphere (containing the neutrosphere and the ionosphere), the hydrosphere (consisting of the oceans and the continental hydrology), the geosphere, i.e. the solid Earth, the cryosphere and the biosphere. The topics of this research field aim on improving the understanding of the dynamic processes and their interactions within these components observed by geodetic measurement techniques. Due to the close connection to other geoscience disciplines, such as geophysics, meteorology, oceanography or hydrology, complementary data from other sensors are integrated into the modelling process. The combination of all data allows for a reliable estimation of the dynamic processes, which are of great importance for monitoring climate change.

In 2014, we focused on topics related to three components of the Earth system. In Section 3.1, we present first results of two new projects on global ionosphere modelling using alternative modelling approaches and combining various observation techniques including DORIS. Section 3.2 deals with several topics in the field of continental hydrology, especially studies on water level using altimetry data and spatio-temporal modelling of continental hydrological conditions. Finally, in Section 3.3, two topics on ocean modelling are presented, namely the validation of the instantaneous dynamic ocean topography and minor tides.

3.1 Ionosphere

The project "Multi-scale model of the ionosphere from the combination of modern satellite techniques" (MuSIK), funded by DFG as of January 2011 for three years, expired at the end of 2013. Final results of this project related to modelling the electron density of the ionosphere were presented by Liang et al. (2014) and Limberger et al. (2014). In 2014, two new projects abbreviated by the acronyms OPTIMAP and ADAPIO started; in context to first results they will be introduced in the following. Both projects aim at the estimation of appropriate model parameters from the combination of space geodetic measurement techniques including DORIS.

Using DORIS measurements for ionosphere modelling

The DORIS system was originally developed for precise orbit determination of low Earth orbiting (LEO) satellites. Beyond that, it is highly qualified for monitoring and modelling the distribution of electrons within the ionosphere, as it measures with two frequencies in the L-band with a relative frequency ratio close to five. The terrestrial ground beacons are homogeneously distributed, and several LEOs are equipped with DORIS receivers. Thus, a good applicability for global vertical total electron content (VTEC) modelling is expected. However, due to the orbit configuration of the LEOs the measurement distribution with local time is not as homogeneous as with geographic longitude. As a consequence, the DORIS observations should be combined with measurements from other space geodetic techniques, e.g. the Global Navigation Satellite Systems (GNSS), in order to derive reliable global models with high spatial and temporal resolution.

We investigated the capability of DORIS dual-frequency phase observations from DORIS RINEX files of four missions (Jason-2, Cryosat-2, HY-2A, and Saral) to derive VTEC and the contribution of these data to global VTEC modelling. The DORIS pre-processing is performed similarly to the commonly used GNSS pre-processing. However, since the DORIS data contain no absolute information, the absolute DORIS VTEC level is taken from Global Ionospheric Maps (GIM) provided by the International GNSS Service (IGS). DORIS-derived VTEC values are in good agreement with IGS GIMs with an RMS value between 2 and 3 total electron content units (TECU) depending on the solar activity which can be reduced

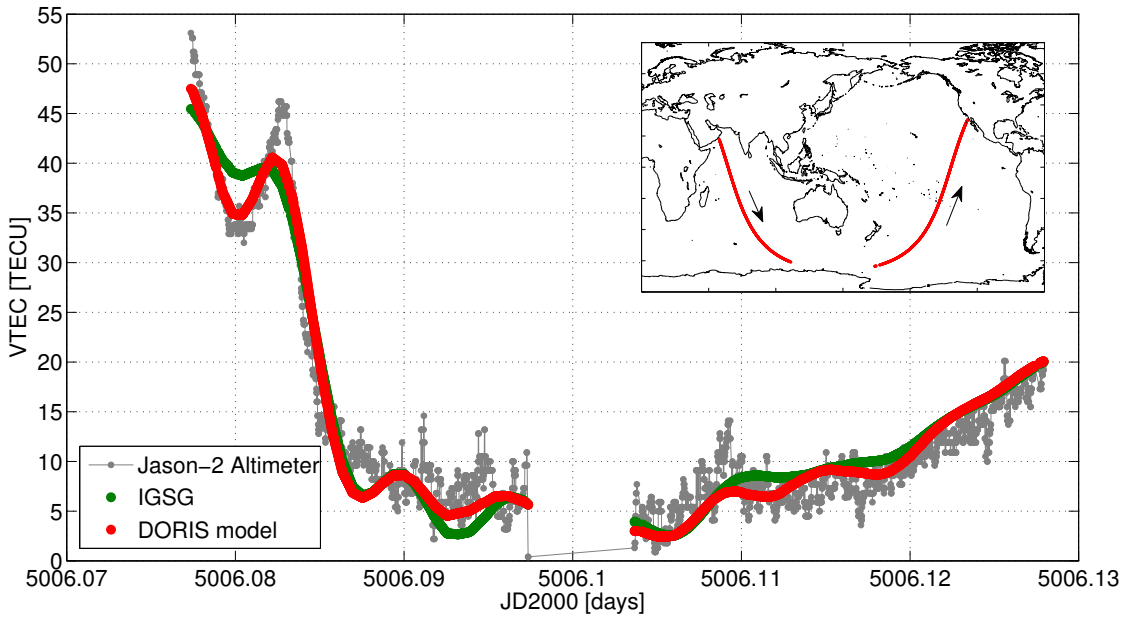

Fig. 3.1: *VTEC in TECU on two Jason-2 altimeter passes on September 15, 2013 from three different data sources: altimeter data is plotted in gray, IGS GIM in green and DORIS-based model in red (from Dettmering et al. 2014)*

to less than 2 TECU if only observations with elevation angles above 50° are used. The combination of DORIS VTEC with data from other space geodetic measurement techniques improves the accuracy of global VTEC models significantly. If DORIS VTEC data is used to update IGS GIMs, an improvement of up to 12% can be achieved for single days. The accuracy directly beneath the DORIS satellites' ground tracks ranges between 1.5 and 3.5 TECU assuming a precision of 2.5 TECU for altimeter-derived VTEC values which were used for validation purposes. Figure 3.1 illustrates the improvements of DORIS (red) w.r.t. IGS GIM (green) when compared with altimetry (Jason-2, gray). More details can be found in Dettmering et al. (2014).

Operational Tool for Ionospheric Mapping and Prediction (OPTIMAP)

The project OPTIMAP aims at the computation and prediction of VTEC maps from various space geodetic observation techniques; it is funded by the Bundeswehr Geoinformation Centre (BGIC), located in Euskirchen. Project partners are the German Space Situational Awareness Centre (GSSAC) in Uedem and the Institute of Astrophysics (IAG) at the University of Göttingen. Key part of OPTIMAP is the deployment of an operational service for the provision of ionospheric information. Therefore, a software application has to be developed that allows to model VTEC as well as the electron density (ED) distribution on a global scale.

Observation-driven ionosphere models significantly benefit from the large amount of measurements that become available through the increasing number of space missions improving the spatial and temporal data distribution. The temporal distribution refers to the sampling of measurements but also to the latency, i.e. the time gap between the measurement and the provision of the data through online data servers. The latter aspect plays a key role in the challenge of running operational monitoring services to model ionospheric key quantities such as VTEC or ED in space and time as a sequential process.

Therefore, the combination of different satellite observation techniques is considered for sounding the ionosphere with different geometries and sensitivities. In a first step, a preprocessor performs a batch processing of raw observations to extract ionospheric information to be saved in a local data base. Currently, GPS and GLONASS measurements, provided as hourly RINEX batch files from terrestrial IGS tracking stations, are processed. The steps include the calculation of the geometry-free linear combina-

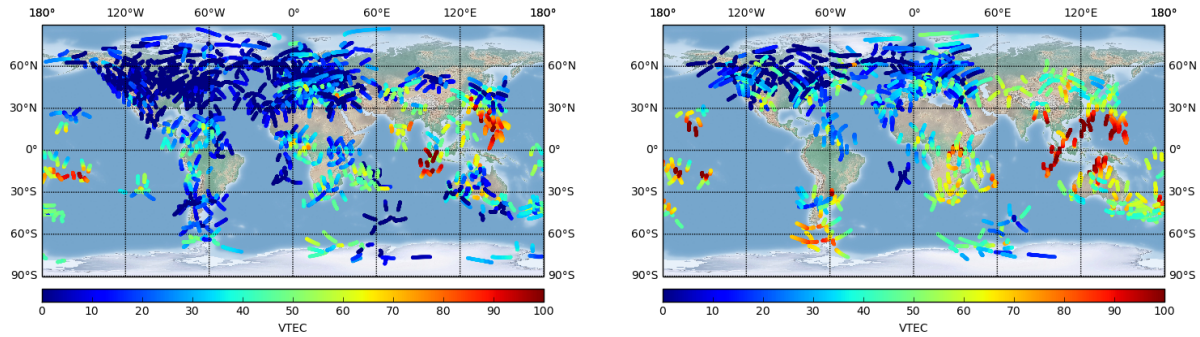

Fig. 3.2: Ionospheric pierce points between 06:00 UT and 07:00 UT on January 16, 2015 for GPS (left) and GLONASS (right). The VTEC is indicated by coloured patches.

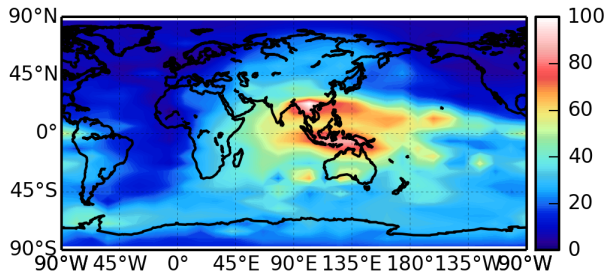

Fig. 3.3: Global VTEC distribution for 6:00 UT on January 16, 2015 as modelled from GPS and GLONASS data by means of the OPTIMAP Kalman filter approach. The parameterization is based on level 5 for the PBS in latitude and level 3 for the TBS in longitude direction.

tion, phase levelling and mapping of TEC from slant into the vertical direction under consideration of a single-layer mapping function. The distribution of ionospheric pierce points, i.e. the intersection of the line of sight from the satellite to the receiver with the single layer is depicted in Fig. 3.2 for GPS (left) and GLONASS (right) for the time between 06:00 UT and 07:00 UT on January 16, 2015. Coloured circular patches indicate the measured VTEC values that are affected by the so- called differential code biases (DCBs). In particular, in the southern regions of Africa and South America, strong VTEC differences between GPS and GLONASS can be observed due to these biases. However, the equatorial anomaly along the geomagnetic equator becomes clearly visible in the region of Indonesia with a local time (LT) of 14:00 LT to 15:00 LT (Central Indonesia: UT + 8 h). The implementation of additional observation techniques such as DORIS, radar altimetry and ionospheric radio occultations is already in progress.

The VTEC observations are forwarded to a Kalman filter that sequentially processes the data according to the sampling of the observation epochs, e.g., 30 s in case of GNSS. The global representation of the data is realized by localizing B-splines where polynomial B-splines (PBS) and trigonometric B-splines (TBS) are considered for the parameterization w.r.t. latitute and longitude, respectively; for details see Schmidt et al. (2014). VTEC parameters as well as DCBs for satellites and receivers are estimated by the Kalman filter approach. The ionospheric state of VTEC is provided in Fig. 3.3 in terms of Sun-fixed coordinates, exemplarily as a snapshot at 06:00 UT on January 16, 2005.

Development of a novel adaptive model to represent global ionosphere information from combining space geodetic measurement systems (ADAPIO)

The ADAPIO project, funded by the German Aerospace Centre (DLR), focuses on data adaptive techniques which can be utilized in a near real-time (NRT) processing framework to resolve the problem of inhomogeneous data distribution for global ionospheric representations. In this context, Multivariate Adaptive Regression B-Splines (BMARS) were used to assimilate ionospheric observations within

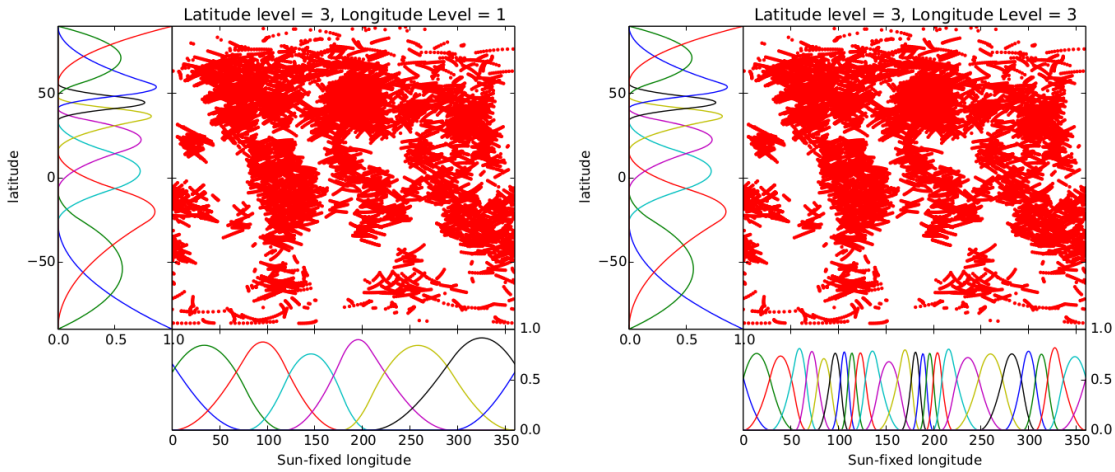

Fig. 3.4: Adaptive basis formation with PBS (latitude) and TBS (longitude); left: PBS basis with adaptive knots over latitude at level 3 and TBS basis with adaptive knots over longitude at level 1; right: PBS basis with adaptive knots over latitude at level 3 and TBS basis with adaptive knots over longitude at level 3.

a convenient filtering method (e.g., least-squares (LS) or (unscented) Kalman filter (KF)) using proper regularization methods in order to provide improved global VTEC maps in NRT.

As mentioned before, VTEC can be estimated from different space geodetic measurement techniques. Dual-frequency observations from GNSS provide increased spatial and temporal resolution. Since the spatial distribution of GNSS observations is not homogeneous (cf. Fig. 3.2), the inclusion of other observation techniques such as satellite altimetry, radio occultations, or DORIS improves the spatial distribution of global ionospheric observations. Nevertheless, the problem of an inhomogeneous data distribution and data gaps still persists.

BMARS is a non-parametric modelling method. The basis functions of classical BMARS are compactly supported PBS with adaptive knot placements depending on the data distribution. Algorithms in BMARS were altered to use both PBS and TBS to achieve a global approach. The basis formation with adaptive knot placement using real GPS data is shown in Fig. 3.4 for different levels.

A data assimilation method carried out in this project is currently based on GPS and GLONASS observations. The adaptive B-spline coefficients (each pair of TBS and PBS in Fig. 3.4 defines one coefficient), receiver and satellite DCBs as well as altimeter biases are the elements of the unknown state vector. Its estimation is based on a combined filtering approach as depicted in Fig. 3.5. It consists of two processes, namely a LS estimator and a KF. The LS part is responsible for the estimation of the unknowns; it includes prior information and regularization techniques. The main task of the KF is to provide predicted prior information feeded to the LS estimator.

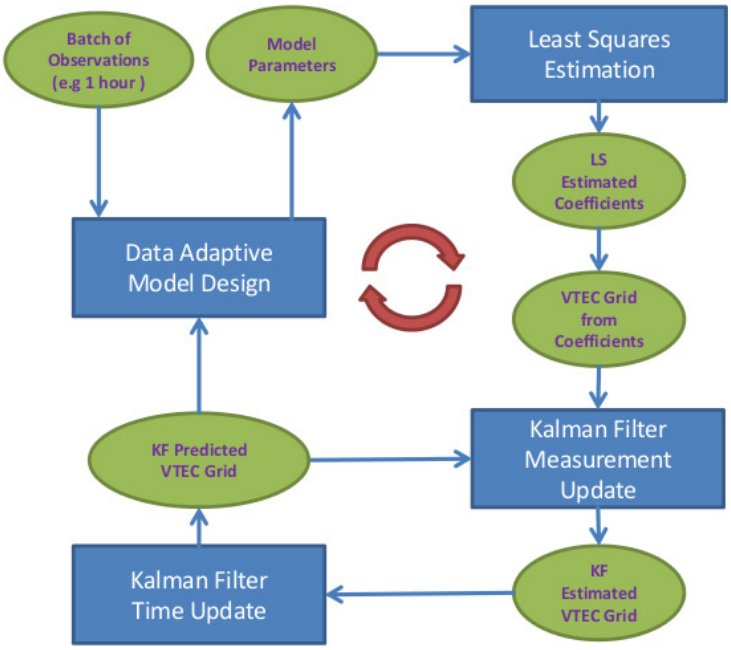

Fig. 3.5: Sequential combined filtering framework consisting of a LS estimation and a KF step.

A detailed view into the cycle of the data assimilation framework can be

taken from Fig. 3.5: The filter starts at an initial time epoch t by running the "Data Adaptive Model Design" module. Its input are the current observations collected within the time interval $[t-d, t+d]$ and an a priori model, which provides VTEC values on a regular spatial grid. Here, the knot points of the B-spline model are formed adaptively w.r.t. the spatial distribution of the available data (cf. Fig. 3.4). Next, all model parameters (including the observation vector and the design matrix) are sent to the "LS Estimation" module to estimate the B-spline coefficients and the auxiliary parameters. Then, pseudo VTEC "observations" on a predefined grid are computed using the LS results and sent to the "KF Measurement Update" module to provide updated VTEC values for the grid points. In the "KF Time Update" module, these gridded VTEC values are propagated in time using a proper temporal variation model. Later on, these predicted VTEC values are admitted as prior information and used to feed both the "Data Adaptive Model Design" module and the measurement update step of the KF at the next epoch $t+1$.

Since ionospheric inverse problems are usually ill-posed, mainly due to data gaps, a suitable regularization procedure has to be be developed within ADAPIO to stabilize the solution. The best-known regularization method is the Tikhonov regularization. Assume a linear observation equation system $\boldsymbol{Ax} = \boldsymbol{b} + \boldsymbol{e}$, where $\boldsymbol{A}$ is the design matrix, $\boldsymbol{x}$ denotes the unknown parameter vector, $\boldsymbol{b}$ is the observation vector and $\boldsymbol{e}$ the measurement error vector, the Tikhonov regularization selects the solution $\boldsymbol{x}_\lambda$ that solves the following minimization problem

$$\min\{\|\boldsymbol{Ax}-\boldsymbol{b}\|_2^2 + \lambda^2\|\boldsymbol{Lx}\|_2^2\} \tag{3.1}$$

with λ the regularization parameter, controlling the relative weight between minimizing the seminorm $\|\boldsymbol{Lx}\|_2$ of the solution and minimizing the residual norm $\|\boldsymbol{Ax}-\boldsymbol{b}\|_2$. Automatic strategies, such as L-curve, Generalized Cross Validation (GCV) and Variance Component Estimation (VCE) were investigated. To illustrate the methods, $\boldsymbol{L}$ is set to the identity matrix $\boldsymbol{I}$ in the following.

The methods were firstly applied to VTEC observations simulated from the International Reference Ionosphere. The left panel of Fig. 3.6 shows the pierce points of the observed satellite-to-receiver ray paths during a selected time period from 17:00 UT to 19:00 UT within a test area. Following DGFI's regional ionosphere modelling approach, we represent the corrections ΔVTEC, i.e. the differences between the simulated observations and a chosen background model as a series expansion in PBS w.r.t. latitude and longitude; in this example, the series consists of altogether $18 \cdot 18 = 324$ terms. The right panel of Fig. 3.6 shows the singular values of the corresponding design matrix $\boldsymbol{A}$; as can be seen, the singular values gradually decay to zero; the rank deficiency is equal to the number of non-supported coefficients within the test area.

In order to obtain a reliable solution, regularization is needed. Figure 3.7 illustrates selections of λ by L-curve (left) and GCV (right). The L-curve searches λ at the L-shaped corner which is assumed to be

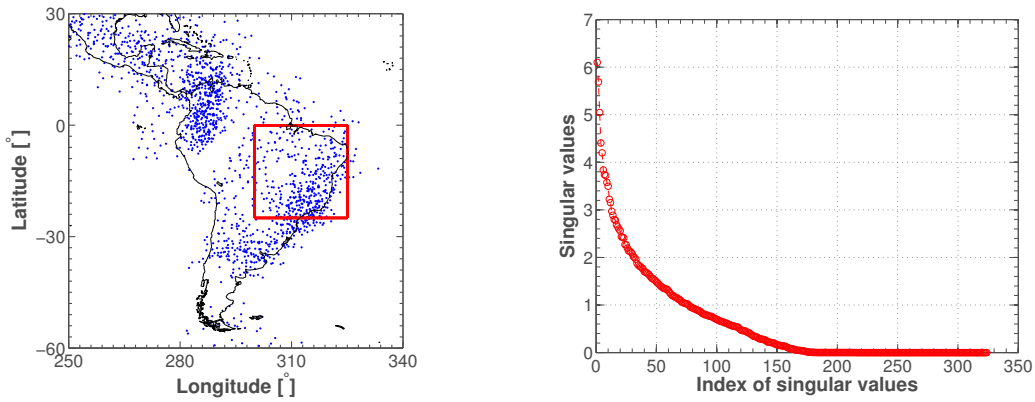

Fig. 3.6: Data distribution of the selected GPS observation sites (pierce points at a height of 400 km) for a short time interval (17:00 to 19:00 UT) of the SIRGAS network (left), and the singular values of the design matrix $\boldsymbol{A}$ *established from the observations (right).*

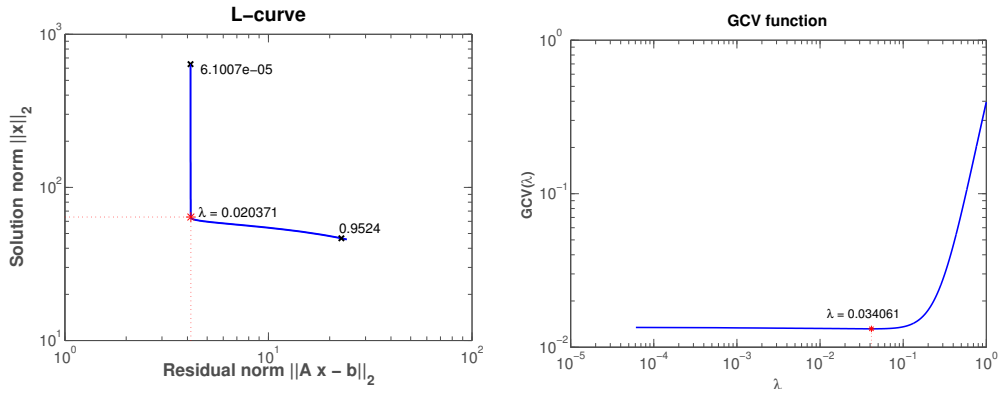

Fig. 3.7: Selections of λ by L-curve (left) and GCV (right). The chosen values are illustrated with red stars.

a good balance between the norm of the residual vector and the norm of the solution, whereas the GCV method searches for λ which minimizes the GCV function $\|\boldsymbol{A}\boldsymbol{x}_\lambda - \boldsymbol{b}\|_2^2/(T(\lambda))^2$ where the quantity $T(\lambda)$ depends on the degree of freedom, the singular values, and the regularization parameter.

The selected regularization parameters derived with the two methods mentioned before as well as from VCE and the corresponding RMS values of the differences between the estimated ΔVTEC and the simulated input data are shown in Table 3.1 for a small region (red box in the left panel of Fig. 3.6) . As can be seen, the three methods yield similar λ values and the RMS values are relatively small compared to 4.7 TECU, the mean of absolute values of the simulated ΔVTEC signal.

Table 3.1: Selected λ values from different methods and the corresponding RMS values of the differences between the estimated $\Delta VTEC$ and the simulated input data.

Method	λ	RMS [TECU]
L-curve	0.020	0.070
GCV	0.034	0.074
VCE	0.022	0.071

3.2 Continental hydrology

Database for hydrological time series of inland waters (DAHITI)

In recent years, satellite altimetry has become more and more important for continental hydrology. The fact that altimetry – originally designed for open ocean applications – can also provide reliable results over inland waters makes it a very useful tool for continental hydrology, as it helps to understand the water cycle of the Earth system.

The Database for Hydrological Time Series of Inland Waters (DAHITI) developed at DGFI provides time series for about 200 inland water targets (lakes, rivers, reservoirs and wetlands) from multi-mission satellite altimetry. DAHITI is part of DGFI's Open Altimeter Database (OpenADB) which is available at http://openadb.dgfi.tum.de. All data sets are freely available, but provided without guarantee.

The processing strategy for the estimation of water level time series is based on a Kalman filter approach. In 2014, significant improvements of the processing strategy could be achieved. First of all, the hooking effect occurring near land-water transitions of small rivers and lakes can now be corrected automatically to achieve improved water level time series for these targets (see next section). Another improvement of our methodology is the error propagation of the Kalman filter approach which enables us to provide

water level heights for each period of time with an additional formal error. Until now, the resulting errors provided information about the relative error between different water level heights of a time series. The resulting errors mainly depend on the standard deviation of each water level height along the altimeter track which are introduced as ”measurement” error for the Kalman filtering. In the near future, the determination of reliable absolute errors of water level heights will be possible.

Figure 3.8 shows two DAHITI water level time series (blue) for Lake Taupo in New Zealand (top) and the Amazon river near Manaus (bottom) based on the altimeter missions Envisat (2002-2010) and SARAL/AltiKa (since 2013). Both time series are compared with in-situ data (red). The very good agreement between the time series is demonstrated by small RMS values: 12.2 cm for Lake Taupo and 13.0 cm for the Amazon river. Furthermore, the formal errors of the water level heights are plotted as green bars. The formal errors for Lake Taupo and the Amazon river are about 2.5 cm and 4.3 m, resp. Thereby, the formal errors decreased for SARAL/AltiKa compared to Envisat.

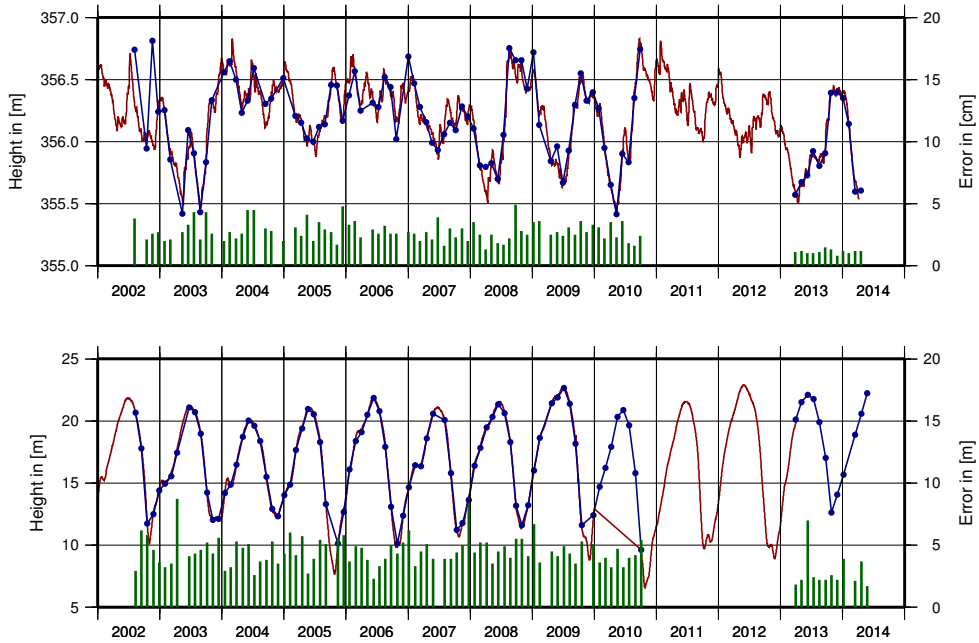

Fig. 3.8: *DAHITI water level time series (blue) for Lake Taupo (top) and the Amazon river (bottom) compared with in-situ data (red). The formal error of each water level height is plotted as green bar.*

Estimating water levels of rivers with radar altimetry by correcting the hooking effect

For many years, the numbers of in-situ gauging stations has been declining. To achieve reliable time series of inland water levels without in-situ data, satellite altimetry observations can be used. However, measuring water table elevations of medium and smaller scale rivers from space is a major challenge. It is necessary to develop methods for reliably identifying such small water bodies in the altimeter footprint of about 5 to 10 km. Without preprocessing of the data it would not be possible to retrieve reliable water level data from altimetry over rivers with a width of less than 1 km. The heights measured by the altimeter feature a parabolic shape with increasing distance to the river. This originates from the fact that the water surface reflects the radar signal much stronger than the surrounding land. Consequently, the satellite also registers reflections from water surfaces in off-nadir direction. Those slant distances are longer than the actual height of the satellite over the water surface. This effect is called hooking or off-nadir effect.

Figure 3.9 shows one altimetry pass crossing the upper Mekong River impacted by this effect. The hooking effect expands over many km away from the actual river (in blue). The vertex of the hooking parabola is identical with the water level. The parabola allows to measure the water level of a river even

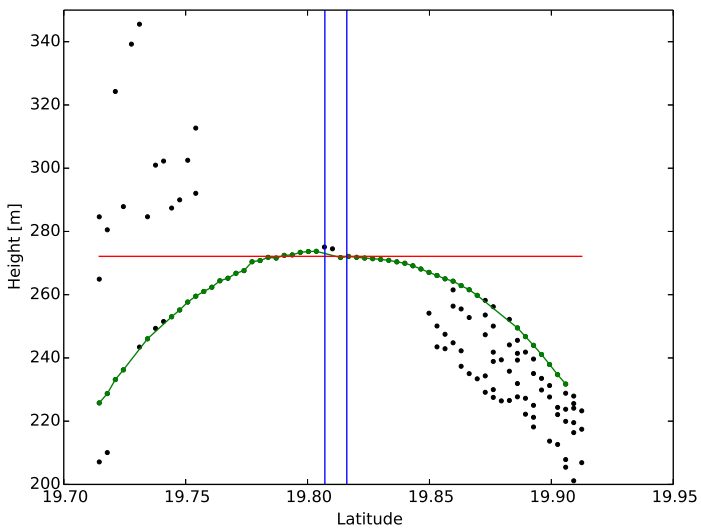

Fig. 3.9: *Hooking effect over the Mekong River. The river is located between the blue lines but the hooking parabola extends to both sides. The red line indicates the water level height estimated from the hooking parabola (green).*

if there are no altimeter measurements directly over the river. Unfortunately, not all measured heights are affected by the hooking effect. Hence, the RANSAC (random sample consensus) is used to detect the points lying on the hooking parabola. The advantage of this algorithm is that it can handle large proportions of outliers from the model (here the parabola), which is the case for our altimeter height data. Finally, the height data extracted by the RANSAC algorithm are used in a least squares adjustment to estimate the parameters of the parabola. With this method it is possible to derive water level time series over small rivers with poor data quality. It is even possible to measure the water level height if no direct measurement over the river exists, as long as parts of the hooking parabola are present.

We developed a new retracking method specially designed for the water level height estimation by fiting a hooking parabola. This retracker is based on a subwaveform retracker but does not only use the first or most prominent subwaveform but all. This leads to more than one measured height for each observation. The RANSAC algorithm is capable to extract from this bundle of heights the height belonging to the parabola. In addition to the heights, also their standard deviations are derived by the retracker. Figure 3.9 shows the resulting estimated parabola for one Envisat track over the upper Mekong River. In Figure 3.10, three exemplary time series are presented derived with the hooking correction over the lower Mekong River. The widths of the Mekong River at the sites of the time series vary between 500 m and 2 km.

This work was conducted in the WLDYN project (Assessing the spatio-temporal dynamics of water volumes in large wetlands and lakes by combining remote sensing with macro-scale hydrological modelling). The project aims at characterizing the quantities of water storage dynamics of large lakes and wetlands by combining satellite information (altimetry and remote sensing) on water level height changes and water surface extent with global scale hydrological modelling.

Altimetry-derived water level time series of Pantanal Wetland

Radar altimetry was designed to provide highly accurate measurements of sea surface heights over open oceans on a global scale. However, nowadays, satellite altimetry is also used for inland water level monitoring, mainly for lakes, reservoirs, and rivers. In 2014, we investigated the potential of altimetry to estimate water levels of inundation areas, especially in the area of the Pantanal.

The Pantanal is one of the largest wetlands worldwide. It is located in South America, mostly in Brazil with smaller extents in Bolivia and Paraguay and comprises an area of about 400 by 250 km. The region

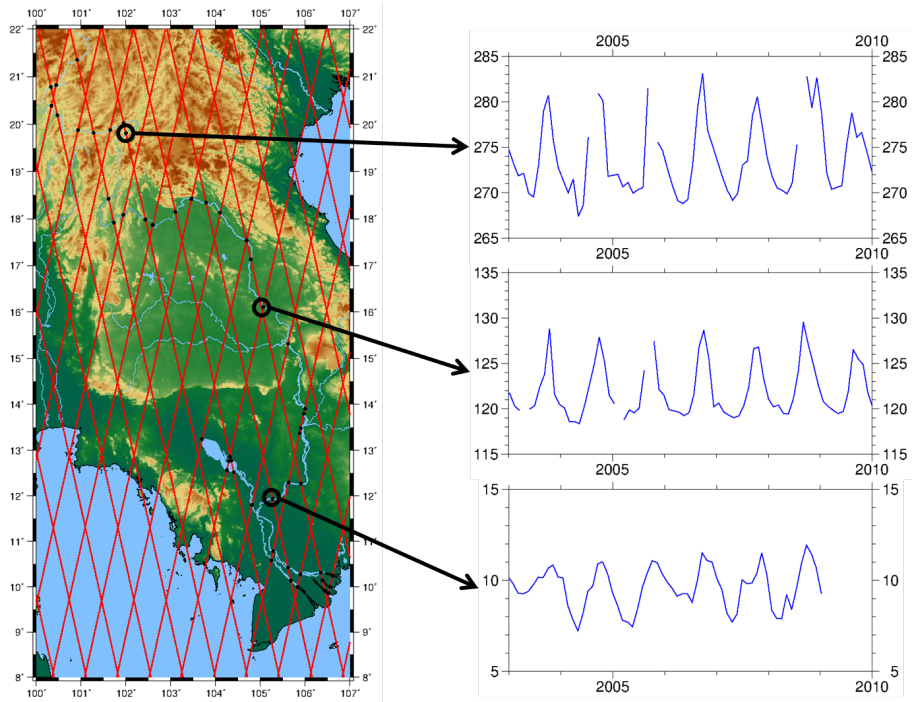

Fig. 3.10: The lower Mekong River basin with all crossings of the Envisat/Saral altimeters and three exemplary height time series.

is relatively flat with elevations between 80 and 150 m and terrain slopes of only about 25 cm/km with some isolated mountains interspersed. We divided the area of investigation into 0.1 by 0.1 degree grid cells and computed one water level time series for each grid cell. The data processing was performed by the DAHITI software and comprised waveform retracking, robust outlier detection, terrain correction (in order to account for changing land elevations within a single grid cell), and complete error propagation.

Most of the derived time series show a clear annual behaviour and the estimated formal errors clearly depend on water level. In case of low water, the errors are higher due to "land contamination" of the waveforms (see Fig. 3.11).

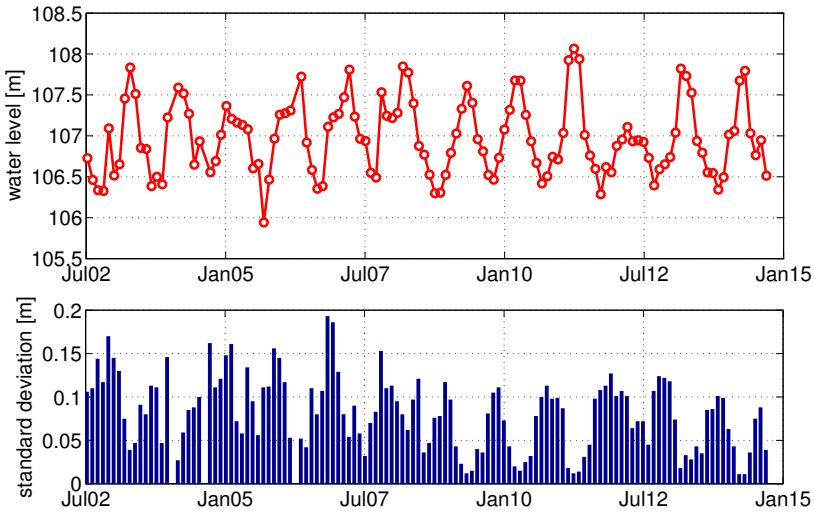

Fig. 3.11: Estimated water level from Envisat and Jason-2 for one single grid cell (with mean location 303.15°/-16.85°). The top panel illustrates the water level, the bottom panel shows the estimated formal errors.

A comparison with a nearby in-situ gauging station (Pousada Taiama at Rio Cuiaba) reveals a correlation of 88% and an RMS difference of 0.40 m (see Fig. 3.12). In addition, the altimeter data also show a good agreement with GRACE total water storage time series as well as with laser altimeter measurements of the IceSat mission.

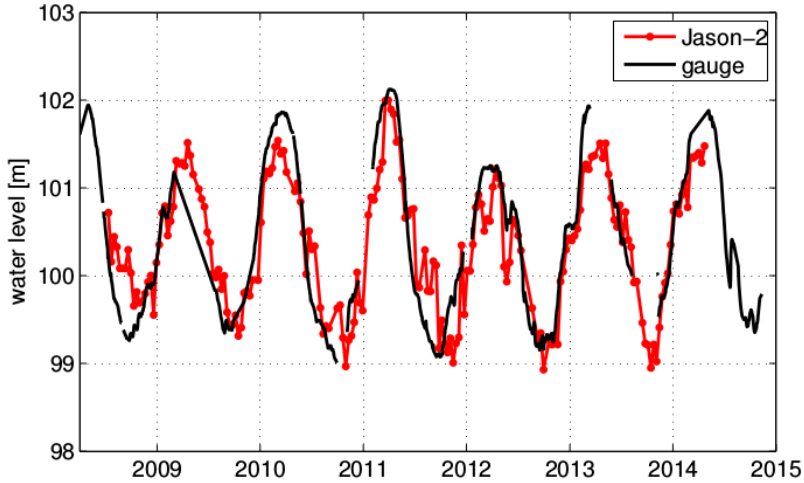

Fig. 3.12: Validation of estimated water level time series. The plot shows the estimated water level from Jason-2 (red) together with in-situ gauge data (black).

After fitting harmonic functions to the times series one can extract information on the annual behaviour of the water level, i.e. on the amplitude and the month of maximum water level. The amplitude can reach up to 1.5 m which occurs mainly in the south-west region of the Pantanal. Also the maximum flooding varies as illustrated in Fig. 3.13. The maximum level occurs between February and May, depending on the location.

Our investigations show that altimetry can be used to derive accurate and reliable water levels of wetlands with sub-meter precision. Especially for remote inundation areas, altimetry can provide unique and highly valuable information for hydrological research. When combined with water extent derived from remote sensing missions such as Landsat, important information on surface water storage can be derived.

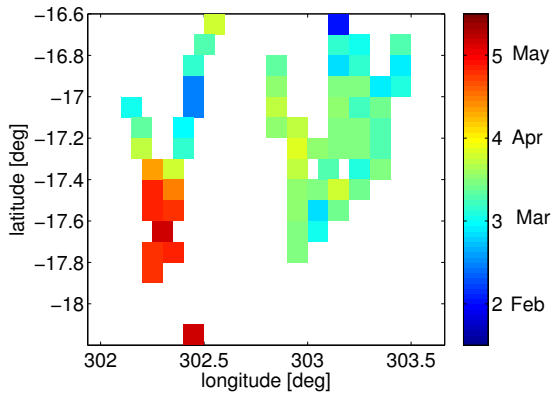

Fig. 3.13: Month of maximum water level in the Pantanal region (per grid cell).

Regional spatio-temporal modelling of continental hydrological conditions influenced by climate anomalies and weather extremes (REWAP)

The project REWAP (Monitoring and Prediction of Regional Water Availability for Agricultural Production under the Influence of Climate Anomalies and Weather Extremes) established within the focus area "Water" and funded by the TUM International Graduate School of Science and Engineering (IGSSE) is situated at the link between hydrological conditions and water availability for human consumption and agriculture. It will enhance the benefit of existing regional monitoring systems through its emphasis on understanding the connection between regional water availability and large-scale hydrological conditions as observed by global satellite systems. Of particular interest is the development and application of novel regional mathematical approaches for the analysis of data from the dedicated gravity field satellite mission GRACE (Gravity Recovery And Climate Experiment). One of the main results of the project should be refined estimates of hydrological variations from GRACE data over different spatial and temporal scales.

Gravity field observations, i.e. mass variations observed by GRACE are used in order to investigate how hydrological conditions evolved in certain regions. Traditionally, the spatio-temporal behaviour of the Earth's gravity field is modelled as a series expansion in terms of global spherical harmonics. Here, we apply a series expansion based on spherical radial basis functions for regional modelling of hydrological

variations in a test area, namely the Amazon region. For initial studies we decided to focus on areas with high signal amplitudes before investigating further regions with less significant variations. Monthly GRACE L1C data were kindly provided by our project partner C.K. Shum and his group from the Ohio State University. With the GRACE L1C data serving as input for our regional gravity modelling approach we computed time series of monthly grids of equivalent water heights (EWH) for the time interval between April 2002 and May 2014. Exemplary approximations using Blackman scaling functions of level 5 (until degree 31) show the typical seasonal mass variations of about ±30 cm EWH between January 2009 and June 2010 (Fig. 3.14).

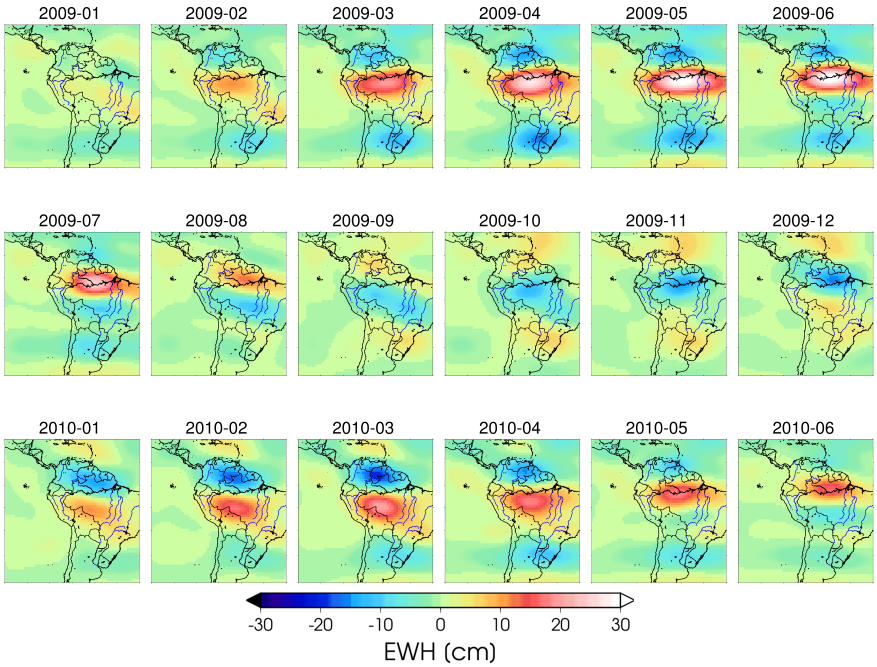

Fig. 3.14: *Spatio-temporal variations in the Amazon region using a series expansion in Blackman scaling functions of level 5.*

Additional regions of interest will be investigated in the course of this study. Special emphasis is placed on areas where, on the one hand, a transition of hydrological conditions is being observed (e.g., a degradation of groundwater level) and, on the other hand, a link between this transition and climate anomalies and weather extremes is assumed.

3.3 Ocean

Validation of iDOT profiles using ARGO floats and surface drifters

Since the Earth's gravity field has been significantly improved by satellite missions like GRACE and GOCE, it is possible to infer the Dynamic Ocean Topography (DOT) by just subtracting the satellite-based marine geoid from sea surface heights, derived from satellite altimetry. Within the last years, a dedicated approach for estimating so-called (instantaneous) iDOT profiles on individual ground tracks of altimeter satellites has been developed at DGFI. In contrast to long-term averaged mean DOT fields (MDT) computed by several other institutions, the DGFI iDOTs represent also temporal variations within the ocean topography. Thus, the iDOT profiles of the most prominent altimeter missions allow to derive gridded time series of DOT states, which represent their seasonal (monthly or even 10-day) variations. Moreover, when using the geostrophic assumption, the iDOT gradients (i.e., the derivatives of the topographic heights) can be used to estimate ocean surface currents.

Recently, first steps to validate the time-variable iDOT were performed as part of a master's thesis. We validate the product by gridding the DOT profiles, computing the associated geostrophic velocity field

Table 3.2: *Comparison between gridded velocities of iDOT and in-situ data for different study areas.*

area	mean differences u [m/s]	mean differences v [m/s]	number of measurements
area 1	0.0236 ± 0.1045	-0.0068 ± 0.1033	1574
area 2	-0.0052 ± 0.1291	-0.0013 ± 0.1084	1317
area 3	0.0439 ± 0.1216	0.0019 ± 0.1180	1472
area 4	0.0152 ± 0.1303	0.0141 ± 0.1192	1595
area 5	0.0134 ± 0.1286	0.0129 ± 0.1156	1633
area 6	0.0281 ± 0.1619	-0.0106 ± 0.1505	1457
global	0.0060 ± 0.1357	-0.0027 ± 0.1236	28322

and comparing this with gridded surface currents observed by ARGO floats and surface drifters, both corrected for wind and Ekman drift. ARGO floats and drifting buoys are independent ocean observing systems, providing, at least since 2004, a rather dense sampling for assessing the surface velocity field.

For the comparison, all data sets (in-situ, correction, and iDOT) are interpolated to the same global grid (1°x1°). As the in-situ global coverage is limited we use quarterly grids for the validation in order to have sufficient density of the in-situ data. The differences are built separately for both velocity components (u and v). All analyses are done globally as well as for six different study areas covering all strong western boundary currents (cf. Fig. 3.15). The mean differences are summarized in Tab. 3.2.

Although the gridded iDOT time series is a smoothed snapshot of the ocean topography, the differences to the in-situ data (smoothed accordingly) are rather small. On average the residual vector field exhibits velocities below ± 0.1 m/s (even at western boundary currents) with no systematic deviation in azimuth (see Fig. 3.16 for the Gulf Stream).

The comparison of a $1° \times 1°$ grid on a quarterly basis cannot cope with the potentially high temporal and spatial resolution of the multi-mission iDOT profiles. In order to avoid any unnecessary smoothing we started to perform also a pointwise comparison, where the geodetic DOT and the geostrophic velocity components are interpolated to individual observations of ARGO floats and surface drifters. This part of the study is still under investigation.

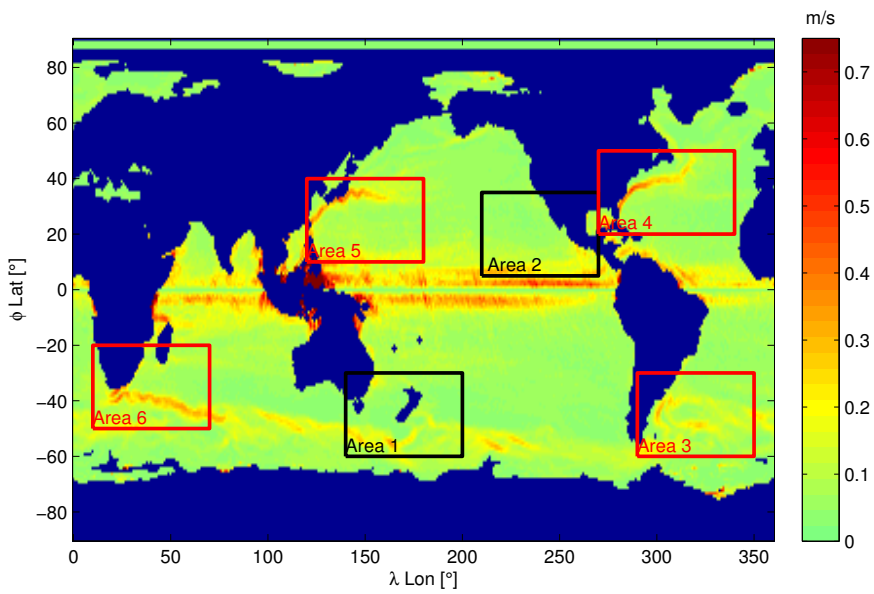

Fig. 3.15: *Study areas with different streaming conditions (red: strong currents; black: calm regions). The background colour represents the associated velocity pattern of the gridded ocean topography derived from iDOT between 2007 and 2010.*

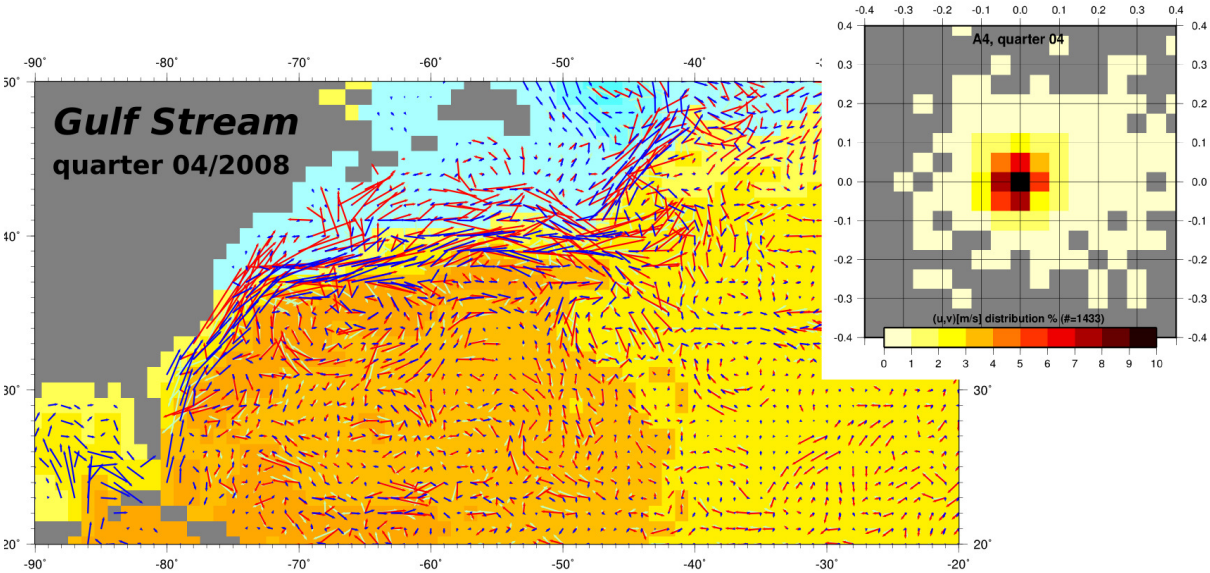

Fig. 3.16: Zoom to area 4 indicated in Fig. 3.15 (Gulf Stream) with the geostrophic velocity fields derived from iDOT profiles (blue) and the in-situ velocity vectors of ARGO floats and drifters (red). The plot shows the scenario for one particular quarter (04/2008). The background colour represents the associated pattern of the gridded ocean topography derived from IDOT profiles for the same quarter. Attached to the area plot is a scatter plot indicating the distribution of the residual vector field (in-situ minus iDOT). The percentage of vector differences for a cell size of 0.05 m/s in each component is colour-coded from light yellow (1%) to dark red (10%).

Study on minor tides

The increasing long-time series of precise altimetry by repeat pass missions (more than two decades) gradually improves the potential to empirically estimate even minor tidal constituents like J1, M1, OO1, T2, L2, $\mu 2$ and $\nu 2$. Except for FES2012, global ocean tide models such as GOT4.8, TPX0.8, or EOT11a do not provide tabulated amplitudes and phases for these minor tides. They are usually inferred by admittance theory, which assumes that their response to the gravitational attraction of Sun and Moon is a smooth function of frequency relationship to neighbouring major tides within the same tidal species (diurnal or semi-diurnal).

Unfortunately, there is no common convention to treat admittances. The IERS conventions (Petit and Luzum 2010) and the prediction software of Ray suggest linear functions, while developers of FES and EOT models apply linear admittance for diurnal and quadratic admittance for semi-diurnal tides. The difference between linear and quadratic admittances can reach several cm.

Aliasing is also critical if high-frequency tidal signals (with 12 or 24 hours period) are sampled by altimetry with repeat cycles of 10 or even 35 days. Table 3.3 shows, however, that alias periods of the minor tides are rather small and even the longest Rayleigh periods, required to separate neighbouring tides are short compared to the two decade record available from satellite altimetry.

Amplitudes of minor tides are generally small and close to the noise level of precise altimetry. To achieve an optimal signal-to-noise ratio the empirical estimates were realized by:

- least-squares analysis on the common ground tracks of CNES/NASA missions
- using the concatenated long-time series (21 years) of Topex/Jason1/Jason2
- blunder detection by a 3σ criterion for every mission
- estimating mission-specific biases and common drift terms beside the tidal constituents
- variance component estimation for an objective weighting of different mission data

As the analysis is performed with DGFI's OpenADB holdings (already de-tided by the FES2004 model) the estimates are residual tides w.r.t. FES2004. The study focuses on the question how the empirical

Table 3.3: *Alias periods (on the diagonal) and Rayleigh periods (off-diagonal, both in [days]) for some minor tides if sampled by Topex or Jason with 10 day repeat cycle. The minor tides $\mu 2$, $\nu 2$ and $T2$ are augmented by 2N2, N2 and S2, respectively, as their frequencies are close to each other.*

	J1	M1	OO1	$\mu 2$	2N2	$\nu 2$	N2	L2	T2	S2
J1	32.7	86.6	344.2	53.5	72.2	65.9	96.8	55.7	93.0	74.1
M1		23.8	115.7	139.7	434.1	37.4	45.7	156.4	44.8	39.9
OO1			29.9	63.3	91.4	55.3	75.6	66.5	73.2	61.0
$\mu 2$				20.3	205.9	29.5	34.4	1302.9	34.0	31.1
2N2					22.5	34.4	41.4	244.5	40.6	36.6
$\nu 2$						65.2	205.9	30.2	225.8	591.7
N2							49.5	35.4	2330.6	315.8
L2								20.6	34.8	31.8
T2									50.6	365.3
S2										58.7

estimates of minor tides compare to results derived by admittance theory (which is dubious in shallow water areas where non-linear tidal effects are relevant). Also a comparison with the hydrodynamic modelling of minor tides, provided by FES2012 is valuable. First controversial results were presented at the EGU2014 conference and the OSTST2014 meeting with examples for the Patagonian shelf shown in Fig. 3.17. A validation by tidal constants from tide or bottom pressure gauges is therefore an urgent issue.

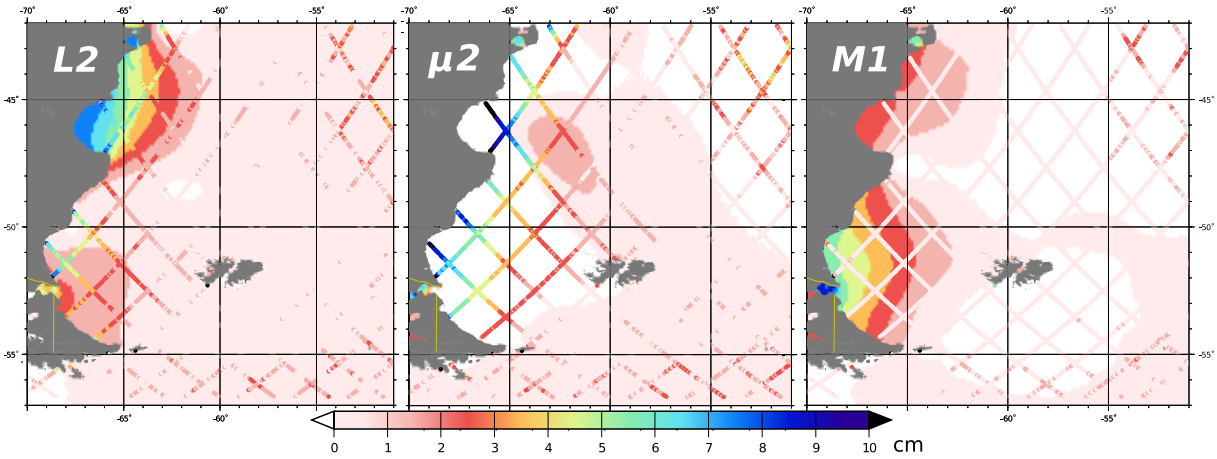

Fig. 3.17: *The colour-coded dots on Topex/Jason ground tracks are empirical amplitudes (present study) while the background colour shows FES2012 amplitudes – both relative to FES2004 amplitudes derived by admittance theory. For L2 (left), empirical estimates and FES2012 are consistent but differ from admittance. The empirical $\mu 2$ estimates (middle) differ significantly from FES2012 (coinciding with FES2004 admittance). The empirical amplitudes of M1 (right) are negligible, but FES2012 differs significantly from admittance theory.*

Related publications

Dettmering D., Limberger M., Schmidt M.: Using DORIS measurements for modeling the vertical total electron content of the Earth's ionosphere. Journal of Geodesy 88(12): 1131-1143, 10.1007/s00190-014-0748-2, 2014

Göttl F., Schmidt M., Seitz F., Bloßfeld M.: Separation of atmospheric, oceanic and hydrological polar motion excitation mechanisms based on a combination of geometric and gravimetric space observations. Journal of Geodesy, accepted, 2014

Liang W., Limberger M., Schmidt M., Dettmering D., Hugentobler U., Bilitza D., Jakowski N., Hoque M., Wilken V., Gerzen T.: Regional modeling of ionospheric peak parameters using GNSS data - an update for IRI. Advances in Space Research (online first), 10.1016/j.asr.2014.12.006, 2014

Limberger M., Liang W., Schmidt M., Dettmering D., Hernández-Pajares M., Hugentobler U.: Correlation studies for B-spline modeled F2 Chapman parameters obtained from FORMOSAT-3/COSMIC data. Annales Geophysicae 32(12): 1533-1545, European Geosciences Union, 10.5194/angeo-32-1533-2014, 2014

Schmidt M., Dettmering D., Seitz F.: Using B-spline expansions for ionosphere modeling. Handbook of Geomathematics (Second Edition), Springer, accepted, 2014

Schwatke C., Dettmering D., Boergens E.: Potential of SARAL/AltiKa for inland water applications. Marine Geodesy, accepted, 2014

Seitz F., Hedman K., Meyer F.J., Lee H.: Multi-sensor space observation of heavy flood and drought conditions in the Amazon region. In: Rizos C., Willis P. (Eds.) Earth on the Edge: Science for a Sustainable Planet, IAG Symposia 139: 311-317, Springer, 10.1007/978-3-642-37222-3_41, 2014

4 Methodological Foundations

4.1 Numerical methods and parameter estimation

DOGS-OC development

Processing of SLR observations to Jason-2 with DOGS-OC

The DGFI software DOGS-OC was upgraded by the modeling of non-gravitational perturbations due to solar radiation pressure, Earth infrared (IR) radiation, Earth albedo and atmospheric drag for non-spherical satellites such as Jason-2 (CNES, NASA, EUMETSAT, NOAA). Jason-2 was launched in 2008 and is still in orbit. It was selected to be implemented since it currently is the satellite mission with the highest number of SLR observations. Indeed, the assessment of non-gravitational perturbations is one of the major problems for the definition of a precise dynamical model of an orbiting satellite. For a non-spherical satellite, this is particularly difficult due to the complex satellite geometry, the incomplete knowledge of the reflective and thermal properties of the satellite surfaces and the uncertainty in the satellite attitude and the orientation of all its parts (antennas, solar panels, etc.). In order to model the complete radiation pressure force for a given direction of the incident radiation, the CNES macro model of Jason-2 was implemented (see Table 4.1), which provides the optical and IR coefficients (absorption, specular and diffuse reflection) of the satellite surfaces in the simplified spacecraft geometry of the "box-wing" model comprising a 6-face box and 2 solar panels with a specific orientation in the satellite reference frame (see Fig. 4.1).

Table 4.1: *Jason-2 macro model (CNES) including the surface areas of the "box-wing" satellite model and the solar panels, the normals to these surfaces in the satellite reference frame and their optical and IR coefficients for absorption (abs), specular (spec) and diffuse reflection (diff).*

				optical properties			infrared properties		
surf. [m^2]	normal in sat. ref. frame			spec	diff	abs	spec	diff	abs
1.65	1.0	0.0	0.0	0.0938	0.2811	0.2078	0.4250	0.1780	-0.0260
1.65	-1.0	0.0	0.0	0.4340	0.2150	0.0050	0.4080	0.1860	-0.0120
3.0	0.0	1.0	0.0	1.1880	-0.0113	-0.0113	0.3340	0.3420	0.2490
3.0	0.0	-1.0	0.0	1.2002	-0.0044	-0.0044	0.2740	0.3690	0.2970
3.1	0.0	0.0	1.0	0.2400	0.4020	0.3300	0.2360	0.3820	0.3090
3.1	0.0	0.0	-1.0	0.3180	0.3700	0.2670	0.2980	0.3360	0.2400
solar array									
9.8	1.0	0.0	0.0	0.3440	0.0060	0.6470	0.0970	0.0980	0.8030
9.8	-1.0	0.0	0.0	0.0040	0.2980	0.6970	0.0350	0.0350	0.9310

The Jason-2 attitude was modeled through the use of quaternions and solar panel orientation angles, conveniently interpolated to define the attitude matrix at each integration and observation epoch. This matrix describes the rotation from the inertial reference frame to the satellite reference frame and allows to compute radiation pressure and atmospheric drag perturbations acting on all the satellite surfaces. Moreover, this matrix describes the satellite attitude control which keeps the $+z$-plane of the satellite nadir-pointed and simultaneously the solar panels oriented towards the Sun to maximize their power absorption

As the satellite center of mass (CoM) varies during the mission lifetime due to fuel consumption, offsets

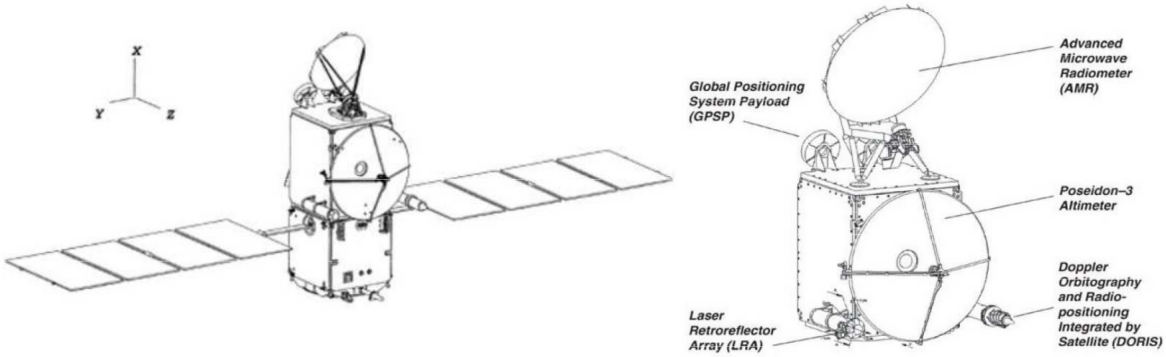

Fig. 4.1: *Jason-2 satellite reference frame (CNES and http://sealevel.jpl.nasa.gov/files/ostm/Spacecraft-OSTM_Fact_Sheet_Final.pdf): the origin is located at the center of the attachment ring; x-axis is along the satellite's main axis of inertia (axis from the satellite CoM pointing from the attachment ring towards the radiometer antenna; y-axis is transverse, along the rotation axis of the solar panels; z-axis is radial, pointing towards the Earth (nadir).*

for mass and CoM from the corresponding history files[1] have to be added to the initial values (see Table 4.2) to obtain the actual values of the satellite mass and the CoM coordinates in the satellite reference frame. By knowing the actual values for the CoM and the laser retroreflector array (LRA) offset in the satellite reference frame (see Table 4.3), it is possible to compute the offset between the variable CoM and the LRA optical center at each integration and observation epoch. The concept diagram of the SLR CoM correction is shown in Fig. 4.2. An additional correction of 4.9 cm was finally subtracted from the computed range to account for the LRA phase center offset of Jason-2.

Table 4.2: *Initial mass and CoM values in the satellite reference frame at the launch epoch of Jason-2.*

mass [kg]	X_{CoM} [m]	Y_{CoM} [m]	Z_{CoM} [m]
505.9	0.9768	0.0001	0.0011

Table 4.3: *LRA offset in the satellite reference frame.*

X_{LRA} [m]	Y_{LRA} [m]	Z_{LRA} [m]
1.194	0.598	0.684

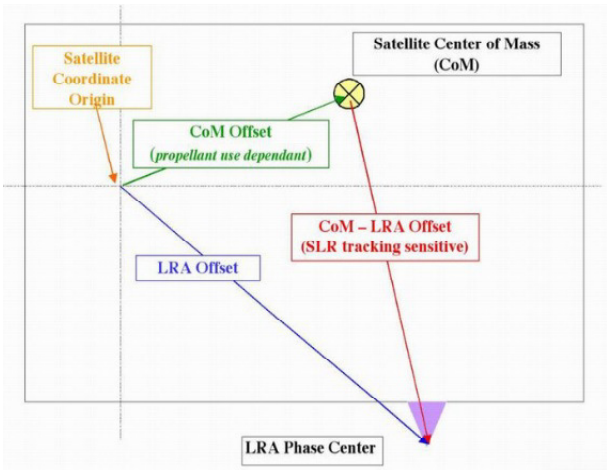

Fig. 4.2: *SLR center of mass correction concept.*

Through this modified version of DOGS-OC, Jason-2 SLR observations from July 20, 2008 to September 20, 2014 were processed using 3.5-day arcs (half a GPS week) except for those arcs containing orbital maneuvers. In fact, orbit parameters tend to change over time as a result of the perturbing forces. In order to keep the satellite in an adequate orbit, maneuvers are necessary. To handle the maneuvers, we decided to split the 3.5-day arcs into sub-arcs (or to attach very short sub-arcs to the previous or following arc) in such a way that the first sub-arc ends approximately at the end of the maneuver in order to estimate good initial orbital elements for processing the second sub-arc. Indeed, without this expedient, we observed a correlation between high SLR RMS values and the maneuver events.

[1] DORIS satellites models implemented in POE processing; url: ftp://ftp.ids-doris.org/pub/ids/satellites/DORISSatellite Models.pdf

During a first processing of the Jason-2 data, no EOP, station coordinates or gravity field coefficients were estimated in order to identify possible outliers in the observations based on an SLR RMS threshold of 70 cm. Afterwards, the SLR RMS threshold was systematically decreased to 20 cm, and geodetic parameters were estimated. The final arc-dependent SLR RMS values are shown in Fig. 4.3. In this figure, a correlation between the SLR RMS and the yaw steering events is visible. The nominal attitude model of Jason-2 ("yaw steering" model) should be used to compute the satellite attitude when the quaternions and solar panel orientation angles are missing. Handling the maneuvers as mentioned above, allowed to eliminate their correlation with the SLR RMS (see Fig. 4.3). However, a correlation with the yaw steering events which are currently modeled with the quaternions and solar panel orientation angles remains. This issue has to be further investigated.

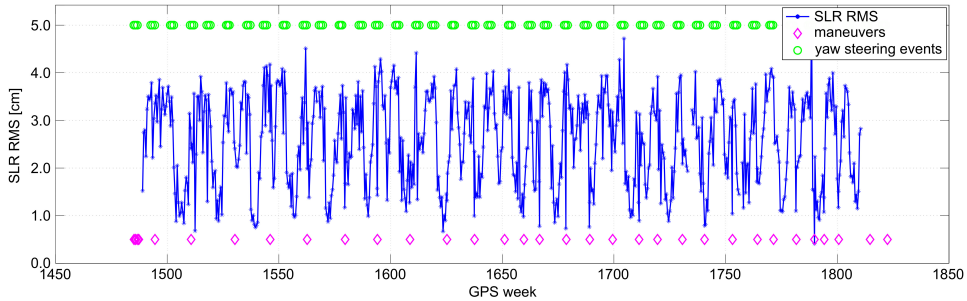

Fig. 4.3: *SLR RMS for Jason-2 arcs between July 2008 and September 2014. The correlation between RMS and yaw steering events is clearly visible but cannot be explained yet; the correlation with the maneuvers could be removed by splitting the arcs containing maneuvers into sub-arcs.*

Finally, Figs. 4.4 and 4.5 show the differences between the DOGS and ESOC Jason-2 orbits for 3.5-day arcs processed with the spherical satellite model and the box-wing model, respectively (no estimation of EOP, station coordinates and gravity field). For the considered arcs, we obtained an SLR RMS of 75.8 cm in the spherical model case and an SLR RMS of 6.3 cm in the box-wing model case.

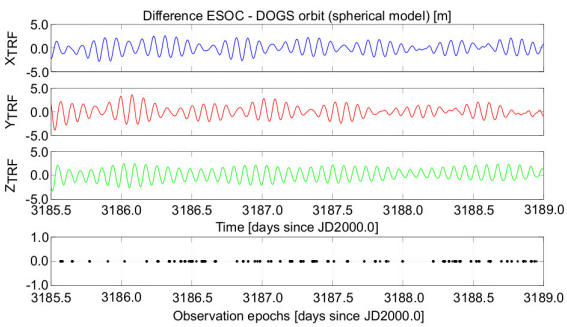

Fig. 4.4: *Differences of the DOGS 3.5-day arcs for Jason-2 (spherical satellite model) w.r.t. ESOC (SLR RMS = 75.8 cm).*

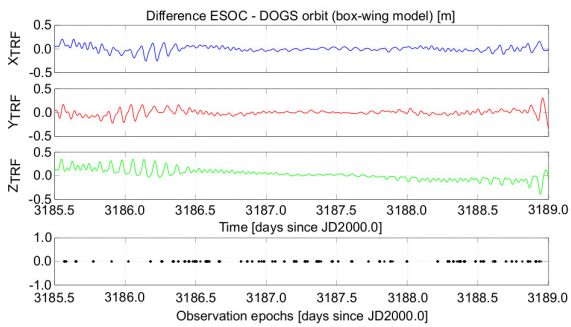

Fig. 4.5: *Differences of the DOGS 3.5-day arcs for Jason-2 (box-wing satellite model) w.r.t. ESOC (SLR RMS = 6.3 cm).*

DOGS-CS development

Correction of SLR observations due to non-tidal loading effects (implementation in DOGS-OC and DOGS-CS)

In the framework of the ILRS pilot project on correcting SLR observations for non-tidal atmospheric effects, DGFI implemented the ability to correct for various non-tidal loading effects in its software package DOGS-OC. Through a joint project with the Bundesamt für Kartographie und Geodäsie (BKG) within the DFG research unit on "Reference Systems", models to account for non-tidal atmospheric, oceanic and hydrological loading effects were made available. Besides the direct geometrical effect on

the observing station, also the gravitational perturbing acceleration has to be taken into account for a consistent correction of the non-tidal effects.

Besides the implementation of non-tidal corrections in DOGS-OC, the ability to correct for non-tidal loading effects at the normal equation level was implemented in DOGS-CS. At this level of the Gauß-Markov model, only the site displacements can be corrected in global TRF computations since the gravitational field parameters are fixed to their corresponding a priori values (as it is the case for the ITRF2014 processing). In order to quantify the impact of the non-tidal atmospheric loading (NT-ATML) corrections on global reference frames and the EOP, three test solutions using SLR data were computed:

(A) conventional TRF: No NT-ATML corrections applied. This TRF is named "conventional" TRF in the following and is the basis for the comparison of the similarity transformation parameters (Fig. 4.6), the station coordinates and velocities (Fig. 4.7) and the squared sums of the observations and residuals (Table 4.4).

(B) TRF + NT-ATML corrections applied a posteriori: Only site displacements at the normal equation/parameter level are applied using DOGS-CS. The applied site displacements are a mean of all displacements during a week. Consequently, since only displacements at observation epochs should be used (for ITRF2014 processing, this information is not available), the mean correction applied a posteriori is not the same mean correction which is applied a priori.

(C) TRF + NT-ATML corrections applied at the observation level (a priori): Within DOGS-OC, both the site displacement and the gravitational acceleration (i.e. the complete effect) are applied. The corrections are applied at the observation epochs only. This approach to correct the NT-ATML effect is the most rigorous one since it accounts for both effects exactly at the observation epochs.

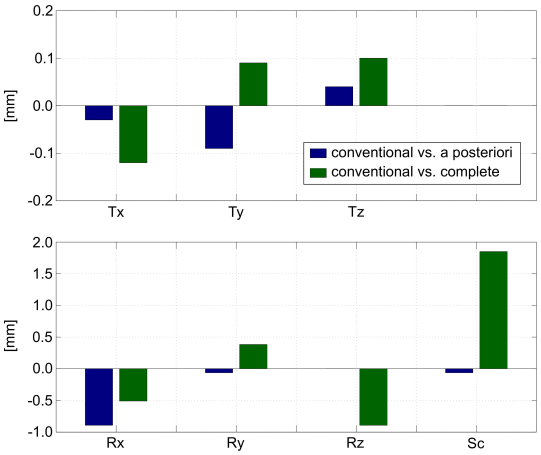

Fig. 4.6: Similarity transformation parameters of the conventional TRF (A) w.r.t. the other two TRF solutions (B) and (C).

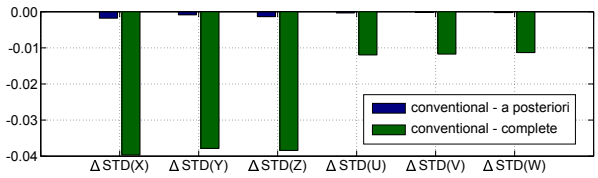

Fig. 4.7: Mean standard deviation differences between the conventional TRF (A) and the two other TRF solutions (B) and (C) for the three station coordinate components in [mm] and for the three velocity components in [mm/a].

Table 4.4: $\mathbf{l}^T\mathbf{Pl}$ *and* $\mathbf{v}^T\mathbf{Pv}$ *of the different TRF solutions.*

TRF solution	$\mathbf{l}^T\mathbf{Pl}$	$\mathbf{v}^T\mathbf{Pv}$
(A)	$5.166 \cdot 10^6$	$3.092 \cdot 10^6$
(B)	$5.172 \cdot 10^6$	$3.099 \cdot 10^6$
(C)	$5.120 \cdot 10^6$	$2.990 \cdot 10^6$

The Figs. 4.6 and 4.7 and Table 4.4 summarize the TRF comparisons made in order to quantify the effect of applying the NT-ATML correction at different levels of the Gauß-Markov model. It is obvious that the a posteriori application of the NT-ATML correction only marginally affects all similarity transformation parameters w.r.t. the conventional TRF, whereas the complete a priori correction (site displacement and gravitational perturbation) significantly affects the TRF scale. The effect has a magnitude of about 1.8 mm. The mean standard deviations of the estimated coordinates and velocities benefit slightly from the a priori, but only marginally from the a posteriori correction. The squared sum of the observations $\mathbf{l}^T\mathbf{Pl}$ and the squared sum of the residuals $\mathbf{v}^T\mathbf{Pv}$ decrease only slightly for both corrections.

DOGS-RI development

Currently, the VLBI analysis software OCCAM is refined to become part of DOGS. The new module will be called DOGS-RI (radio interferometry). All routines are based on the IERS 2010 Conventions and the celestial intermediate pole (CIP). The theoretical models for the group delay need time derivatives and, in case of delay rate, also the second time derivatives of the input parameters. The OCCAM approach to approximate these derivatives by finite differences with a fixed time step of 2 s was superseded. Parameter and observation models were expanded to provide analytically calculated first and second time derivatives. This conversion is complete except for some routines calculating the equinox-based transformation matrix from the nutation parameters $\Delta\psi$ and $\Delta\varepsilon$. Thus, only the branch based on X_{CIP}, Y_{CIP} and the celestial intermediate origin (CIO) is operative. The correlations between $(X_{\mathrm{CIP}}, Y_{\mathrm{CIP}})$ and $(x_{\mathrm{pol}}, y_{\mathrm{pol}})$ are not yet theoretically modelled; condition equations to prevent subdiurnal retrograde motions still lack in the program.

4.2 Standards and conventions

The GGOS Bureau for Standards and Conventions (BSC) was established as a GGOS component in 2009. The BSC is hosted and supported by DGFI and the Institut für Astronomische und Physikalische Geodäsie (IAPG) of the Technische Universität München, within the Forschungsgruppe Satellitengeodäsie (FGS).

Purpose

The work of the BSC is primarily focused on the IAG Services and the products they derive on an operational basis for Earth monitoring making use of various space geodetic observation techniques such as VLBI, SLR/LLR, GNSS, DORIS, altimetry, gravity satellite missions, gravimetry, etc. The BSC supports GGOS in its goal to obtain products of highest possible accuracy, consistency, and temporal and spatial resolution, which should refer to a unique reference frame, stable over decades in time (Fig. 4.8). To achieve this important goal, it is a fundamental requirement that common standards and conventions are used by all IAG components for the analysis of the different geometric and gravimetric observations.

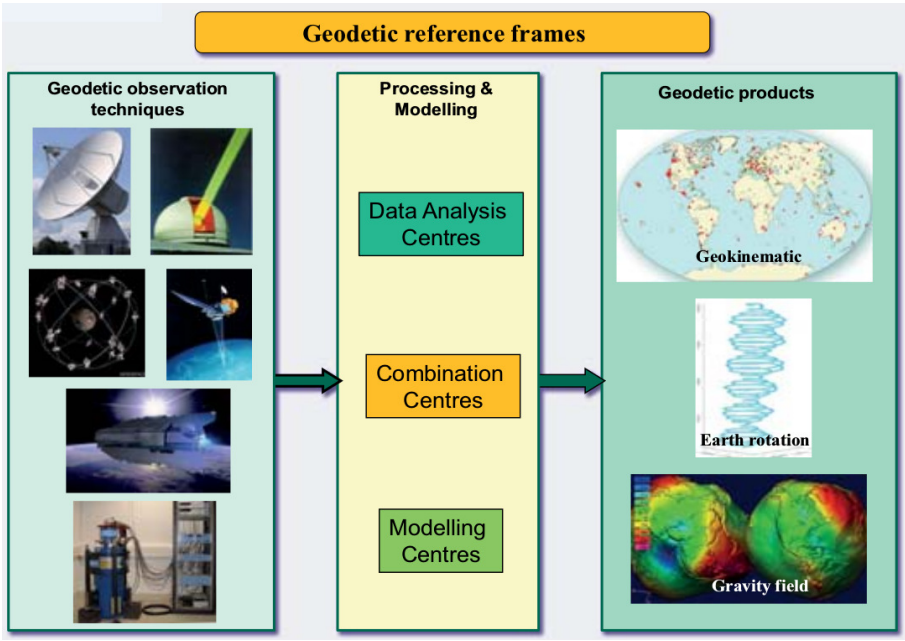

Fig. 4.8: *From geodetic observations to products.*

Objectives

The key objective of the BSC is to ensure that common standards and conventions are adopted and implemented by all IAG components as a fundamental basis for the generation of consistent IAG/GGOS products.

Major tasks of the BSC are:

- To keep track of the strict consideration of adopted geodetic standards, standardized units, fundamental physical constants, resolutions and conventions for the generation of IAG/GGOS products.
- To review, examine and evaluate all standards, constants, resolutions and conventions adopted by IAG or its components and to recommend their use or to propose the necessary updates.
- To identify gaps, inconsistencies and deficiencies in standards and conventions and to initiate steps to remove them.
- To propose the adoption of new standards where necessary.
- To propagate standards and conventions to the wider scientific community and to promote their use.

Inventory of standards and conventions

A key task of the BSC is the compilation of an inventory of standards and conventions currently used for the generation of the IAG/GGOS products. In April 2014, a first version of such a document was completed and distributed to the GGOS Coordinating Board members and to the associated members of the BSC. Additionally, some of these colleagues and also other experts were contacted personally to get feedback and detailed comments on particular topics (sections) of the document. Many of them responded and provided very constructive feedback and valuable comments on the inventory, which is gratefully acknowledged by the authors. A revised version of this document was finalized in December 2014. During the meetings of the GGOS Coordinating Board and the IAG Executive Committee in San Francisco it was decided to conduct an external review of the document by an independent board, which shall be accomplished during the first half of 2015.

The content of the document can be summarized as follows: The introduction part provides general information about GGOS including its mission, goals and organizational structure. This part also deals with standards and conventions from a general point of view along with some relevant nomenclature, such as standards, standardized units, fundamental physical constants, resolutions and conventions, and it also provides the standards and conventions relevant for geodesy. The second chapter presents the BSC, its mission and goals and the personnel structure as well as the interactions with IAG and other entities involved in standards and conventions. Chapter 3 focuses on numerical standards including time and tide systems and the geopotential value W_0. Chapter 4, a key element of this document, addresses the standards and conventions used for the generation of the IAG/GGOS products. The focus is on the following products and topics:

- Celestial reference systems and frames
- Terrestrial reference systems and frames
- Earth orientation parameters
- GNSS satellite orbits
- Gravity and geoid
- Height systems and their realizations

The BSC presents the current status, identifies gaps and inconsistencies as well as interactions between different products. In this context, also open questions and recommendations as regards standards and conventions for the generation of IAG/GGOS products are provided. It shall be noted that the above list

Table 4.5: *Comparison of numerical standards. The IERS Conventions 2010 provide the TCG value for the gravitational constant (GM) in Table 1.1. In addition, the TT-compatible value is given in Section 1.2 of that document.*

Quantity	GRS80	Fundamental Parameters[1]	IERS2010	EGM2008	Unit
Gravit. constant (GM)					
– TCG value	398.6005	398.6004418	398.6004418		$[10^{12}\mathrm{m}^3\mathrm{s}^{-2}]$
– TT value			398.6004415	398.6004415	
Equatorial radius (a)					
– zero-tide value	6378137.0		6378136.6		
– mean-tide value		6378136.7			[m]
– tide-free value				6378136.3	
Dyn. form factor (J_2)					
– zero-tide value	1082.63	1082.6359	1082.6359	1082.6361	$[10^{-6}]$
Ang. rot. velocity (ω)	7.292115	7.292115	7.292115	7.292115	$[\mathrm{rad\ s}^{-1}]$

[1] Groten E., 2004. Fundamental parameters and current (2004) best estimates of the parameters of common relevance to astronomy, geodesy, and geodynamics. J Geod 77(10-11), 724-797, doi:10.1007/s00190-003-0373-y

of topics and IAG/GGOS products is by far not complete and can be extended by adding other products in an updated version of the document.

In the following, we present the status regarding numerical standards. Table 4.5 contains values from different sources aiming at different purposes. The GRS80 is still used as a conventional ellipsoid, although the values do no longer truly represent reality. Except for the angular rotation velocity ω, all values differ from the consistent set of fundamental parameters estimated by Groten (2004) about 25 years later. The latter set of values was kept for the IERS Conventions 2010. Although the equatorial radius a differs by 0.1 m, the IERS Conventions 2010 are consistent with Groten (2004), since this difference is only due to the expression in different tide systems. However, concerning the numerical standards given in Table 1.1 of the IERS Conventions 2010 it shall be mentioned that in parallel the GRS80 values are recommended for transforming Cartesian coordinates into ellipsoidal coordinates (the difference between both standards is 0.4 m for the equatorial radius a). The standards adopted for the EGM2008 were defined in the geodetic reference systems as adopted for EGM96 to ensure consistency between both gravity field models. For a comparison of the values displayed in Table 4.5, it has also to be considered that they are partly expressed in different time and tide systems. A fundamental parameter for the definition of height systems is the geopotential value W_0. Some selected examples from recent computations are shown in Table 4.6.

Table 4.6: *Examples of global W_0 estimates. The values are extracted from Table 3 of Sanchez (2012)*[1].

W_0 [m^2/s^2]	Comments	References
62636860.850	GRS80 ($W_0 = U_0$)	Moritz, 2000
62636856.16	Mean sea surface T/P (1993–2001), EGM96	Burša, 2002
62636856.0	IERS Conventions 2010 (best W_0 estimate in 1998, T/P (1993 - 1996), EGM96)	IERS, 2010
62636854.6	Mean sea surface T/P (1993–2003), EGM96	Burša, 2007
62636853.4	Mean sea surface T/P, EIGEN-GC03C, epoch 2000.0	Sánchez, 2007
62636854.38	Mean sea surface CLS01, EIGEN-GL04S, epoch 2000.0	Sánchez, 2009
62636854.2	Mean sea surface DNSC08, ECCO2, EGM2008, epoch 2005.0	Dayoub, 2012

[1] Sanchez L., 2012. Towards a vertical datum standardisation under the umbrella of GGOS. Journal of Geodetic Science, 2(4):325-342, doi:10.2478/v10156-012-0002-x.

In summary, the inventory shows that several open issues, deficiencies and gaps need to be addressed by the geodetic community. The fact that the numerical standards are partly given in different time and tide systems needs to be considered by the users and respective transformations have to be performed. For a correct interpretation and use of geodetic products, the applied standards and conventions must be clearly documented, which is currently not always the case. The inventory of standards and conventions provides some recommendations on how to resolve inconsistencies and gaps, which are summarized at the end of each section. The recommendations given in this inventory shall be discussed and priorities should be defined together with all experts in the field. Finally, an action plan with tasks and responsibilities including a time schedule should be compiled.

Representation of IAG Services and other entities

A close interaction with the IAG Services is essential to accomplish the tasks of the BSC, in particular for the evaluation of the standards and conventions currently adopted by all IAG components and other entities involved. This could be achieved by selecting representatives from the IAG Services, the IAU and other entities as associate members of the BSC. The status of December 2014 is summarized in Table 4.7.

Table 4.7: *Representatives of IAG Services, IAU and other entities in the BSC (status: December 2014).*

T. Herring, USA, G. Petit, France	International Earth Rotation and Reference Systems Service (IERS)
U. Hugentobler, Germany	International GNSS Service (IGS)
E. Pavlis, USA	International Laser Ranging Service (ILRS)
J. Gipson, USA	International VLBI Service for Geodesy and Astrometry (IVS)
F. Lemoine, J. Ries, both USA	International DORIS Service (IDS)
R. Barzaghi, Italy	International Gravity Field Service (IGFS)
F. Barthelmes, Germany	International Centre for Global Gravity Field Models (ICGEM)
S. Bonvalot, France	International Gravimetric Bureau (BGI)
R. Heinkelmann, Germany	International Astronomical Union (IAU), Working Group "Numerical Standards for Fundamental Astronomy"
M. Craymer, Canada	Chair of Control Body for the ISO Geodetic Registry Network
J. Ádám, Hungary	Chair of the IAG Communication and Outreach Branch
J. Ihde, Germany	IAG representative to ISO/TC211
J. Kusche, Germany	Representative of the gravity community
P. Steigenberger, Germany	Representative of the GNSS community

Organizational issues

A realignment of the GGOS organization has been initiated in 2014. The existing GGOS components are kept, but their responsibilities are defined and clarified. During the GGOS Coordinating Board Meeting in Vienna (April 2014), it was decided that the responsibilities and tasks of both GGOS Bureaus shall be extended. Within this realignment, the BSC shall be transferred to a Bureau of Products and Standards. This transition is still in progress, and the charter and implementation plan for the new Bureau is under development.

5 Information Services and Scientific Transfer

It is of particular importance for fundamental research on geodesy (a rather unacquainted field in geosciences) to provide information on research projects, scientific results, value-added data and products to both the scientific community and the public. Exchange of knowledge and scientific results is a basic requirement for any research that is more and more based on international cooperation. Publications in peer-reviewed scientific journals are still the most acknowledged way of scientific transfer. Section 5.2 provides a list of the papers printed or published online in 2014. It is followed by a list of posters and oral presentations that wered presented by DGFI staff at numerous workshops, symposia and conferences.

Besides, the internet is intensively used as a platform for information exchange. DGFI maintains a homepage on which all research activities, projects and cooperations of the institute are described in detail. Under the heading of "hot stories" we call attention to the most recent results. Quite a number of additional web sites are maintained by DGFI, particularly those of the Office of the International Association of Geodesy (IAG) and of the German Geodetic Commission (Deutsche Geodätische Kommission, DGK) including an online catalogue with about 1000 publications (predominantly dissertations) published by the DGK. Further internet sites are set up and maintained for large projects, services and national research programmes.

5.1 Internet representation

The Internet has become an indispensable medium for the exchange of data and scientific information. The DGFI maintains several independent internet sites and wikis to meet growing demands for information about different scientific aspects.

Internet sites set up and maintained by DGFI

Internet sites maintained by the DGFI:

- Deutsches Geodätisches Forschungsinstitut (DGFI)
- Deutsche Geodätische Kommission (DGK)
- Office of the International Association of Geodesy (IAG)
- Geocentric Reference System for the Americas (SIRGAS)
- EUROLAS Data Center (EDC)
- Open Altimeter Database (OpenADB)
- GGOS Bureau for Standards and Conventions (BSC)
- International Altimetry Service (IAS)
- ESA projects
- IAG Working Groups
- IAG Joint Study Groups

DGFI

The DGFI home page, available at

http://dgfi.tum.de,

informs about the structure and results of the current research programme, ongoing research topics, the national and international projects DGFI is involved in and the multiple contributions of DGFI to international services. The web site (see Fig. 5.1) also provides a complete list of papers and reports published since 1994 by the employees as well as a compilation of all posters and oral presentations. Annual reports and DGFI reports are available in electronic form.

DGK

Another web site is maintained for the "Deutsche Geodätische Kommission" (DGK). It is available at

http://dgk.badw.de

and informs about the structure of the DGK, the membership, sections, geodetic research institutes in Germany, and the numerous publications of DGK. The complete catalogue of DGK publications can be downloaded as a pdf file or browsed by means of a user-friendly search function (see Fig. 5.1).

IAG Office

At the General Assembly of IUGG in Perugia, Italy, the IAG was reorganized. The position of the IAG Secretary General was handed over to the retired director of DGFI, and the IAG Office was established at DGFI. The web site

http://iag.dgfi.tum.de

was installed to support the work of the Office.

SIRGAS

SIRGAS is the Geocentric Reference System for the Americas. The web site is operated by the SIRGAS Vice-President at DGFI and located at

http://sirgas.org.

The SIRGAS web site comprises (see Fig. 5.2)

- a scientific description presenting definition, realization, and kinematics of the SIRGAS reference frame,

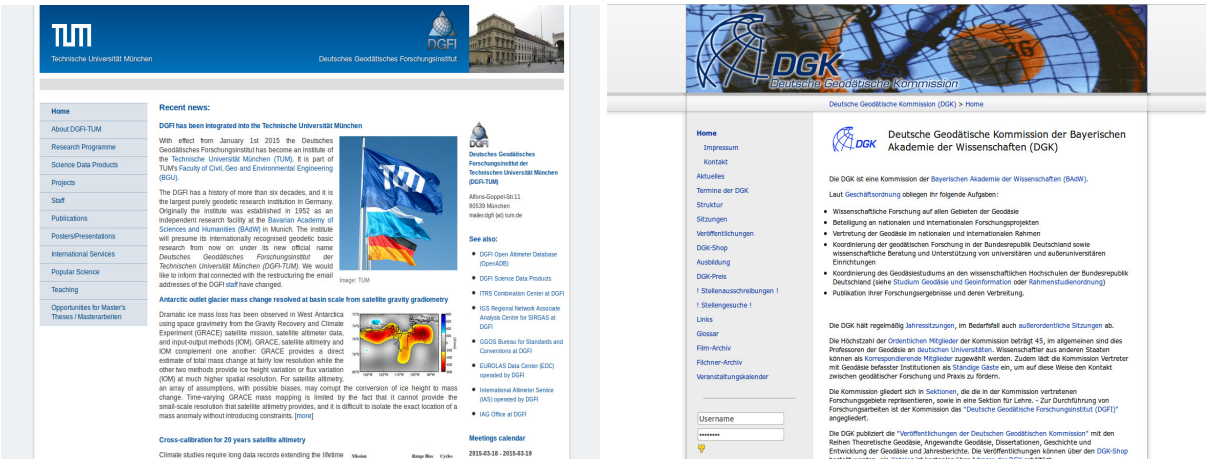

Fig. 5.1: Screenshots of the home pages of DGFI (left) and DGK (right)

- an organizational summary showing the operational structure and functions of the different components of SIRGAS,
- a bibliographic compilation with reports, articles, presentations, and posters related to the SIRGAS activities.

EUROLAS Data Center (EDC)

The EUROLAS Data Center (EDC) provides access to the database of SLR observations and derived products (see Fig. 5.2). This web site informs about the data flow within the Operation Centre (OC) and the data holding of the Data Centre (DC). This site is available at

http://edc.dgfi.tum.de.

Open Altimeter Database (OpenADB)

OpenADB is a database for multi-mission altimeter data and derived high-level products. It is designed for users with little experience in satellite altimetry and scientific users evaluating data and generating new products, models and algorithms. OpenADB allows fast parameter updates and enables database extracts with user-defined formats and parameters. The usage of OpenADB is open after registration to anyone (see Fig. 5.3). This site is available at

http://openadb.dgfi.tum.de.

GGOS Bureau for Standards and Conventions (BSC)

The GGOS Bureau for Standards and Conventions (BSC) was established as a GGOS component in 2009. The BSC is hosted and supported by DGFI and the Institut für Astronomische und Physikalische Geodäsie (IAPG) of the Technische Universität München, within the Forschungsgruppe Satellitengeodäsie (FGS). The web site is located at

http://ggos-bsc.dgfi.tum.de.

International Altimetry Service (IAS)

The home page of the International Altimetry Service

Fig. 5.2: Screenshots of the web sites of SIRGAS (left) and the EUROLAS Data Center (right)

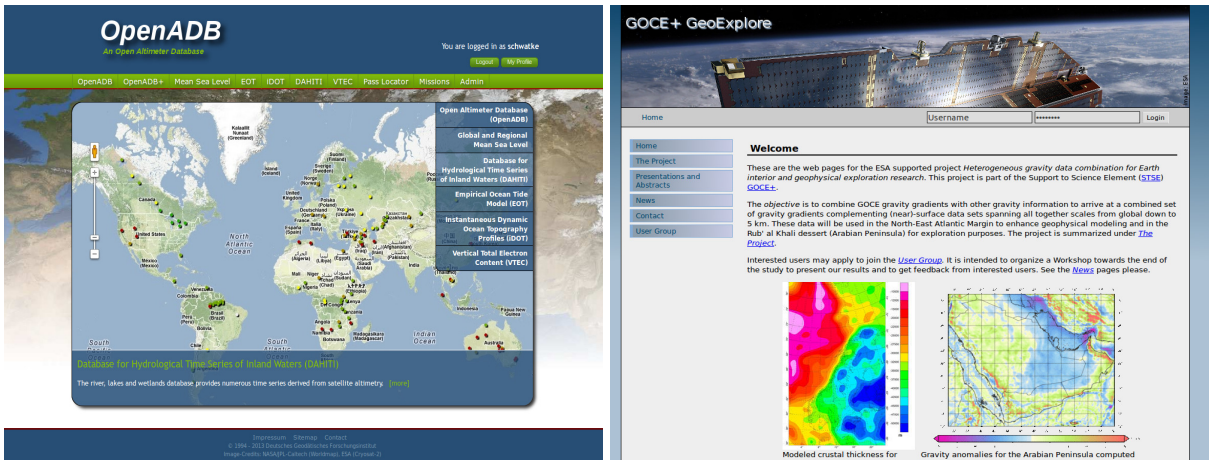

Fig. 5.3: Screenshots of the web sites of the EUROLAS Data Center (left) and the ESA project "GOCE+ GeoExplore" (right)

- provides a point of contact for general information on satellite altimetry and its applications;
- communicates and interfaces with altimeter mission data providers and with centres which process, archive and analyze altimeter data and other related services and organizations;
- promotes satellite altimetry as a core element of Global Earth Observing Systems;
- helps users to compile and analyze data and to respond to altimeter user requirements.

This site is available at

http://ias.dgfi.tum.de.

ESA projects

The web sites of the GOCE+ GeoExplore (see Fig. 5.3) and the GOCE+ Time-Variations are available at

http://goce4interior.dgfi.tum.de

and

http://gocedt.dgfi.tum.de.

Both web sites provide information about the progress of the projects. Presentations related to the projects are also available.

IAG Working and Joint Study Groups

The DGFI maintains web sites of three IAG Working (IAG-WG) and Joint Study Groups (IAG-JSG).

- IAG Joint Working Group 0.1.1 – "Vertical Datum Standardisation" (*http://whs.dgfi.tum.de/*)
- IAG Joint Working Group 1.3 – "Strategies for Epoch Reference Frames" (*http://erf.dgfi.tum.de/*)
- IAG Joint Study Group 0.3 – "Methodologies of Regional Gravity Field Modelling" (*http://jsg03.dgfi.tum.de/*)

Wikis mainted by DGFI

In addition to the different web sites, the DGFI currently maintains eight wikis which are used for information exchange within projects or working groups.

Mailing lists

Mailing lists are maintained by DGFI to fulfill the requirements for information exchange within the ILRS Global Data Centre, the Reference System SIRGAS and CGE. The mailing lists are realized by the 'mailman' program which transforms submitted e-mails to a specific format which can then be viewed by any internet browser sorted according to date, thread or author.

Intranet

Another server behind a firewall is used to provide Intranet functionality, on the basis of the Typo3 CMS. The internal information exchange is supported by a black board, a meeting calendar, the access to the library database, and numerous pages which can be created, modified or deleted by any of the employees. The pages compile internal information for the work of particular research topics, links to data sets, formats, internal documentation and the necessary meta data.

5.2 Publications

Albertella A., Savcenko R., Janjic T., Rummel R., Bosch W., Schröter J.: *Mean dynamic ocean topography in the Southern Ocean from GRACE and GOCE and multi-mission altimeter data*. In: Rizos C., Willis P. (Eds.) Earth on the Edge: Science for a Sustainable Planet, IAG Symposia 139: 81–87, Springer, doi:10.1007/978-3-642-37222-3_10, 2014

Alothman A., Bouman J., Gruber T., Lieb V., Alsubaei M., Alomar A., Fuchs M., Schmidt M.: *Validation of regional geoid models for Saudi Arabia using GPS/levelling data and GOCE models*. In: Marti U. (Ed.) Gravity, Geoid and Height Systems (GGHS2012), IAG Symposia 141: 193–199, doi:10.1007/978-3-319-10837-7_25, 2014

Bachmann S., Lösler M., Messerschmitt L., Schmid R., Bloßfeld M., Thaller D.: *BKG/DGFI Combination Center Annual Report 2013*. In: Baver K.D., Behrend D., Armstrong K.L. (Eds.) International VLBI Service for Geodesy and Astrometry 2013 Annual Report, 257-260, NASA/TP-2014-217522, 2014

Bloßfeld M., Gerstl M., Hugentobler U., Angermann D., Müller H.: *Systematic effects in LOD from SLR observations*. Advances in Space Research 54(6): 1049-1063, doi:10.1016/j.asr.2014.06.009, 2014

Bloßfeld M., Seitz M., Angermann D.: *Non-linear station motions in epoch and multi-year reference frames*. Journal of Geodesy 88(1): 45–63, Springer, doi:10.1007/s00190-013-0668-6, 2014

Bloßfeld M., Stefka V., Müller H., Gerstl M.: *Consistent estimation of Earth rotation, geometry and gravity with DGFI's multi-satellite solution*. Proceedings of the 18th International Workshop on Laser Ranging, 13-0113, 2014

Böhm J., Bloßfeld M., Fritsche M., Steigenberger P.: *Tagungsbericht IAG Scientific Assembly 2013, Thema 1: Definition, Implementation and Scientific Applications of Reference Frames*. Zeitschrift für Geodäsie, Geoinformation und Landmanagement (zfv) 139(1), 2014

Bosch W., Dettmering D., Schwatke C.: *Multi-mission cross-calibration of satellite altimeters: constructing a long-term data record for global and regional sea level change studies*. Remote Sensing 6(3): 2255–2281, doi:10.3390/rs6032255, 2014

Bouman J., Fuchs M., Broerse T., Vermeersen B., Visser P., Schrama E., Schmidt M.: *Modelling and observing the Mw 8.8 Chile 2010 and Mw 9.0 Japan 2011 earthquakes using GOCE*. In: Rizos C., Willis P. (Eds.) Earth on the Edge: Science for a Sustainable Planet, IAG Symposia 139: 303–310, Springer, doi:10.1007/978-3-642-37222-3_40, 2014

Bouman J., Fuchs M., Lieb V., Bosch W., Dettmering D., Schmidt M.: *GOCE gravity gradients: combination with GRACE and satellite altimetry*. In: Flechtner F., Sneeuw N., Schuh W.-D. (Eds.) Observation of the System Earth from Space - CHAMP, GRACE, GOCE and future missions, Advanced Technologies in Earth Sciences, 89–94, Springer, doi:10.1007/978-3-642-32135-1_11, 2014

Bouman J., Fuchs M., Ivins E., van_der_Wal W., Schrama E., Visser P., Horwath M.: *Antarctic outlet glacier mass change resolved at basin scale from satellite gravity gradiometry*. Geophysical Research Letters 41(16): 5919-5926, doi:10.1002/2014GL060637, 2014

Dettmering D., Bosch W.: *Performance of ESA CryoSat-2 GDR data over open ocean*. In: Ouwehand L. (Ed.) Proceedings of "CryoSat Third User Workshop", March 2013, Dresden, Germany, ESA SP-717 (CD-ROM), ISBN 978-92-9221-281-0, ESA/ESTEC, 2014

Dettmering D., Limberger M., Schmidt M.: *Using DORIS measurements for modeling the vertical total electron content of the Earth's ionosphere*. Journal of Geodesy 88(12): 1131–1143, doi:10.1007/s00190-014-0748-2, 2014

Dettmering D., Schwatke C., Bosch W.: *Global calibration of SARAL/AltiKa using multi-mission sea surface height crossovers*. Marine Geodesy (in press), doi:10.1080/01490419.2014.988832, 2014

Ebbing J., Bouman J., Fuchs M., Gradmann S., Haagmans R.: *Sensitivity of GOCE gravity gradients to crustal thickness and density variations: case study for the Northeast Atlantic region*. In: Marti U. (Ed.) Gravity, Geoid and Height Systems (GGHS2012), IAG Symposia 141: 291–298, doi:10.1007/978-3-319-10837-7_37, 2014

Forootan E., Kusche J., Loth I., Schuh W.-D., Eicker A., Awange J., Longuevergne L., Diekkrüger B., Schmidt M., Shum C.K.: *Multivariate prediction of total water storage changes over West Africa from multi-satellite data*. Surveys in Geophysics 35(4): 913-940, Springer, doi:10.1007/s10712-014-9292-0, 2014

Forootan E., Rietbroek R., Kusche J., Sharifi M.A., Awange J.L., Schmidt M., Omondi P., Famiglietti J.: *Separation of large scale water storage patterns over Iran using GRACE, altimetry and hydrological data*. Remote Sensing of Environment 140: 580–595, Elsevier, doi:10.1016/j.rse.2013.09.025, 2014

Jacobs C.S., Arias F., Boboltz D., Boehm J., Bolotin S., Bourda G., Charlot P., de_Witt A., Fey A., Gaume R., Gordon D., Heinkelmann R., Lambert S., Ma C., Malkin Z., Nothnagel A., Seitz M., Skurikhina E., Souchay J., Titov O.: *ICRF-3: roadmap to the next generation ICRF*. In: Capitaine N. (Ed.) Proceedings of the Journées 2013 "Scientific developments from highly accurate space-time reference systems", 51–56, Observatoire de Paris, ISBN 978-2-901057-69-7 , 2014

Kirschner S., Seitz F.: *Recursive adjustment approach for the estimation of physical Earth parameters from polar motion*. In: Rizos C., Willis P. (Eds.) Earth on the Edge: Science for a Sustainable Planet, IAG Symposia 139: 453–459, Springer, doi:10.1007/978-3-642-37222-3_60, 2014

Liang W., Limberger M., Schmidt M., Dettmering D., Hugentobler U., Bilitza D., Jakowski N., Hoque M., Wilken V., Gerzen T.: *Regional modeling of ionospheric peak parameters using GNSS data - an update for IRI*. Advances in Space Research (online first), doi:10.1016/j.asr.2014.12.006, 2014

Limberger M., Liang W., Schmidt M., Dettmering D., Hernández-Pajares M., Hugentobler U.: *Correlation studies for B-spline modeled F2 Chapman parameters obtained from FORMOSAT-3/COSMIC data*. Annales Geophysicae 32(12): 1533-1545, European Geosciences Union, doi:10.5194/angeo-32-1533-2014, 2014

Männel B., Rothacher M., Kodet J., Schreiber U., Schmid R.: *GLONASS satellites simultaneously observed by VLBI, GNSS and SLR*. In: Behrend D., Baver K.D., Armstrong K.L. (eds.) VGOS: The New VLBI Network, Proceedings of the 8th IVS General Meeting, pp 461–465, Science Press, Beijing, China, 2014

Müller H., Bloßfeld M.: *Quality and possible improvements of the official ILRS products*. Proceedings of the 18th International Workshop on Laser Ranging, 13-0202, 2014

Rodriguez-Solano C.J., Hugentobler U., Steigenberger P., Bloßfeld M., Fritsche M.: *Reducing the draconitic errors in GNSS geodetic products*. Journal of Geodesy 88(6): 559-574, Springer, doi:10.1007/s00190-014-0704-1, 2014

Rudenko S., Dettmering D., Esselborn S., Schöne T., Förste C., Lemoine J.-M., Ablain M., Alexandre D., Neumayer K.-H.: *Influence of time variable geopotential models on precise orbits of altimetry satellites, global and regional mean sea level trends*. Advances in Space Research 54(1): 92–118, doi:10.1016/j.asr.2014.03.010, 2014

Sánchez L.: *IGS Regional Network Associate Analysis Centre for SIRGAS (IGS RNAAC SIR)*. In: Dach R., Jean Y. (Eds.) International GNSS Service Technical Report 2013, 103–114, 2014

Sánchez L., Dayoub N., Cunderlík R., Minarechová Z., Mikula K., Vatrt V., Vojtísková M., Síma Z.: *W0 estimates in the frame of the GGOS Working Group on Vertical Datum Standardisation*. In: Marti U. (Ed.) Gravity, Geoid and Height Systems (GGHS2012), IAG Symposia 141: 203–210, doi:10.1007/978-3-319-10837-7_26, 2014

Schmid R.: *IGS Antenna Working Group*. In: Dach R., Jean Y. (Eds.) International GNSS Service Technical Report 2013, 133–136, IGS Central Bureau, 2014

Schmid R., Gerstl M., Seitz M., Angermann D.: *DGFI Analysis Center Annual Report 2013*. In: Baver K.D., Behrend D., Armstrong K.L. (Eds.) International VLBI Service for Geodesy and Astrometry 2013 Annual Report, 263-264, NASA/TP-2014-217522, 2014

Schmidt M., Göttl F., Heinkelmann R.: *Towards the combination of data sets from various observation techniques*. In: Kutterer H., Seitz F., Alkhatib H., Schmidt M. (Eds.) The 1st International Workshop on the Quality of Geodetic Observation and Monitoring Systems (QuGOMS'11), IAG Symposia 140: 35–43, Springer, doi:10.1007/978-3-319-10828-5_6, 2014

Seitz F., Hedman K., Meyer F.J., Lee H.: *Multi-sensor space observation of heavy flood and drought conditions in the Amazon region*. In: Rizos C., Willis P. (Eds.) Earth on the Edge: Science for a Sustainable Planet, IAG Symposia 139: 311-317, Springer, doi:10.1007/978-3-642-37222-3_41, 2014

Seitz F.: *Geodätische Erdbeobachtungsdaten als Fundament für die Beobachtung und das Verständnis des globalen Wandels*. Allgemeine Vermessungs-Nachrichten (avn), 05/2014, 169, 2014

Seitz M., Angermann D., Bloßeld M., Gerstl M., Müller H.: *ITRS Combination Centre at DGFI*. In: Dick W.R., Thaller D. (Eds.) IERS Annual Report 2013, 100-105, IERS Central Bureau, Verlag des Bundesamts für Kartographie und Geodäsie, Frankfurt/Main, ISBN 978-3-86482-073-1, 2014

Seitz M., Steigenberger P., Artz T.: *Consistent adjustment of combined terrestrial and celestial reference frames*. In: Rizos C., Willis P. (Eds.) Earth on the Edge: Science for a Sustainable Planet, IAG Symposia 139: 215–221, Springer, doi:10.1007/978-3-642-37222-3_28, 2014

Stammer D., Ray R.D., Andersen O.B., Arbic B.K., Bosch W., Carrère L., Cheng Y., Chinn D.S., Dushaw B.D., Egbert G.D., Erofeeva S.Y., Fok H.S., Green J.A.M., Griffiths S., King M.A., Lapin V., Lemoine F.G., Luthcke S.B., Lyard F., Morison J., Müller M., Padman L., Richman J.G., Shriver J.F., Shum C.K., Taguchi E., Yi Y.: *Accuracy assessment of global barotropic ocean tide models*. Reviews of Geophysics 52(3): 243–282, doi:10.1002/2014RG000450, 2014

Thaller D., Angermann D.: *Tagungsbericht IAG Scientific Assembly 2013, Theme 5: Global Geodetic Observing System*. Zeitschrift für Geodäsie, Geoinformation und Landmanagement (zfv) 139(1), 2014

Visser P.N.A.M., van_der_Wal W., Schrama E.J.O., van_den_IJssel J., Bouman J.: *Assessment of observing time-variable gravity from GOCE GPS and accelerometer observations*. Journal of Geodesy 88(11): 1029-1046, doi:10.1007/s00190-014-0741-9, 2014

5.3 Posters and oral presentations

Abdul Fattah, Meekes S., Bouman J., Ebbing J., Haagmans R.: *Modeling Tectonic Heat Flow and Source Rock Maturity in the Rub*. IPTC 2014: International Petroleum Technology Conference , 2014-01-19

Angermann D., Gruber T., Gerstl M., Hugentobler U., Sánchez L.: *GGOS-Büro für Standards und Konventionen*. Geodätische Woche, Berlin, Germany, 2014-10-08 (Poster)

Angermann D.: *GGOS Bureau of Products and Standards*. GGOS Coordinating Board Meeting, San Francisco, USA, 2014-12-13

Angermann D., Seitz M., Bloßfeld M., Gerstl M.: *ITRS Combination Centre at DGFI: Strategy and first results of ITRF2013 analysis*. EGU General Assembly 2014, Vienna, Austria, 2014-04-30

Angermann D., Gruber T., Gerstl M., Hugentobler U., Sánchez L., Heinkelmann R., Steigenberger P.: *Inventory of standards and conventions used for the generation of IAG/GGOS products*. AGU Fall Meeting, San Francisco, USA, 2014-12-15 (Poster)

Angermann D.: *GGOS Bureau of Products and Standards*. GGOS Consortium Meeting, San Francisco, USA, 2014-12-13

Angermann D., Nothnagel N., Thaller D.: *Linking Earth and Space*. Begutachtung DFG Forschergruppe "Referenzsysteme", Bonn, 2014-11-10

Angermann D., Gruber Th., Gerstl M., Hugentobler U., Sánchez L., Heinkelmann R., Steinberger P.: *GGOS Bureau for Standards and Conventions*. Symposium SIRGAS 2014, La Paz, Bolivia, 2014-11-24/26 (Poster)

Angermann D., Schmid R.: *DGFI part of project PN 5 - concept for 2nd phase*. Projekttreffen der DFG-Forschergruppe FOR1503, Zurich, Switzerland, 2014-06-03

Angermann D., Seitz M., Bloßfeld M., Gerstl M.: *Report of ITRS Combination Centre at DGFI*. IERS DB Meeting, Vienna, Austria, 2014-04-26

Bloßfeld M., Roggenbuck O., Seitz M., Angermann D., Thaller D.: *Non-tidal atmospheric pressure loading corrections in global reference frame computations: a case study using SLR*. IAG Commission 1 Symposium: REFAG, Luxemburg, Luxemburg, 2014-10-13

Bloßfeld M., Müller H., Gerstl M., Panafidina N., Bouman J., Göttl F.: *Low-degree spherical harmonics from multi-satellite SLR*. EGU General Assembly 2014, Vienna, Austria, 2014-04-30 (Poster)

Bloßfeld M., Müller H., Hugentobler U., Angermann D., Gerstl M.: *LOD systematics from SLR observations*. 19th International Workshop on Laser Ranging, 2014-10-27/31 (Poster)

Boergens E., Schwatke C., Dettmering D.: *Performance of Saral/AltiKa over inland water on effects of atmospheric water content*. 8th Coastal Altimetry Workshop, Lake Constance, Germany, 2014-10-24

Boergens E., Schwatke C., Dettmering D.: *Performance of Saral/AltiKa over inland water*. SARAL/AltiKa Workshop, Lake Constance, Germany, 2014-10-27 (Poster)

Bosch W., Dettmering D., Schwatke C., Panzetta F.: *Case study on minor tides - modeling, computation or estimation?*. Ocean Surface Topography Science Team Meeting, Lake Constance, Germany, 2014-10-30 (Poster)

Bosch W., Müller F., Dettmering D., Schwatke C.: *Validating space-based time-variable dynamic ocean topography by surface currents observed by ARGO floats and surface drifters*. Ocean Surface Topography Science Team Meeting, Lake Constance, Germany, 2014-10-30 (Poster)

Bouman J,: *The Earth's temporal gravity field observed by GOCE*. AGU Fall Meeting, San Francisco, 2014-12-16

Bouman J., Haberkorn C., McMillan M., Ivings E., Bloßfeld M., Fuchs M., Horwath M.: *Comparison of Antarctic basin scale mass change from GRACE/GOCE and CryoSat-2*. AGU Fall Meeting 2015, San Francisco, USA, 2014-12-17

Brunini C., Azpilicueta F., Limberger M., Schmidt M., Dettmering D., Liang W.: *An indirect assessment of the precision of the NmF2 maps computed from the ITU-R database and FORMOSAT-3/COSMIC ionospheric radio-occultations* . EGU General Assembly 2014, Vienna, Austria, 2014-05-02 (Poster)

Brunini C., Sánchez L., Mackern M.V., de Freitas: *SIRGAS: reference system for the Americas*. Symposium SIRGAS 2014, La Paz, Bolivia, 2014-11-24

Dettmering D., Schwatke C., Bosch , W. : *Global calibration of SARAL/AltiKa using multi-mission sea surface height crossovers*. SARAL/AltiKa Workshop, Lake Constance, Germany, 2014-10-27 (Poster)

Dettmering D., Limberger M., Schmidt M.: *Using DORIS for modeling the Vertical Total Electron Content of the Earth's Ionosphere*. EGU General Assembly, Vienna, Austria, 2014-05-02 (Poster)

Dettmering D., Limberger M., Schmidt M.: *Using DORIS for modeling the Vertical Total Electron Content of the Earth's Ionosphere*. IDS Workshop, Lake Constance, Germany, 2014-10-27

Dettmering D.: *Satellite Altimetry I*. DFG SPP1257 Summerschool, 2014-09-17

Drewes H., Sánchez L.: *Actualization of the SIRGAS velocity model*. Symposium SIRGAS 2014, La Paz, Bolivia, 2014-11-26

Ebbing J., Bouman J., Abdul Fattah, Haagmans R., Holzrichter N., Lieb V., Meekes S.: *Lithospheric structure of the Arabian peninsula from modeling of satellite gravity gradients*. EGU, Vienna, Austria, 2014-05-02

Ebbing J., Bouman J., Abdul Fattah, Haagmans R., Holzrichter N., Lieb V., Meekes S.: *Lithospheric structure of the Arabian peninsula from modeling of satellite gravity gradients*. 74. Jahrestagung der Deutschen Geophysikalischen Geschellschaft, 2014-03-13

Ebbing J., Bouman J., Fattah R., Haagmans R., Nils Holzrichter, Lieb V., Meekes S.: *Lithospheric structure of the Arabian peninsula from modeling of satellite gravity gradients*. EGU General Assembly, Vienna, Austria, 2014-04-28 (Poster)

Eicker A., Schall J., Lieb V., Bentel K., Schmidt M., Buße K., Kusche J., Gerlach C.: *Regional gravity field modeling using radial basis functions: results from IAG*. EGU General Assembly, Vienna, Austria, 2014-04-28

Erdogan E., Liang W., Limberger M., Schmidt M., Durmaz M., Dettmering D.: *Estimation of global VTEC in near real-time using B-Splines in support of IRI*. XXXIth URSI General Assembly and Scientific Symposium (URSI GASS), Beijing, China, 2014-08-16/23

Fuchs M., Haberkorn C., Bouman J., Lieb V., Schmidt M.: *Die GOCE Mission (RegGrav II)*. RegGrav II, Munich, Germany, 2014-05-22

Fuchs M., Bouman J.: *GOCE gradient processing and error assessment*. GOCE+/GDC: Final Meeting, 2014-10-29

Fuchs M., Broerse T., Bouman J., Hooper A.: *Integrated Inverse Modeling of Coseismic and Postseismic Deformation from Space Borne Gravimetric Measurements for the 2011 Tohoku-Oki Earthquake*. GENAH 2014, Matsushima, Japan, 2014-07-22

Göttl F., Boergens E., Dettmering D., Schwatke C.: *Cryosat-2 SAR altimetry for recovering sea surface heights in the open ocean and inland water - First results*. SAR Altimetry Training Course, Lake Constance, Germany, 2014-10-21/22 (Poster)

Göttl F., Schmidt M., Seitz F., Bloßfeld M.: *Separation of atmospheric, oceanic and hydrological polar motion excitation mechanisms by a combination of geometric and gravimetric space observations*. EGU General Assembly 2014, Vienna, Austria, 2014-04-29 (Poster)

Haase C., Bouman J., Ebbing J., Gradmann S., Lieb V.: *Inversion of multi-level gravity data to improve lithospheric modelling ? A case study for the North Atlantic region*. EGU General Assembly, Vienna, Austria, 2014-04-28 (Poster)

Haase C., Bouman J., Ebbing J., Gradmann S., Lieb V.: *Inversion of multi-level gravity data to improve lithospheric modelling ? A case study for the North Atlantic region*. EGU General Assembly, Vienna, Austria, 2014-04-28 (Poster)

Haase C., Bouman J., Ebbing J., Gradmann S., Lieb V.: *Inversion of multi-level gravity data to improve lithospheric modelling - A case study for the North Atlantic region*. EGU, Vienna, Austria, 2014-05-02 (Poster)

Haberkorn C., Bloßfeld M., Bouman J.: *Estimation of the Earth's gravity field by combining normal equation matrices from GRACE and SLR*. EGU General Assembly 2014, Vienna, Austria, 2014-05-01

Hernández-Pajares M., Limberger M., Garcia-Rigo A., Olivares G., Aragón-Àngel A., Schmidt M., Hugentobler U.: *Towards an optimal overall description of electron density information gathered during GNSS satellite occultations*. EGU General Assembly 2014, Vienna, Austria, 2014-05-02 (Poster)

Hugentobler U., Seitz M., Angermann D., Bloßfeld M., Panafidina N., Yi W.: *Consistent dynamic satellite reference frames and terrestrial geodetic datum parameters - PN6 -*. Statusseminar FG Referenzsysteme, Zurich, Switzerland, 2014-06-02

Kirschner S., Reinwald M., Schmidt M., : *Long-term simulations of polar motion: Variations of the Chandelr oscillation over two centuries* . EGU General Assembly 2014, Vienna, Austria, 2014-04-29 (Poster)

Legrand J., Bruyninx C., Craymer M., Dawson J., Griffiths J., Kenyeres A., Rebischung P., Sánchez L., Santamaría-Gómez A., Saria E., Altamimi Z.: *IAG WG "Integration of Dense Velocity Fields in the ITRF": Results and Lessons learned*. IGS Workshop 2014, Pasadena, California, USA., 2014-06-24 (Poster)

Liang W., Dettmering D., Schmidt M., Limberger M.: *An adapted multi-resolution representation of regional VTEC*. EGU General Assembly 2014, Vienna, Austria, 2014-05-02 (Poster)

Liang W., Erdogan E., Schmidt M., Durmaz M., Dettmering D., Limberger M., Hugentobler U.: *Multi-scale ionosphere model with data-adapted spatial resolution*. XXXIth URSI General Assembly and Scientific Symposium (URSI GASS), Beijing, China, 2014-08-21 (Poster)

Lieb V., Schmidt M., Dettmering D., Liebsch G.: *Analysing the accuracy of airborne gravity field observations and their contribution to regional gravity field models* . EGU General Assembly, Vienna, Austria, 2014-04-28

Lieb V., Buße K., Schmidt M., Dettmering D., Bouman J.: *Closed-loop tests of a regional gravity field modelling approach using radial basis functions*. EGU General Assembly, Vienna, Austria, 2014-04-28 (Poster)

Lieb V.: *Comparison of regional gravity models*. GOCE+ GeoExplore Project Meeting, Pilsen, Czech Republic, 2014-03-12

Lieb V.: *Patchwork of regional gravity models*. GOCE+ GeoExplore Project Meeting, Pilsen, Czech Republic, 2014-03-12

Limberger M., Hernández-Pajares M., García A., Schmidt M., Hugentobler U.: *Ionospheric electron density retrieval from FORMOSAT-3/COSMIC occultation data for a period of more than half a Solar Cycle*. EGU General Assembly 2014, Vienna, Austria, 2014-05-02 (Poster)

Lu C., Mora-Diaz J.A., Heinkelmann R., Schwatke C., Karbon M., Liu L., Nilsson T., Raposo-Pulido V., Soja B., Schuh H.: *IVS rapid tropospheric parameter re-combination and comparison with GNSS products*. 8th IVS General Meeting, Shanghai, China, 2014-03-02/07

Panafidina N., Hugentobler U., Seitz M.: *Subdaily Earth rotation model and GPS solutions*. EGU General Assembly 2014, Vienna, Austria, 2014-04-30 (Poster)

Rudenko S., Dettmering D., Esselborn S., Schöne T., Förste C., Lemoine J-M., Neumayer K-H.: *Impact of time variable Earth global gravity field models on precise orbits of altimetry satellites, global and regional mean sea level trends*. EGU General Assembly, Vienna, Austria, 2014-05-01

Sánchez L., H. Drewes, C. Brunini, M.V. Mackern, W. Martínez-Díaz, M. Fuchs: *Modelling seismic effects in regional geodetic reference frames*. International Symposium on Geodesy for Earthquake and Natural Hazards (GENAH 2014). Matsushima, Miyagi, Japan, 2014-07-22 (Poster)

Sánchez L.: *Vertical datum standardisation in South America*. Symposium SIRGAS 2014, La Paz, Bolivia, 2014-11-24

Sánchez L., Drewes H., Brunini C., Mackern M.V., Martínez-Díaz W., Schmid R.: *Improved modelling for the SIRGAS reference frame computation*. IGS Workshop 2014, Pasadena, USA, 2014-06-25 (Poster)

Sánchez L., Cunderlík R., Dayoub N., Minarechová Z., Mikula K., Vatrt V., Síma Z., Vojtísková M.: *Towards a new best estimate for the conventional value of W0*. Symposium SIRGAS 2014, La Paz, Bolivia, 2014-11-24/26 (Poster)

Sánchez L.: *Towards a unified vertical reference frame for SIRGAS*. XXVII Scientific Meeting of the Argentinean Association for Geodesy and Geophysics. San Juan, Argentina, 2014-11-12

Sánchez L., Cunderlík R., Dayoub N., Mikula K., Minarechová Z., Síma Z., Vatrt V., Vojtísková M.: *Towards a new best estimate for the conventional value of W0*. 3rd International Gravity Field Service (IGFS) General Assembly, 2014-07-02 (Poster)

Sánchez L.: *Report on the analysis of the SIRGAS reference frame at the IGS RNAAC SIRGAS*. Symposium SIRGAS 2014, La Paz, Bolivia, 2014-11-24/26 (Poster)

Santacruz A., de Freitas, Sánchez L.: *Towards a unified vertical reference frame for South America in view of the GGOS specifications*. 3rd International Gravity Field Service (IGFS) General Assembly. Shanghai, China., 2014-07-02

Santacruz A., de Freitas, Sánchez L., Luz R.T., Philippi S.: *Review of the South American heights systems to meet the new IAG/SIRGAS requirements*. Symposium SIRGAS 2014, La Paz, Bolivia, 2014-11-24

Schmid R., Bloßfeld M., Angermann D.: *Impact of non-linear station motions*. Geodätische Woche 2014, Berlin, Germany, 2014-10-07

Schmid R., Bloßfeld M., Angermann D.: *DGFI part of project PN 5 - status report*. Projekttreffen der DFG-Forschergruppe FOR1503, Zurich, Switzerland, 2014-06-02

Schmid R.: *Splinter Meeting of the IGS Antenna Working Group*. IGS Workshop 2014, Pasadena, USA, 2014-06-26

Schmidt M., Durmaz M., Limberger M., Erdogan E., Dettmering D., Liang W.: *A Global Ionospheric B-Spline VTEC Model from GNSS Measurements* . Conference on Satellite Methods for Positioning, Olsztyn, Poland, 2014-06-23

Schmidt M., Gerlach C., Bentel K., Dai C., Dettmering D., Eicker A., Herceg M., Kusche J., Lieb V., Schall J., Shang K., Shum C.K., Tscherning C.C.: *Results from IAG's Joint Study Group JSG0.3 on the Comparison of Current Methodologies in Regional Gravity Field Modeling*. EGU General Assembly, Vienna, Austria, 2014-04-28 (Poster)

Schwatke C., Dettmering D., Bosch W., Göttl F., Boergens E.: *Database for Hydrological Time Series of Inland Waters (DAHITI)*. Ocean Surface Topography Science Team Meeting, Lake Constance, Germany, 2014-10-30 (Poster)

Schwatke C., Dettmering D., Bosch W., Göttl F., Boergens E.: *OpenADB: An Open Altimeter Database providing high-quality altimeter data and products*. Ocean Surface Topography Science Team Meeting, Lake Constance, Germany, 2014-10-30 (Poster)

Schwatke C., Dettmering D., Bosch W., Göttl F., Boergens E.: *Database for Hydrological Time Series of Inland Waters (DAHITI)*. 8th Coastal Altimetry Workshop, Lake Constance, Germany, 2014-10-23 (Poster)

Schwatke C.: *Historical development of the SLR data holding at EDC between 1976 and 2014*. 19th International Laser Ranging Workshop, Annapolis, USA, 2014-10-29 (Poster)

Seitz M., Angermann D., Bloßfeld M., Gerstl M., Schmid R.: *The 2013 DGFI realization of the ITRS*. AGU Fall Meeting 2014, San Francisco, USA, 2014-12-14 (Poster)

Seitz M., Angermann D., Bloßfeld M.: *DTRF2013: Results of the analysis and impact of the contribution of the International DORIS Service*. IDS Workshop, Konstanz, Germany, 2014-10-27

Seitz M., Angermann D., Bloßfeld M., Gerstl M., Schmid R.: *The 2013 DGFI realization of the ITRS: DTRF2013*. IERS DB Meeting, San Francisco, USA, 2014-12-14

Seitz M., Nothnagel A.: *Consistent realization of ITRS and ICRS from a multi-technique combination*. IAG Commission 1 Symposium REFAG2014, Luxembourg, 2014-10-15

Woo J., Schwatke C., Müller H., Kim J.: *Station Procedures*. 19th International Laser Ranging Workshop, Annapolis, USA, 2014-10-31

5.4 Membership in scientific bodies

Centre National d'Etudes Spatiales (CNES) / National Aeronautics and Space Administration (NASA)

- Ocean Surface Topography Science Team for Jason-2,
  Member: Bosch W., Dettmering D.

Deutsche Geodätische Kommission (DGK)

- *Member: Seitz F.*

Deutsche Gesellschaft für Geodäsie, Geoinformation und Landmanagement (DVW)

- Working Group 7: Experimentelle, Angewandte und Theoretische Geodäsie,
  Member: Seitz F., Guest: Schmidt M.

European Geosciences Union (EGU)

- Geodesy Division,
  President: Schmidt M., Deputy President: Bouman J.

European Space Agency (ESA) / European Organisation for the Exploitation of Meteorological Satellites (EUMETSAT)

- Sentinel-3 Validation Team, Altimetry sub-group,
  Member: Dettmering D.

International Association of Geodesy (IAG)

- Commission 1, Sub-Commission 1.3b: Regional reference frame for South and Central America,
  Vice-Chair: Sánchez L.
- Commission 1, Sub-Commission 1.4: Interaction of celestial and terrestrial reference frames,
  Member: Seitz M.
- Commission 4, Study Group 4.3.1: Ionosphere modelling and analysis,
  Chair: Schmidt M., Member: Dettmering D., Limberger M., Liang W.
- GGOS Bureau for Standards and Conventions,
  Director: Angermann D.
- GGOS Consortium,
  Member: Angermann D.
- GGOS Coordinating Board,
  Member: Angermann D.
- GGOS Executive Committee,
  Member: Angermann D.
- GGOS Working Group on Performance Simulations and Architectural Trade-Offs (PLATO),
  Member: Seitz M.
- ICCT Joint Study Group 0.1: Application of time series analysis in geodesy,
  Member: Schmidt M.
- ICCT Joint Study Group 0.3: Methodology of regional gravity field modelling,
  Chair: Schmidt M., Member: Lieb V.

- ICCT Joint Study Group 0.5: Multi-sensor combination for the separation of integral geodetic signals,
  Chair: Seitz F., Member: Schmidt M., Seitz M.
- ICCT Joint Study Group 0.6: Applicability of current GRACE solution strategies to the next generation of inter-satellite range observations,
  Member: Bouman J., Haberkorn C., Schmidt M.
- Joint Working Group 0.1.1: Vertical datum standardization,
  Chair: Sánchez L.
- Joint Working Group 1.1: Tie vectors and local ties to support integration of techniques,
  Member: Seitz M.
- Joint Working Group 1.3: Strategies for epoch reference frames,
  Chair: Seitz M., Member: Bloßfeld M., Sánchez L.
- Symposia Series,
  Associate Editor: Sánchez L.
- Working Group 1.3.1: Integration of dense velocity into the ITRF,
  SIRGAS representative: Sánchez L.
- Working Group 1.3.2: Deformation models for reference frames,
  Member: Sánchez L.

International Astronomical Union (IAU)

- Commission 19, Rotation of the Earth,
  Secretary: Seitz F.
- Division A Working Group: Third Realisation of International Celestial Reference Frame,
  Member: Seitz M.

International Earth Rotation and Reference Systems Service (IERS)

- ITRS Combination Centre,
  Chair: Seitz M.
- Working Group on Combination at the Observation Level,
  Member: Angermann D., Bloßfeld M., Co-Chair: Seitz M.
- Working Group on SINEX Format,
  Member: Seitz M.
- Working Group on Site Coordinate Time Series Format,
  Member: Seitz M.
- Working Group on Site Survey and Co-location,
  Member: Angermann D., Schmid R., Seitz M.

International GNSS Service (IGS)

- Antenna Working Group,
  Chair: Schmid R.
- Governing Board,
  Member: Schmid R., Network Representative: Sánchez L.

- GPS Tide Gauge Benchmark Monitoring - Working Group,
  Member: Sánchez L.

International Laser Ranging Service (ILRS)

- Analysis Working Group,
  Member: Bloßfeld M., Müller H.
- Data Centre (EDC),
  Chair: Schwatke C., Member: Müller H.
- Governing Board,
  Member: Müller H.
- Operations Centre (EDC),
  Chair: Schwatke C.
- Study Group on ILRS Software Library,
  Member: Schwatke C.
- Working Group on Data Formats and Procedures,
  Chair: Müller H., Member: Schwatke C.

International VLBI Service for Geodesy and Astrometry (IVS)

- Operational Analysis Centre,
  Member: Schmid R., Seitz M.

Modelado de movimientos no lineales en el establecimiento de marcos de referencia

- *Member: Sánchez L.*

Sistema de Referencia Geocéntrico para las Américas (SIRGAS)

- *Vice president: Sánchez L.*
- Working Group 1: Reference frame,
  Member: Sánchez L.

5.5 Participation in meetings, symposia, conferences

2014-01-23/24 : **Retreat of the Faculty of Civil, Geo and Environmental Engineering of the TU München, Wildbad Kreuth, Germany**
Seitz F.

2014-01-28/29 : **Horizon2020 National Launch Event, Berlin, Germany**
Seitz F.

2014-02-24/26 : **DFG SPP1257 Workshop on Outreach, Bonn, Germany**
Seitz F.

2014-03-13 : **Valedictory lecture of Prof. Wilfried Schwarz, Weimar, Germany**
Seitz F.

2014-03-13/14 : **GOCE+ GeoExplore Meerting, Plsen, Czech Republic**
Bouman J., Lieb V.

2014-03-21 : **DFG-Forschergruppe FOR1503, Projects PN 5/6, Progress Meeting, Munich, Germany**
Angermann D., Bloßfeld M., Schmid R., Seitz M.

2014-03-24 : **Annual meeting of DGK section Geodesy, Stuttgart, Germany**
Seitz F.

2014-03-26/27 : **Munich Satellite Navigation Summit 2014, Munich, Germany**
Sánchez L., Schmid R.

2014-04-03/04 : **Discussion of the DFG proposal RU Global Freshwater System, Stuttgart, Germany**
Dettmering D., Seitz F.

2014-04-26 : **GGOS Coordinating Board Meeting, Vienna, Austria**
Angermann D.

2014-04-27 : **IERS Directing Board Meeting, Vienna, Austria**
Angermann, D.

2014-04-28 : **ILRS Analysis Working Group Meeting, Vienna, Austria**
Bloßfeld M.

2014-04-28 : **GGOS Study Group: LAser Ranging to GNSS s/c Experiment (LARGE), Vienna, Austria**
Bloßfeld M.

2014-04-28/05-02 : **European Geosciences Union General Assembly, Vienna, Austria**
Angermann D., Bloßfeld M., Haberkorn C., Lieb V., Schmidt M., Seitz F.

2014-05-12 : **REWAP Kick-off meeting, Munich, Germany**
Boergens E., Dettmering D., Lieb V., Ressler G., Schmidt M., Seitz F.

2014-05-21 : **Status Seminar of Project RegGRAV II, Munich, Germany**
Dettmering D., Haberkorn C., Lieb V., Schmidt M., Seitz F.

2014-05-22 : **OPTIMAP Kick-off meeting, Munich, Germany**
Dettmering D., Durmaz M., Limberger M., Schmidt M., Seitz F.

2014-06-02/03 : **Status Seminar of the DFG Research Unit FOR1503 (Reference Systems), Zurich, Switzerland**
Angermann D., Schmid R., Seitz M.

2014-06-03/06 : **Arctic Days, Tromso, Norway**
Bouman J.

2014-06-13 : **Discussion of the DFG proposal SPP1811 (Sea Level), Hamburg, Germany**
Dettmering D.

2014-06-13 : **Kolloquium Götze/Ebbing, Kiel, Germany**
Bouman J.

2014-06-16/18 : **IGSSE Forum, Burghausen, Germany**
Boergens, E., Lieb V., Ressler G.

2014-06-22 : **43rd IGS Governing Board Meeting, Pasadena, USA**
Schmid R.

2014-06-22/25 : **International Symposium on Geodesy for Earthquake and Natural Hazards (GENAH 2014), Matsushima, Japan**
Fuchs M.

2014-06-23/24 : **Conference on Satellite Methods for Positioning, Olsztyn, Poland**
Schmidt M.

2014-06-23/27 : **IGS Workshop 2014, Pasadena, USA**
Schmid R.

2014-07-03/04 : **1st Workshop of DFG priority programme 1788: Dynamic Earth, Potsdam, Germany**
Schmidt M.

2014-07-23 : **WLDYN Kick-off meeting, Munich, Germany**
Boergens E., Dettmering D., Schwatke C., Seitz F.

2014-09-15/18 : **ESA 3D Earth pre-meeting, Barcelona, Spain**
Bouman J.

2014-09-15/19 : **DFG SPP1257 Summerschool, Mayschoss, Germany**
Boergens E., Dettmering D., Ressler G.

2014-09-22 : **Status Seminar of Project RegGRAV II, Uedem, Germany**
Haberkorn C., Schmidt M., Seitz F.

2014-09-23/24 : **Status Seminar of Project OPTIMAP, Uedem, Germany**
Limberger M., Schmidt M., Seitz F.

2014-10-07/09 : **Geodätische Woche, Berlin, Germany**
Angermann D.

2014-10-13/17 : **IAG Commission 1 Symposium: Reference Frames for Applications in Geosciences (REFAG2014), Luxembourg, Luxembourg**
Bloßfeld M.

2014-10-21/22 : **SAR Altimetry Training Course, Constance, Germany**
Göttl F.

2014-10-23/24 : **8th Coastal Altimetry Workshop, Constance, Germany**
Boergens E.

2014-10-26 : **ILRS Analysis Working Group Meeting, Annapolis, USA**
Müller H., Schwatke C.

2014-10-27 : **IDS Workshop, Constance, Germany**
Bloßfeld M., Dettmering D.

2014-10-27 : **SARAL/AltiKa Workshop, Constance, Germany**
Dettmering D.

2014-10-27/31 : **19th International Workshop on Laser Ranging, Annapolis, USA**
Müller H., Schwatke C.

2014-10-28/31 : **Ocean Surface Topography Science Team Meeting, Constance, Germany**
Dettmering D.

2014-10-29 : **Valedictory lecture of Prof. Reinhard Dietrich, Dresden, Germany**
Sánchez L., Seitz F.

2014-11-10 : **Begutachtung DFG Research Unit FOR1503 "Reference Systems", Bonn, Germany**
Angermann D., Seitz M.

2014-11-10/14 : **XXVII Scientific Meeting of the Argentinean Association for Geodesy and Geophysics, San Juan, Argentina**
Sánchez L., Drewes H.

2014-11-12/14 : **Annual meeting of DGK, Munich, Germany**
Hornik H., Seitz F.

2014-11-20/22 : **SIRGAS School on Vertical Reference Systems, La Paz, Bolivia**
Sánchez L., Drewes H.

2014-11-24/26 : **Symposium SIRGAS 2014, La Paz, Bolivia**
Sánchez L., Drewes H.

2014-11-25/26 : **Status Seminar of Project OPTIMAP, Göttingen, Germany**
Limberger M., Schmidt M., Seitz F.

2014-11-25/27 : **GOCE User Workshop, Paris, France**
Bouman J.

2014-11-28 : **Annual meeting of the Munich GeoCenter, Munich, Germany**
Seitz F.

2014-12-03/04 : **Sentinel-3 Validation Team (S3VT) Meeting, Darmstadt, Germany**
Dettmering D.

2014-12-11 : **Status Seminar of Project WLDYN, Potsdam, Germany**
Boergens E., Seitz F.

2014-12-13 : **GGOS Coordinating Board Meeting, San Francisco, USA**
Angermann D.

2014-12-13 : **GGOS Consortium Meeting, San Francisco, USA**
Angermann D

2014-12-14 : **IERS Directing Board Meeting, San Francisco, USA**
Angermann D.

2014-12-15/19 : **American Geophysical Union (AGU) Fall Meeting, San Francisco, USA**
Angermann D., Bouman J., Lieb V.

5.6 Guests

2014-01-01/02-26 :	Romina de los Angeles Galvan, Universidad Nacional de La Plata, La Plata, Argentina
2014-01-01/03-08 :	Prof. Dr. Claudio Brunini, Universidad Nacional de La Plata, La Plata, Argentina
2014-01-01/11-30 :	Dr. Murat Durmaz, Middle East Technical University, Ankara, Turkey
2014-01-20 :	Dr. Annette Eicker, Universität Bonn, Germany
2014-02-01/28 :	Dr. Virginia Mackern, Universidad Nacional de Cuyo, Mendoza, Argentina
2014-03-21 :	Dr. Daniela Thaller, Ole Roggenbuck, Bundesamt für Kartographie und Geodäsie (BKG), Frankfurt/Main, Germany
2014-05-05 :	Matthieu Talpe, University of Colorado, Boulder, USA
2014-05-21/22 :	Wilhelm Kersten, Zentrum für Geoinformationswesen der Bundeswehr (ZGeoBW), Euskirchen, Germany
2014-05-21/22 :	PD Dr. Klaus Börger, Sylvia Brandert, Weltraumlagezentrum der Bunderswehr (WRLageZ), Uedem, Germany
2014-05-22 :	Dr. Volker Bothmer, Universität Göttingen
2014-06-13 :	Prof. Dr. Jörg Reinking with a group of students, Jade University, Oldenburg
2014-06-26 :	Delegation of 20 professors, Chinese Academy of Sciences (CAS)
2014-07-22/23 :	Dr. Andreas Güntner, GFZ Potsdam
2014-07-23 :	Prof. Dr. Petra Döll, Dr. Felix Portmann, Universität Frankfurt
2014-07-28/08-01 :	Qiang Chen, Universität Stuttgart
2014-07-29/30 :	Prof. Dr. Maik Thomas, GFZ Potsdam
2014-08-19/20 :	Dr. Annette Eicker, Universität Bonn, Germany
2014-10-13/17 :	Prof. Dr. Rodrigo Abarca del Rio, Universidad de Concepcion, Chile
2014-10-22 :	Sarah Quandt, Institute for Baltic Sea Research (IOW), Warnemünde

6 Personnel

6.1 Number of personnel

Total staff of DGFI during the 2014 period:

1	Director
12	Scientists (basic funding)
10	Scientists (third party funding)
7	Technical and administrative staff

6.2 Funding of the following projects is gratefully acknowledged

(in alphabetic ordering)

ADAPIO Development of a novel adaptive model to represent global ionosphere information from combining space geodetic measurement systems (DLR)

AGGA Aeronomy and Geodesy in collaboration between Germany and Argentina (AvH)

CLIVAR-Hydro Signals of climate variability in continental hydrology from multi-sensor space and in-situ observations and hydrological modeling (DFG/IGSSE); at TUM Chair of Geodetic Geodynamics

COMION Investigation of data compression techniques in a multi-scale representation of a regional ionosphere signal (TUM Diversity); at TUM Chair of Geodetic Geodynamics

CRUST-DEF Crustal deformation model in response to regional geophysical fluid variations determined by GRACE (Arcoiris/Erasmus Mundus); at TUM Chair of Geodetic Geodynamics

FOR 584, P6 Integration of Earth rotation, gravity field and geometry using space geodetic observations (DFG)

FOR 1503, PN5 Consistent celestial and terrestrial reference frames by improved modeling and combination (DFG)

FOR 1503, PN6 Consistent dynamic satellite reference frames and terrestrial geodetic datum parameters (DFG)

GOCE HPF Validation and frame transformation of GOCE gravity gradients (ESA/TUM)

GOCE+ GeoExplore Heterogeneous gravity data combination for Earth interior and geophysical exploration research (ESA)

GOCE+ Time Variations Feasibility study to the potential of GOCE data to detect temporal gravity field variations (ESA)

MACOS Mass variations in continental surface water storage from heterogeneous space and in-situ observations (TUM Diversity); at TUM Chair of Geodetic Geodynamics

OPTIMAP Operational Tool for Ionospheric Mapping And Prediction (ZGeoBw)

RegGRAV II Software application for high-resolution regional geoid models (ZGeoBw)

REWAP Monitoring and Prediction of Regional Water Availability for Agricultural Production under the Influence of Climate Anomalies and Weather Extremes (DFG/IGSSE); at TUM Chair of Geodetic Geodynamics

UHR-GravDat Consistent estimate of ultra-high resolution Earth surface gravity data (DFG)

WLDYN Assessing the spatiotemporal dynamics of water volumes in large wetlands and lakes by combining remote sensing with macro-scale hydrological modelling (DFG); at TUM Chair of Geodetic Geodynamics

6.3 Lectures at universities

Bosch W. University lectures "Oceanography and Satellite Altimetry", TUM, WS 2013/14 and WS 2014/15

Bouman J. University lectures "Gravity and Magnetic Field from Space", TUM, WS 2013/14 and WS 2014/15

Schmidt M. University lectures "Numerical Modelling", TUM, WS 2013/14 and WS 2014/15

Schmidt M. University lectures "Numerische Methoden in der Satellitengeodäsie", TUM, SS 2014

Seitz F. University lectures "Earth System Dynamics", TUM, WS 2013/14 and WS 2014/15

Seitz F. University lectures "Seminar ESPACE", TUM, SS 2014

6.4 Lectures at seminars and schools

Dettmering D. SPP1257 Summerschool, Lecture on Satellite Altimetry, Mayschoss, Germany, 2014-09-17

Sánchez L. Lecture on Vertical Reference Systems, XXVII Scientific Meeting of the Argentinean Association for Geodesy and Geophysics. San Juan, Argentina, Universidad Nacional of San Juan. San Juan, Argentina, 2014-11-11/12

Sánchez L. Lecture on Vertical Reference Systems, SIRGAS School on Vertical Reference Systems, Instituto Geografico Militar, La Paz, Bolivia, 2014-11-20/22

Sánchez L. Lecture on kinematic adjustment of vertical reference networks, SIRGAS School on Vertical Reference Systems, Instituto Geografico Militar, La Paz, Bolivia, 2014-11-20/22

6.5 Thesis supervision

Master Theses

Oliveira M. A voxel based approach to retrieve ice mass loss in the Amundson Sea Sector using GOCE and GRACE measurements. (Supervisors: Bouman J., Fuchs M.; institution: TUM)

Doctoral Theses

Schindelegger M. Atmosphere-induced short period variations of Earth rotation. (Co-supervisor: Seitz F.; institution: TU Vienna; day of defense: January 24, 2014)

Forootan E. Statistical Signal Decomposition Techniques for Analyzing Time-Variable Satellite Gravimetry Data. (Co-supervisor: Schmidt M.; institution: University of Bonn; day of defense: September 19, 2014)

7 Miscellaneous

7.1 Dissertations

Sánchez L.

Title: Ein einheitliches vertikales Referenzsystem für Südamerika im Rahmen eines globalen Höhensystems

Supervisors: Prof. (i.R.) Dr.-Ing. habil. Reinhard Dietrich (Technische Universität Dresden), Prof. Dr.-Ing. habil. Dr. h.c. Bernhard Heck (Karlsruhe Institute of Technology), Prof. Dr.-Ing. Martin Horwath (Technische Universität Dresden)

Day of defense: December 19, 2014

Institution: Technische Universität Dresden

7.2 TUM Graduate School

International Research Phase

Liang W.

Academic Institution: George Mason University, Fairfax, U.S.A.

Duration: from June 28 till August 29, 2014

Supervisor: Prof. Dr. Dieter Bilitza

Limberger M.

Academic Institution: Universitat Politècnica de Catalunya, Barcelona, Spain

Duration: from February 2 till April 25, 2014

Supervisor: Prof. Dr. Manuel Hernández-Pajares